ENGINEERING DEVELOPMENT AND CONTROL DESIGN OF A SYSTEM FOR PARAPLEGIC TRICYCLING

By

Markus Rothe

Register No.: 990 99 65

**A thesis submitted in fulfilment of the requirements
for the degree of
Master of Science (M.Sc.) by Research
in the Department of Mechanical Engineering of the
Faculty of Engineering
at the University of Glasgow**

SCOTLAND

FEBRUARY 2001

UNIVERSITY OF GLASGOW
DEPARTMENT OF
MECHANICAL ENGINEERING

The undersigned hereby certify that they have read and recommend to the Faculty of Centre for Systems and Control for acceptance a thesis entitled "**Engineering Development and Control Design of a System for Paraplegic Tricycling**" by **Markus Rothe** in ~~partial~~ fulfillment of the requirements for the degree of **Master of Science**.

Dated: February 2001

Supervisor: ______________________________
Prof. Ken Hunt, University of Glasgow

Readers: ______________________________
Dr. Marion Hersh, University of Glasgow

____
Dr. Malcolm Granat, University of Strathclyde

UNIVERSITY OF GLASGOW

Date: **February 2001**

Author: **Markus Rothe**

Title: **Engineering Development and Control Design of a System for Paraplegic Tricycling**

Department: **Mechanical Engineering**

Degree: **M.Sc.** Convocation: **Oct** Year: **1999**

Signature of Author

To Grandma, Michael, and William.

Table of Contents

Abstract

The aim of this study was the design of a cycle device to be used by patients with Spinal Cord Injury (SCI), using the technique of Functional Electrical Stimulation (FES). A complete literature review of former projects in the areas of Design Engineering, Control Engineering, Physiologic and Psychologic investigations in SCI FES cycling was done. All results achieved so far were summarized.
Based on the review, a commercially available tricycle was modified for the demands of SCI people. A 10 Bit shaft encoder was used to feed back information from the tricycle and the cyclist. A software for the stimulation of the muscles in the lower limbs was developed. The Real Time Toolbox of Matlab was used for the data acquisition between the tricycle and the PC.
A simple approach was invented to find a good first approximation of the individual stimulation pattern for the Gluteal, Hamstring, and Quadriceps muscle groups.
Initial experiments were done. A velocity compensation routine, which was part of the software as well, allowed a healthy subject, stimulated via FES, to increase the pedal frequency to more than 100 rev per minute.
A closed loop controller, based on system identification and analytical controller design, was implemented into the software as well. Experiments showed that the controller was able to fix the pedal frequency to a constant value on one hand, but also to solve dynamic tasks on the other hand. This is a significant original contribution, as this type of feedback controller has not previously been applied in FES cycling.
The system described in the thesis is currently being used in a pilot study of FES cycling with three paraplegic subjects at the Southern General Hospital in Glasgow.

Acknowledgements

There are many people who have made contributions to this thesis.
First, I want to thank Prof. Ken J. Hunt from the University of Glasgow very much for the confidence he put in me, making possible this thesis, and for his outstanding support at any time and his interest in the progress of the work.
I would like to say thank you to Thomas Schauer and Ralf-Peter Jaime for their efforts to answer all my never ending questions on control theory and LaTeXprogramming during the entire time in Glasgow.
3, 2, 1...Thanks to the Norwegian guys Thomas and Nils for late laboratory sessions and discussions about control theory in a more general sense.
'If you want to become rich, just spend enough money'. Very special thanks to Michael and William, who were with me all the time, giving me strength, even in applied instability of car dynamics. 'Its not a problem!'
Thanks to Tilmann, Ben, and Catherine, who were always interested in my well being, on the tennis court as well as during long dinner nights.
Thank you Alan, George, and all the others from the Mechanical Workshop for the support in different tasks to re-design the tricycle. I also want to thank all staff of the Centre for Systems and Control.

On the personal side I would like to say thanks to my Grandma, for her love and her willingness to always listen to my problems and thoughts. Thanks to my family, for their support during the entire study.
Thanks to Marion, Tanja, Heiko, Raphael, Marc, Matthias, and Lutz, who did not forget me and made it easier being so far away for a long time. Special thanks to Anika, for her love and encouragement during the completing period of this thesis, which significantly improved the English.
Last but not least, I want to thank Mr. Missy and the whole Team from the BMW-Company for releasing me from work during the completing phase of the thesis.

Introduction

Functional Electrical Stimulation (FES), at least its effects, were primarily described by Franklin in the 18th century. Franklin described the possibility of evoking involuntary contractions of paralysed muscles by externally applied electricity. After these initial feasibility demonstrations nearly 200 years were to pass until functionally useful applications in paralysed muscles or body functions could be evoked by electrical stimulation. In the research-field of Control Theory and Computation Power the developments that have been made during the last 10 years are currently used to increase the effectiveness of the stimulated muscles, either for the more precise control of a single muscle, or in their collaboration and interaction to restore more complex movements.

Today FES is operated in different areas of the daily life, such as Bowel and Bladder Management, Sexual Function, Walking Quality, Walking Speed and Cosmetic Aspects [74], whereby the ranking of these applications is equal to the demands of improvements in different aspects of disability. In terms of paralysed persons FES has been used in research settings to restore the ability to stand [21], walk [65], rise from a chair [6], climb stairs [21], and grasp objects [1].

There are musculoskeletal problems which typically arise after Spinal Cord Injury (SCI) happened. These problems include disuse atrophy, osteoporosis, and reduced joint mobility. The atrophy of the paralysed muscles can subsequently permit an accompanying loss of support of the skeletal system. This loss of support can result in fractures and other injuries, when combined with osteoporosis. It would be desirable to provide appropriate exercise for the paralysed lower limbs to prevent or reverse these problems [62]. Electrical stimulation-induced exercise is believed to provide therapeutic benefits, such as improved muscle strength and endurance [87], improved cardiopulmonary fitness [31], improved circulation and decreased swelling due to edema [64], prevention of contractures [64], reduction in the rate of osteoporosis [119], and decreased spasticity [64]. One major problem of the applications

mentioned is the rapid muscle fatigue. Uncontrollable body balance and safety problems arise in this regard.
[11] suggested that the muscle force induced during intermittent stimulation produces a longer torque time course. Since cycling transmits intermittent generated muscle forces of different muscle groups in a rotatory movement, it maximises the effectiveness of the electrically stimulated muscles compared to other means of locomotion [38]. For this reason paraplegic cycling on commercially available FES ergometers is supposed to provide long term health maintenance for paraplegic and quadriplegic patients more than any other exercise. Although therapeutic benefits in cycling have been demonstrated [28][32][54] [81][105][112] [133], the general usefulness of this technology as a therapeutic modality is currently limited in terms of cycle time and Power Output (PO) [83][105]. Nevertheless the oxygen consumption (Cardiac Output) in FES-induced computer-controlled cycling reaches 15 litres min^{-1} [94][99][104], whereas the highest cardiac output elicited to lift a weight, described in [97][98], was about 7 litres min^{-1}. As we see computer-controlled aerobic exercise through FES bicycle ergometer has taken on importance in the clinical setting of many rehabilitation centres [112]. An additional advantage of FES cycling is that the individuals with paraplegia can safely perform the exercise [5].

This project was started with a literature survey to get an idea of the work done in this area so far, and to get a first impression of possible problems. The review is also the first Chapter of this thesis.
Chapter 2 treats the tricycle ordered and the modifications made to allow paralysed people cycling.
The muscles of the cyclist's lower limbs are controlled via computer. The software developed and the initial tests done, as well as the first results achieved can be found in the third Chapter.
The fourth Chapter describes the development of a closed loop speed controller for SCI FES cycling.
Chapter 5 reflects the whole project and gives an outlook of the things to be done in future work. It also describes a possibility to increase the performance in SCI FES cycling using a mathematical variation and optimization approach.

Chapter 1

Literature Survey

Research in the area of rehabilitation engineering and neuroprotheses has been carried out for at least 50 years. This Chapter reflects the investigations made and results achieved in terms of muscle stimulation, the design of cycle devices, and also in terms of medical effects observed during up to now.
Different cycle devices will be discussed in the following Section. The focus will be first on unsupported devices operated by muscle-power only (FES-stimulated). Motor-assisted tricycles will be reviewed in the succeeding Subsection. Force sensors developed so far will be specified in the last part of this Section.
The second Section of this Chapter treats the techniques used for the operation of the devices described. The dynamic models established and the muscles involved in cycling are presented.
The problems discovered in previous work in terms of muscle stimulation, cycle parameter optimisation -such as the influence of modified seat positions, and the individual stimulation pattern- are outlined in the third Subsection.
The third Section surveys the results that have been obtained so far in terms of Cardiopulmonary, Metabolic, Skeletal, and Psychological effects.

1.1 Devices

Cycling of paralysed persons usually is performed with three or four wheeled devices because of balance and safety advantages [91][100][108]. Postural stability on a two-wheel cycle is impossible with high levels of spinal cord injury. The seats used are either standard recumbent ones, which normally are fitted on tricycles, or modified ones with shoulder and waist straps to hold the person in place [38][91][100]. In case

of quadriplegic individuals cycling the tricycle, the seat has to be changed to a high-back one to provide postural support [91].
All kinds of control systems need feedback information, the simplest of which is to measure the position of the foot [108]. To do this in FES walking it is necessary to measure the angles of the hip, knee and ankle joints. Cycling is simpler, as the foot motion is constraint by the pedals. With the use of ankle braces the motion is restricted yet further and it becomes possible to use just one angle, that of the crank, to define the geometry of the entire leg, assuming known lengths of shank and thigh. The stimulation can then be synchronised with the crank angle. To provide the computer with information to increase the amount of stimulation to the legs and thereby to increase the speed, every device is endowed with some kind of a throttle, which are well known from motorcycles for example.
In FES cycling the ankle needs to be stabilised against plantar/dorsiflexion, internal/external rotation and inversion/eversion. It is also necessary to prevent varus/ valgus of the legs, although this needs not necessarily be done at the ankle. Stability can be achieved through the use of orthoses, although it should be possible, at least theoretically, to use FES to provide dynamic bracing [103]. Dynamic bracing of the ankle during FES walking has been described by [4][7][92], but bearing in mind the ease with which osteoporotic bones may be broken [103], until now no attempt has been made to use dynamic bracing in cycling.

1.1.1 Unsupported Devices

Petrofsky, Heaton, and Chandler 1983

The three wheel cycle ergometer described in [91] was built from a standard tricycle. This three wheel cycle ergometer had one steered front wheel and two rear wheels. Only one of the rear wheels was driven, to avoid the necessity of a differential gearbox. The cycle position was nearly upright, like on a normal bike, although the seat - not a recumbent one - was modified. Feedback was given from a 360^0 single turn potentiometer with a resistance range between 0 and 10 kΩ. The connection of the crank angle to the sensor was accomplished by placing an additional sprocket on the pedal, linked through a chain drive to the potentiometer. Another potentiometer was used for the manual speed and power adjustment. Five volts were applied through the potentiometers so that the output voltage went from zero to five volts. The computer used was custom built for this application. It utilized a Z80 microprocessor.

Pons, Vaugham, and Jaros 1989

The 'Paracycle' described in [108] is a four wheel device, developed especially for the requirements of paralysed persons. With its two smaller steered wheels in the front and the two larger wheels in the rear, the paracycle device differs from commercial ones. The cycle position is nearly recumbent. It is operable either as a stationary or as a freely moving exercise device. The paracycle was designed to accomodate the smallest (5 percentile female) and largest (95 percentile male) subjects. Features of the paracycle were made adjustable to allow the optimisation of the posture for each individual.

The seat was covered with bands of nylon netting. Each band was tied on with cord so that its tension could be adjusted independently. The armrests may be flexed/extended and internally/externally rotated. Thus they can be moved out of the way to avoid injuring the insensitive hips and buttocks during transfers to and from the seat.

The pedal assembly is movable along the arc of a circle to give height adjustment. The pedals can also be extended and converted into hand cranks to provide upper body exercise.

The steering is performed by supination-pronation of the right forearm. Since the PO of electrical stimulated paraplegics is limited, the paracycle is also equipped with 18 gears. To get feedback from the crank an optical shaft encoder is used. A potentiometer for the throttle is utilized for the manual speed adjustment.

The stimulation hardware and software were developed by [109] around an IBM-compatible PC.

Petrofky and Smith 1992

A commercially available three wheel tricycle in its basic design was modified in '92 from [100]. The tricycle is constructed to acommodate two cyclists in a side by side arrangement of the seats. This arrangement also made the wheelbase wider for better stability. The seats used are high-back bucket-seats which provides better support to sit on and better back support than the ones commonly found. Nevertheless on the side of the tricycle where the individual with paralysis was to ride, a seat belt was added to help stabilize the body.

Another modification of the tricycle involved stabilizer-bars for the legs. They were added on the side where the paralysed individual would ride, so that long aluminium

bars would follow the movement of the knees during cycling to keep the legs from moving in and out. The design was previously published in [94][96][97][98].
The pedals on the side of the tricycle, where the individual who was paralysed would ride, were also modified with toe straps with Velcro linings. These straps held the bottom of the shoe and foot in place.
Potentiometers like the ones described above [91] were used for the feedback of the crank position and manual commands given by the throttle. The microprocessor used for the calculations, the data acquisition converter and the stimulator was a Motorola single chip processor with a sampling rate of approximately 10 000 Hz.

Gföhler, Loicht and Lugner 1998

One of the latest tricycles developed for paraplegic cycling is described in [38]. The cyclist's position on the tricycle is as erect as the one on standard bicycles. The saddle pipe consists of a double effective hydraulic cylinder, which allows the saddle to move up and down. The adjustable height is advantagous in terms of getting on and off the tricycle and to adapt the geometry to the size of the cyclist. The feet are fixed on the two force measurement pedals [82] described below. To reduce the horizontal component of the acceleration, which makes cycling on a tricycle even more difficult for a paraplegic subject who cannot use their hip muscles as stabilizers, the rear axle is a special construction which allows the inclination of the rear wheels and the main cycle frame (see Fig. 1.1).

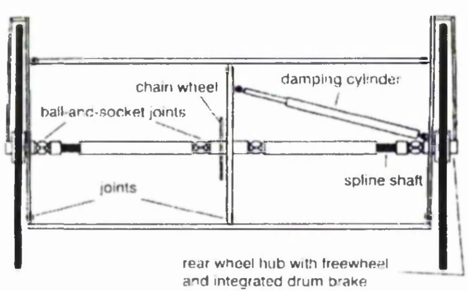

a: Schematic Diagram of Rear Axle.

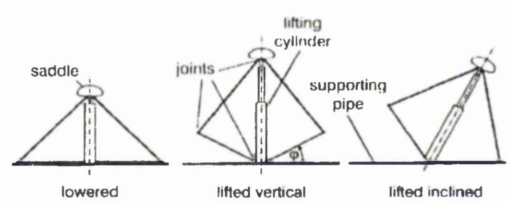

b: Schematic Diagram of the Function of the Articulated Triangles Limiting the Inclination.

Figure 1.1: Inclination System.

The damping of the inclination is adjusted by a double effective hydraulic cylinder, which is controlled by a throttle. This enables subjects with little training to ride the tricycle without employing the inclination function.

In addition to the drive torque generated by the muscle forces, power can be generated by an auxiliary motor (see Section below). The feedback data are fed to a PC and sampled with 50 Hz.

Glaser, Gruner, Feinberg, and Collins 1983

[41] described an intermediate device of a leg propelled wheelchair for locomotion of electrically stimulated individuals. It was assumed that this leg-propelled vehicle (LPV) system could, potentially, alleviate many of the problems associated with conventional arm-propelled wheelchairs, while helping to develop and maintain the fitness of the paralysed legs.
To facilitate the construction of the LPV a universal model wheelchair was modified. The casters were replaced by a single one in the front and a second, swivel incuster, centered in the rear about 2 cm above the ground to prevent backward tipping with forward acceleration. The primary additions to the wheelchair were two movable footplates which were coupled to the drive wheels via ratchet-type transmissions (Fig. 1.2).

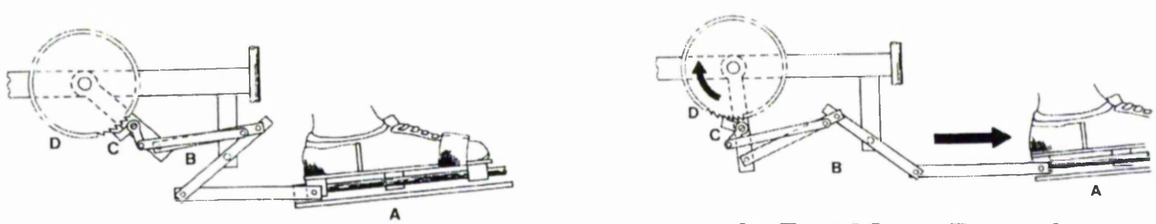

a: Resting Position. **b: Foot Moves Forward.**

Figure 1.2: Ratchet Drive System.

With forward extension of the legs, the pawls of the ratchet systems engage, causing forward rotation of the drive wheels. With backward movement of the legs, through gravity due to the slight upward angle of the footplate, the pawls of the ratchet system disengage, permitting the drive wheels to coast forward. Large-radius steering can be accomplished by consecutive movements of a single leg. Feedback is given from microswitches which are mounted near the end of the forward travel of the LPV footplates which cut off the stimulation. The stimulation pattern is given either manually by three pushbutton-switches to activate either the right leg, or the left leg, or both legs simultaneously, or from a program implemented in the stimulator.

1.1.2 Motor Supported Devices

Classically only very low PO can be sustained by paraplegic subjects cycling and this has been attributed to several factors [44][96][122]. Weakness of the muscles coincident with atrophy of the unused lower limbs is the most obvious cause of low PO [44]. Motor support in tricycles for the use of paraplegic individuals is essential for cycling over gradients in particular. Moreover it guarantees that the cyclist can return to their journeys starting point in case of problems with the generation of muscle force. The auxiliary motor also enables subjects with very weak muscles at the beginning of their training period to use the exercise tricycle and the motor can be used for overcoming the initial inertia when the tricycle is started from rest. It also can help to assist the pedals over the dead spots and increase the cycle time in total in terms of the generally early muscle fatigue in electrically stimulated muscles. In later training sessions the motor can be used as a generator to provide resistance.

The first known cycle device supported by an electric machine functioning as a motor to assist the electrical stimulated muscles was constructed from [41] in 1983.

Pons, Vaugham, and Jaros 1989

The tricycle from Pons, Vaughan, and Jaros [103] was the first known supported device which could be used as a stationary exercise device in the lab or for locomotion outside. The motor was provided to drive the pedals at a speed suitable for passive exercise and to accelerate the vehicle from rest. A Pulse Width Modulator (PWM), built by Popp (1986), was used to control the speed of the motor. The speed was adjusted manually (using a potentiometer) or from within the stimulation program running on the computer. In the latter mode it is possible to control the motor current during each pedal cycle. This microprocessor based PWM allows the cyclist to choose if he wants motor contribution and how much energy the motor should contribute. A variable resistive load is applied to the motor to load the subject. The PWM resistive braking may be controlled manually or from the computer. It is possible to have the motor assist the pedalling during part of the cycle, and retard it during another part of the same cycle.

Gföhler, Loicht, and Lugner 1998 [38]

The tricycle was equipped with an auxiliary motor integrated in the frontwheel. The motor, a hub motor with nominal power of 500 W, is also used as a brake with electrical feedback into the accumulators. The power supply of the motor consists of two lead accumulators, which are mounted on the lower part of the inclination system. In addition to the motor brake, the tricycle has two mechanical drum brakes integrated in the rear wheel hubs.

1.1.3 Measurement of Pedal Forces

A further factor in the low efficiency of paraplegic cycling is the timing and coordination of muscle actions required to produce external forces [101]. The stimulated muscle recruitment patterns during cycling are crude compared to those inherent in voluntary exercise, involving only a few muscle groups and simplistic control of these muscles. If the muscle recruitment patterns are not ideal, it is probable that relatively larger muscle forces will be required to produce a given amount of external work at the pedal. Larger muscle forces would generate higher metabolic costs from both aerobic and anaerobic muscle groups, which may at least explain the lower mechanical efficiency in paraplegic cycling [44][101].
In order to investigate the instantaneous forces produced by paraplegic subjects pedalling via FES-induced muscle contractions, to compare these forces to those generated by able-bodied subjects, and to reject the plane-produced forces to increase the muscle efficiency, force sensors were developed. In motor supported cycle devices the additional data can be used for the combination of the different power sources. The use of force sensors is also advantageous to detect muscle spasms and to switch off the stimulation immediately.
The earliest modern measurement of pedal loading is the work of [52](1968) who used strain gauges on the crank to monitor both the normal pedal force and the crank torque, instead of designing a pedal to measure both forces. [78] (1973) described their design, which relies on two linear potentiometers, to monitor movement of a pedal platform elastically connected to the pedal spindle. Both [49] (1976) and [129] (1979) offer designs using strain gauges. Although implemented differently, both designs are similar in concept, utilizing a double cantilever beam (i.e. two perpendicular beams joined at the center) as the elastic element.
In reviewing the calibration procedures used by [78] (1973), [49] (1976) and [129]

(1979) no information is given regarding cross-sensitivity to out of plane loads. Implicit in a procedure omitting cross-sensitivity measurement is the assumption that either the out of plane loads are insignificant or the dynamometer design offers electrical decoupling from out of plane loads. The measurement of the complete pedal loading by [25] has shown that out of plane loads may be significant while experience by the author has shown that electrical decoupling by element orientation, gauge placement and interconnection, is not especially effective where out of plane loads are concerned. Because the cross sensitive errors are not documented, the accuracy of the driving pedal force measurements previously reported by [49][78] and [129] cannot be firmly assessed.
[82] developed a pedal dynamometer, which measures the driving forces with high accuracy.
In that sensor-device the force components F_x and F_y were electrically decoupled. This was offered by a strain ring in conjunction with a mechanical decoupling to out of plane loads which enables measured loads to be directly indicated to an absolute error of $\pm 5\,\mathrm{N}$. In addition to electrical decoupling, the strain ring geometry enables a stiffness sufficient for high natural frequency, and the necessary overload capability.

1.2 Control Techniques

The musculoskeletal system of a SCI patient and its interaction with the ergometer form a nonlinear and highly coupled complex dynamical system. This makes simulation a necessary adjunct to the experimental investigation of how best to reconfigure or design the stimulation-powered ergometry system [122]. To optimize the utility of existing stimulation-induced leg cycle ergometers and improve the design of future systems, or for the closed loop control of those systems, the knowledge of 1) the muscle force being generated in response to the electrical stimulation, 2) how these muscle forces interact with the skeletal-ergometer linkage to power the crank, and 3) the metabolic energy costs of producing the crank power, is very essential [122].
All the work done so far in earlier research will be outlined in the next Subsection. Results achieved in closed loop controller design will be discussed in the respective Subsection. Subsection Results also treats all the progress in SCI-cycling up to date, particularly in regards to optimal muscle-force conversion depending on pedal frequency and PO, and maximum cycle time.

1.2.1 Dynamic Models

The skeletal ergometer linkage is usually simplified in a 4 or 5 bar linkage system. In case of a 4 bar linkage the ankle joint is fixed, using an orthosis which is attached to the pedal. The resulting system is of one degree of freedom. To model the dynamics of a normal cycle system a 5 bar linkage is required, which results in 2 degrees of freedom in the sagittal plane.

Chen and Yu

The simplest model published [19] uses the simplified 4 bar linkage mechanical system. Nevertheless the design involves the complex interaction between stimulated muscle system and the ergometer system. Due to its complexity a PID controller for FES-induced free swing movement of the lower leg, suggested by [134], was adopted in the FES-cycle control scheme. The aim of previous free-swing control study was to stimulate paralysed lower limbs to maintain a maximum reference angle. Although the mechanisms of free-swing and FES-cycling are quite different, there exist several similarities between these two systems. First, both systems can be modelled as a single input and single output system. In free-swing research, the input is a single channel stimulation strength of quadriceps and the output is the maximum swing of knee angle. Hence, in FES-cycling system, the input is the gain of stimulation pattern and the output is the cycling speed measured. Second the adaptation of both control systems is based on measurements in previous cycling, i.e. the maximal knee angle for the free-swing system and the desired cycling speed for the FES-cycle system. Third fatigue and nonlinear characteristics of the stimulated muscle are the common problems for both systems.

The free-swing movement of the lower leg was modeled as a nonlinear equation

$$M = I\ddot{\Phi} + D\dot{\phi} + K_1 sin\phi + K_2(\phi) \tag{1.1}$$

where M is the generated torque, I is the moment of inertia of the lower leg, and D is a fixed damping coefficient. It is assumed that the nonlinear parts, $K_1 sin\phi$ and K_2 can be combined to a term K. The model is linearized around the equilibrium state of $\phi = \dot{\phi} = 0$ and the equation of motion can be rewritten as

$$M = I\ddot{\Phi} + D\dot{\phi} + K. \tag{1.2}$$

Martin, Millikin, Cobb, Fadden and Coggan

[73] developed a mathematical bicycle model based on physical equations. The model requires a complex, third order, polynomial equation, which predicts power during road cycling. It includes terms for the power required to overcome aerodynamic drag, rolling resistance, wheelbearing friction, the rate of change of potential and kinetic energy, and friction in the drive chain.

It was found that when cycling power was held constant, wind velocity, road grade, rolling resistance, and drag each affected cycling velocity in a quite nearly linear manner ($R^2 > .99$) over the range of values evaluated. These findings allow a simplified understanding of the effects of those parameters. For instance, the findings that wind affects cycling velocity by about two-thirds of the wind velocity, and that road gradient affects cycling velocity by about 11 % for every 1 % change in road gradient, will allow simplified but realistic expectations of how environmental conditions should affect performance.

The model represents a highly accurate image of energy conversion on a tricycle including several environmental parameters. The power prediction could be used for research in cycle projects, where the focus is on the power transmission, such as motor-muscle combination strategies. It doesn't contain any information about masses or energy conversion in human muscles and its interaction with the bicycle geometry and power permutation in overall velocity.

Schutte, Rodgers, Zajac, and Glaser

In [122] a mathematical model based on a four-bar linkage is presented. All joints are assumed to be pin joints except the knee. It was thus modeled using a 3 degree-of-freedom planar joint (i.e. the relative movement between the segments is described by two translations and one rotation), with the two translational degrees of freedom constrained to follow a path specified by the rotational degree of freedom [138]. The knee thus retains a single degree of freedom and the total number of degrees of freedom in the linkage remains one. It was found that the complex knee model has a minimal effect on the kinematics of the linkage.

The dynamics of the one degree of freedom skeletal-ergometer linkage system was thus described by:

$$m(q_{cr})\ddot{q}_{cr} = B(q_{cr})F_t + r_g r_{fly} f_b + f_I + v(q_{cr}, \dot{q}_{cr}) + g(q_{cr}) \tag{1.3}$$

where q_{cr} is the rotation angle of the crank. $m(q_{cr})$, $v(q_{cr}, \dot{q_{cr}})$, and $g(q_{cr})$ are all scalar quantities, $v(q_{cr}, \dot{q_{cr}})$ consist of all velocity ($\dot{q}_{cr}$) terms, and $g(q_{cr})$ contains all gravity terms. $B(q_{cr})$ is a row vector that depends on the moment arms of the muscles and the geometry of the linkage system. Additionally r_g is the gear ratio of the coupling between the crank and the flywheel, r_{fly} the radius of the flywheel and f_b the total braking friction applied to the flywheel.
It was found that simulations, without the inclusion of a presentation of the additional linkage brace that constraints movement, suggest that the brace does not alter the motion in the plane substantially.
The model developed included also terms of 'Activation and Contraction Dynamics of the Muscles', and 'Musculoskeletal Geometry'. Thus the model can be used to investigate different seat positions as well.

Redfield and Hull, Hull and George

[57] and [114] described models based on a closed loop 5 bar linkage to explore the relation between joint moments and pedalling rate. Joint moments were computed by using dynamometer pedal force data and potentiometer crank and pedal position data. The equations were solved by a computer to produce moments at the ankle, knee and hip joints in both cases. The influence of different seat positions, body masses and sizes can be investigated. In the model developed from [114] the kinematic position information was found using vector addition techniques. Both groups separated the equations in static and dynamic fragments to get more detailed information (see Section Results).

Riener

The latest and most accurate model developed is the one from Riener [116]. In this study the model is divided into an activation, contraction and segmental dynamics part. Figure 1.3 shows the SIMULINK flow chart of the general model. Input to the model are the trajectories of the modulated pulse widths and pulse frequencies as obtained from the stimulator. Output is the computed knee joint position as it results from stimulating different muscle groups or, for example, from a passive pendulum test [116].

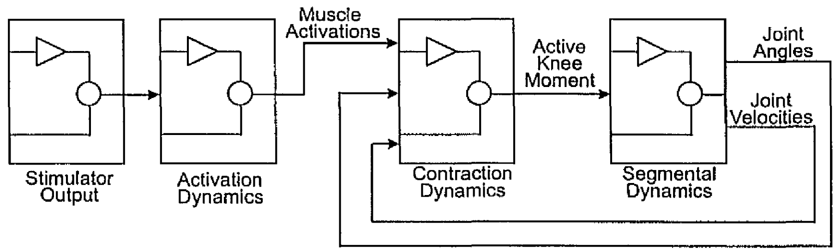

Figure 1.3: Simulink Flow Chart Model by Riener.

1.2.2 Controller Design

PID by Chen, Shih, Huang, Yu, Ju and Huseh

In [19] a PID controller was developed to maintain a desired cycling speed for a trained paraplegic subject. The controller adjusted the gain of stimulation intensity for each cycling period such that the real time control of cycling speed is feasible. The cycle speed (pedal frequency) was fed back to a computer to compare it with the desired cycling speed. The error is processed by the controller. The closed loop FES cycle system became thus a system with a single input - the gain of stimulation intensity, and single output - the cycling speed. The controller output was connected with the channel for each stimulated muscle group. The intermittent stimulation was provided with an overlaid stimulation pattern.
The model derived does not include any geometrical parameters of the tricycle -such as the seat position- nor any information about different sizes and weights of the cyclists' lower limbs.

Fuzzy Control by Yu, Huang, Ann and Chang

In [18] a model free fuzzy logic controller was employed. Using Fuzzy Control avoids exact modeling of the plant to be controlled, which is advantageous especially in case of the complicated musculoskeletal/ergometer system.
The fuzzy control system theory was developed based on fuzzy logic and the fuzzy set developed by Zadeh to describe complicated systems which are difficult to analyze by traditional mathematics [139].
The gain of normalized stimulation intensity was adjusted on the basis of a feedback control algorithm for each cycling period, thereby making real time control feasible.

As described above the measured pedal frequency is fed back to the computer to compare it to the desired cycle speed and the error is processed to the computer. The basic Fuzzy Logic Controller (FLC) comprises four principal procedures: fuzzification interface, decision making, defuzzification and rule table.
For the fuzzification process a subjective evaluation that transforms the measurements (E and ΔE) into linguistic variables had to be done. The process error, E, and the change in error, ΔE, obtained by subtracting the last sampled cycling speed from the present one, were two inputs for the FLC. The input ranges for E and ΔE, [-20,20] $rpm/cycle$ and [-30/30] in $rpm/cycle^2$, were first normalized by scaling factors to [-1/1] range in the defined fuzzy set. A total of seven fuzzy sets were defined by triangular membership functions. Second a set of rules was defined which operates on the fuzzy sets of the error and error change and yields the fuzzy sets for control action. Since a constant cycling speed is desired in the FES cycling control, a set of standard fuzzy control rules, i.e. a seven by seven rule table based on the step response of a second order system, was adopted in this study.
Third the defuzzification step maps the inferred action of decision making to a non-fuzzy control action. Among various defuzzification strategies, the center of area method was employed, due to its better performance in steady state response and its simplicity in implementation.
The distribution of membership function for the fuzzy sets is another possible factor affecting the FLC performance. The symmetric membership function is used for the general physical system, implying the same amount of positive and negative corrections. For FES cycling however, if the cycling speeds drops below a threshold, angular momentum would be insufficient to keep the cycling continuing. To avoid the large correction, the reduction of output gain is a straightforward method. However, lowering the output gain would reduce both positive and negative corrections, which could increase the steady state error. Thus the asymmetric membership function was chosen.

1.3 Cycling Results Up to Now

All the progress that has been made so far in terms of cycle time and loads, and closed loop control of paralysed individuals cycling will be presented in this Chapter. The information derived from the measurements of the force sensors will be discussed.

Cycle Time and Loads

All papers reviewed expressed improvements in cycle time and load. [19] described a 3 month cycle programme in which 9 individuals participated. It was found that all patients increased their time of cycling, while eight of the nine patients also increased their cycling load. The average increase in time was documented with 11.7 minutes while for load it was 30 newtons. The patient who did not increase the load remained without a load throughout the 3 month programme.
[55] described an investigation with ten persons with quadriplegia and eight with paraplegia. FES cycle training was performed 10 to 30 minutes per day, 2 or 3 days per week for 12 to 16 weeks. It was found a significant increase in PO occured during the initial four weeks of training. PO at week 2 was significantly less than at weeks 6, 8, 10, and 12 and training PO at week 4 was significantly less than at weeks 10 and 12. It was reported that there was no significant difference in PO between weeks 6, 8, 10, and 12. Upon completion of the training program, there was one subject still exercising at 0.0 W, two at 6.1 W, six at 12.2 W, four at 18.3 W, four at 24.5 W, and one at 30.6 W.

Closed Loop Control

The PID-control system developed in [19] was tested to maintain a cycling speed of 60 rpm for a subject in two different cases. In the first case, a designed interference of sudden increase in stimulation intensity is initiated. This artificial stimulation interference causes instantaneous increase in cycling speed, but goes back to original cycling speed within 20 cycles. This indicates that the controller adopted from a free-swing system can be applied to the FES cycling system [19]. The second case was for the adaptation of muscle fatigue in which the tested subject was first exercised to approximately muscle fatigue, before the beginning of FES cycling. It was shown that the closed-loop FES cycling system has an increasing trend of stimulation intensity in order to maintain the desired cycle speed.
The controller was able to overcome muscle fatigue, at least if the pedal frequency and power output was fixed at a constant value far below from the border of maximum PO.
In [18] the Fuzzy Controller was tested in four male subjects with paraplegia. First the FLC control strategy was utilized to achieve a speed of 35 rpm, the lowest cycling speed generally used in clinical setups, in which the effect of mechanical friction to

cycling smoothness is more evident [5]. Since the controllers aimed to control various cycling speeds, FLC controllers with symmetric and asymmetric membership functions were primarily compared with a PD-controller with the same configuration as FLC for tracking three different cycling speeds at a fixed load. For performance evaluation, a specific speed tracking pattern was designed which consisted of six continuous sections with 100 cycles each. The first section was assigned at 45 rpm as a warm up, which was designed to overcome the initial cycling friction and to accommodate the paralysed muscles to the electrical stimulation. The next 5 cycling sections were formed by an upward and then downward cycling speed pattern, in a sequence of 35, 45, 55, 45, and 35 rpm.

The results found indicate that all the controllers exhibit comparable results at a high cycling speed. FLC systems with symmetrical membership function, like conventional PD, can not adapt to slower cycling speeds and thus produce higher cycling variation [18]. By a simple change in the distribution of membership functions, the FLC with asymmetric membership function has an improved performance compared to the other controllers, particularly with a stable steady state response for various cycling speeds. Although longer transient time during downward change of speed can be observed in asymmetrical FLC, the controller characteristics can prevent the cycling from dropping below the threshold for continuous cycling during the initial transient state.

Compared to the conventional PD-controller, the results found demonstrated that FLC has the advantages of a flexible architecture and a simple algorithm, and no requirement of identifying system parameters a priori.

Forces Acting During Cycling

For the investigations made in [124] six spinal cord injured subjects (1 female, 5 male) with complete or nearly complete spinal lesions between vertebrae T_4 and T_{10} were recruited. Six able bodied individuals matched by weight and leg length were also recruited.

Muscle activation in paraplegic subjects was achieved through a relatively crude paradigm, in which muscle forces could be produced in only three muscle groups over very limited ranges of crank angles. In contrast voluntary cycling undertaken by the able bodied individuals revealed that effective muscle forces could be produced over the complete crank revolution. It was found that while able bodied subjects overcame external resistance by effecting small increments of force production throughout each crank revolution, the paraplegic group needed to produce much higher torques during the relatively shorter period that their muscles were stimulated. This effect must certainly contribute to the low efficiency and rapid muscle fatigue previously reported for FES induced cycling [44][101].

It was initially expected that the differences between the passive and the active curves at each workload might relate to the component of external forces and torques produced by muscle contractions, so that when there were no muscle forces the active forces and torques would be equal to passive values. This was not the case, because small changes in the kinematic parameters at different workloads resulted in concomitant alterations in the weight and inertial effects upon pedal forces. As ergometer resistance increased the subjects were required to push harder against the pedals and this changed the pedal orientation at each workload. Consequently the inertial forces acting upon the pedals varied with each workload rather than being exactly the same as the passive trial.

[57] and [114] analyzed the relation between joint moments and pedalling rate by measuring the pedal forces and calculating the resultant joint moments with a mathematical moment described in Section Dynamic Models. Using the model analysis both the kinematic and quasi static contribution to the total joint moment time history were examined. (Kinematic moments are moments to accelerate the leg segments only, whereas the quasi static moments result from pedal forces. By setting the pedal forces equal to zero, the kinematic joint moments could be examined. Similarly by setting acceleration terms to zero, quasi static moments were produced. Further details of this partitioning of the joint moments into kinematic and quasi static contributions can be found in [57]).

A constant PO of 98 W per leg was chosen. The cadence varied in a range which spans the typical pedalling speeds for the utility cyclist (63 rpm), the average tourer (80 rpm), and the long distance competitor (100 rpm) (see [136]). First of all it was found that, by increasing rpm the absolute average kinematic moments increase, whereas the average quasi static moments decrease. This result is of major significance for this analysis, because as rpm increases, the necessary pedal force to maintain constant average power decreases. This is seen in the definition of average power $\bar{P}$ as

$$\bar{P} = \frac{1}{2\pi} \int_0^{2\pi} R_D(\theta)\dot{\theta}\, d\theta \tag{1.4}$$

where R_D is the component of the pedal force driving the crank and $\dot{\theta}$ is the crank angular velocity. Also as cadence increases, link segment accelerations increase and thus kinematic joint moments increase to provide these accelerations. In conclusion the interaction between the quasi static and kinematic moments can be graphically outlined as in Figure 1.4a. At low rpm the pedal power must come from a higher torque and thus from higher quasi static joint moments. As cadence is increased, the required torque and thus quasi static joint moment decrease. In contrast at low cadence, kinematic moments are small, because link accelerations are small. As rpm increases, the kinematic joint moments, necessary for increased link accelerations, increase. Accordingly at either low rpm (≤ 80) or high rpm (≥ 120) the total joint moments are high. In the middle of this range, in this case about 105 rpm for both the knee and hip joints, the joint moment average is a minimum. At this rpm the rider achieves the minimum joint moment possible for this given power. Further interpretations of the results in Figure 1.4a can be seen in a semi-quantitative way in Figure 1.4b, where the moment due to power generation (quasi static) plots as hyperbolic because

$$power = torque * angular\, velocity \tag{1.5}$$

and thus

$$torque = power/angular\, velocity. \tag{1.6}$$

The moment due to the inertial terms (kinematic) plots as parabolic because accelerations are functions of the square of the angular velocity. Summing these effects produces an overall moment curve, which includes a minimum point.

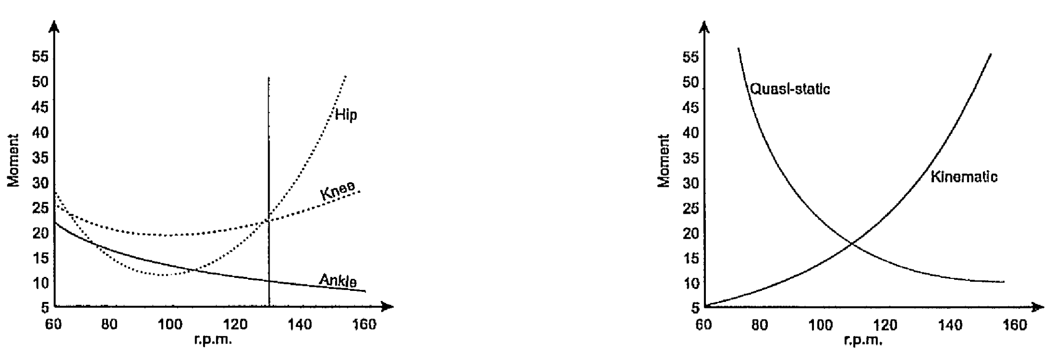

a: Absolute Joint Moments. b: Kinematic and Static Moments.

Figure 1.4: Forces Acting.

Considering how increasing the power demand affects the optimal cadence produces further results. Increased power demand shifts the hyperbole in Figure 1.4b to the right and thus shifts the minimum moment in the same direction. Hence higher power implies a higher optimal cadence.

1.4 Uncertainties in SCI FES-Cycling

Electrically stimulated muscles are weaker than voluntarily controlled muscles. The muscle groups recruited using FES are fewer and the stimulation patterns are crude in comparison with the natural pattern. The apparatus needed for the stimulation (sensors, cables, stimulator, control unit) makes the cycle device even heavier and reduces thus the effectiveness of those systems.
These and other problems in paraplegic and quadriplegic cycling will be discussed in this Section.

1.4.1 Muscle Weakness

Stimulation systems and electrodes can be grouped into external, percutaneous and implanted systems. In external systems control unit and stimulator are outside the body. Surface electrodes are used that are attached to the skin above the muscle or peripheral nerve, whereas in percutaneous systems wire electrodes pierce the skin near the motor point of the muscle. In implanted systems both stimulator and electrodes are inside the body. Different kinds of implanted electrodes are used. They can be inserted into muscle (e.g. on muscle surface: epimysial electrodes), nerve (epineural electrodes), fascicle (intrafascicular electrodes) or surround the nerve (nerve cuff electrodes) [115].
At present, the most common method of stimulation in clinical practice is to use surface electrodes. These have some advantages but also several disadvantages. For the re-strengthening of muscles, patient training and evaluation of the patients abilities, surface electrodes appear to be a practical solution. The main advantage is certainly that no surgical intervention is necessary. On the other hand, the stimulation is rather diffuse. It is not possible to obtain satisfactory stimulation selectivity because of the relatively large surface electrodes. High amplitudes of stimuli are necessary because of the resistance of the skin and the subcutaneous tissue. The electrical stimulation can effect skin burns. When the electrode remains on the same position and the

muscles are constantly stimulated, the skin and the subcutaneous tissue can be seriously damaged. Another disadvantage of surface electrodes is the need to position the electrodes, which is sometimes inconvenient and time consuming. Last but not least, the unattractive appearence of surface electrodes can be detrimental to acceptance by the patient [60][115].
The main advantages of implanted electrodes are the low stimulation currents or voltages required for activation and a better selectivity of stimulation. The implanted electrodes must be made from material which has no side effects. The stimulus signals as well as the energy can be remotely transferred e.g. by radio.

An action potential evoked by FES and propagating to the muscle, is indistinguishable from a physiologically triggered action potential. However there are fundamental differences between FES and the natural physiology of nerve activation. Compared to the physiological recruitment order, recruitment with FES is inverted. When low muscle forces are desired and thus low intensity, the same motor units remain activated, which defeats the goal of spatial summation. In addition to these recruitment problems, most current neuroprostheses trigger the action potential in the recruited motor neurons of the respective nerve simultaneously. This is opposed to the central nervous system (CNS) which triggers action potentials asynchronously. Therefore in artificial activation the stimulation frequency must be above the range of 12-16 Hz to achieve a relatively smooth tetanus. All these differences compared to the natural way of nerve activation cause early fatigue of the muscles. Additional factors which decrease the fatigue resistance of paralysed muscles are atrophy and changes in fibre type composition [60] [115].

Protocol

Before any of the cycle attempts described were started, the individuals had to participate in a FES Protocol to re-strengthen the atrophied muscles. Almost all protocols described consisted of 3 phases, primarily described by Newington. Phase 1 usually consisted of quadriceps muscle strengthening. Stimulation was applied to provide 45 ° of active knee extension followed by passive knee flexion. Treatment initially started with gravity as the only resistance. After the patient completed 45 extension/flexion sequences in two consecutive sessions without external weight, 0.5 lb of weight were applied until 45 sequences could be accomplished, again in two consecutive sessions. This was repeated until the patient could lift 3 to 5 lbs.

Phase 2 consisted of pedal progression. FES was applied to the quadriceps, gluteals, and hamstrings sequentially, to achieve a rhythmical pedalling motion on the ergometer/cycle device. Initially patients pedalled against a 0-kilopound (kp) resistive load 5 min or as long as the patients could tolerate (30 min maximum). In each succeeding session, the time increased until the patient was able to pedal for 30 min continuously in two consecutive training sessions.
In phase 3 resistance was added to the cycling motion. The ergometer unit was programmed to add from zero to $\frac{7}{8}$ kp of resistance, depending on the fitness of the patient. Typically patients reached maximum resistance levels of only $\frac{4}{8}$ to $\frac{5}{8}$ kp. If the cycle rate fell below 35 rpm, the unit automatically shut off because the resistance level was too high for the patient to overcome. When this occured, either the patient resumed cycling at a lower level of resistance, or a therapist would assist the patient by hand pedalling the unit, so that the patient would be able to continue the exercise. [5] measured variables for six months during phase 3 to obtain an average. All patients continued the FES resistance phase after measurements were obtained. Stretching exercises were added to the Newington protocol to lessen the increased muscle spasticity that some of the patients were having. Fifteen to twenty minutes before the electrodes were applied, a therapist helped each patient do a series of stretching exercises for the hamstrings', quadriceps', and gluteals' muscles.
The protocol described in [28] differed from the Newington protocol. Here the subjects were equipped with the electrodes and seated on the ergometer/cycle device. They were allowed to rest for about 5 minutes after that. During the rest blood pressure and heart rate were determined. After rest, subjects started their 30 min exercise. If fatigue occurred, up to three bouts were permitted (bouts separated by 5 min rest periods) to complete the session. All the subjects initiated their training at the 0-W PO for the first three sessions. When they were capable of completing 30 minutes of continuous exercise at a given PO for three consecutive sessions, the load was increased by 6.1 W (0.125 kp braking force at 50 rpm) for the next session. This protocol was repeated during the 12-week / 36-session training period.

To enhance performance of spinal cord injured subjects in cycling further [42] developed a system, which increased the current applied to the muscle from 140 mA to 300 mA. The shank muscles were added to the quadriceps, gluteals, and hamstrings as well. A current controller enabled the amplification of the FES current to each muscle from the maximum limit of about 140 mA (monophasic) to 300 mA (biphasic

pulses). A separate front panel control permits setting of current limit for each muscle before and during exercise bouts.
The system didn't fulfill the expectations. It was found that the lack of greater PO was probably due to the fatiguing effects of longer contraction duty cycle with wider firing angle ranges. Otherwise the metabolic and cardiopulmonary peak responses were greater with the incorporated modifications. This effect was explained with the recruitment of additional muscle fibers.

Electrodes

Traditionally only a single pair of electrodes is applied above active skeletal muscle in electrical stimulation experiments or in the clinical setting. However studies [93][110] have shown that sequential activation of motor units can result in smooth contractions of muscle within normal physiological frequencies of activation. In contrast the high frequencies necessary to tetanize the muscles by a single pair of electrodes can result in rapid fatigue. This fatigue is due to the depletion of acetylcholine at the neuromuscular junction [14]. The contractions obtained are also very smooth [100]. Using sequential stimulation, a central electrode is placed diagonally across each muscle. The centre electrode is the reference electrode and the two outside electrodes are active electrodes. Stimulation is applied first to the active electrode and then, 180° out of phase, to the other electrode. A complete description of the advantages and disadvantages is given elsewhere [30][86].
One major problem of surface electrodes is the poor contact with the skin. In cycling, where the subjects slide up and down in the seat with every crank rotation, the probability that the electrodes come off, or at least have a poor contact, is rather high. [95] used a custom manufactured garment instead of the placement of 18 electrodes. The garment was manufactered by Trend Corp. to allow conductive cloth patches with gel pockets to be used to stimulate muscle. Therefore, using the garment, only one plug on the top of the garment is needed for the computer. A complete description of the garment is given in [47]. [108] described a method to find out the optimal electrode placement.

Fatigue

The presence of fatigue during prolonged FES causes a substantial decrease in the force output of the quadriceps muscle [68]. The metabolic parameters recorded by magnetic resonance spectroscopy (MRS) revealed a variation of these parameters parallel to that of the force output [69]. Specifically the decrease in intra-cellular pH was highly correlated with the decay found in the force output. Therefore the intracellular pH level was designated to represent fatigue within the active contractile element. Intracellular acidification is not solely responsible for the contractile change during fatigue and additional factors [10][69] may have to be taken in account for future modeling. A model based on intracellular acidification is described in [69].

[91] described a fatiguemeter which was placed on a tricycle in order to quantify fatigue of the stimulated subject. It consisted of a high impedance operational amplifier and a capacitor. The capacitor on the high impedance operational amplifier is set to charge from the throttle control (see Section Motor Supported Devices). The throttle control output is thus integrated to provide a rough indication for the subject of the degree of muscle fatigue. If the throttle is left in High for short periods of time or Low for long periods of time, the total accumulative output is shown to the subject on a panel meter. The gain adjustment on the output of the operational amplifier was used to calibrate the panel meter for each individual subject with precision settings to get a rough idea of how fatigued the muscle was becoming.

A more accurate and sophisticated method to measure fatigue is described in [20]. EMG response, also called compound muscle action potential (CMAP) or M-wave, as direct measurement of muscle force as fatigue index was used. In contrast to the stochastic properties of EMG obtained from ordered-recruitment of motor units in able bodied subjects, the CMAP measures the muscle activity of simultaneous contraction of stimulated muscle. Measurement of the Peak-To-Peak (PTP) amplitude of the stimulus-evoked EMG has been found to be a reliable muscle fatigue indicator for effective characterization of the FES-elicited force output in continuous static stimulation [48][77]. In [20] it was found that the relationship between PTP amplitude and muscle fatigue observed in isometric contraction can be applied to dynamic movement, such as cycling.

1.4.2 Seat Position

All changes in seat configuration can be resolved into three independent components: the inclination of the seat back (Fig. 1.5a), the overall orientation of the ergometer and SCI subject with respect to gravity (Fig. 1.5b), and the distance from the hip centre to the crank centre (Fig. 1.5c). Only the latter (Fig. 1.5c) changes the four bar linkage.

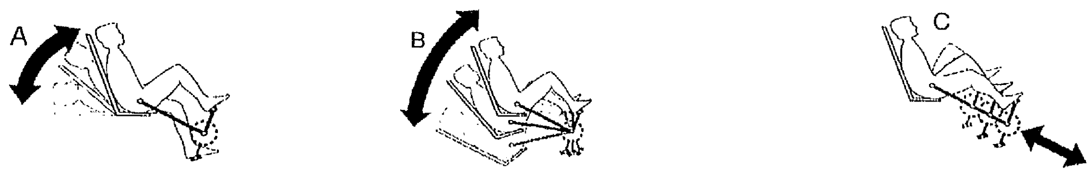

a: Recline Angle. **b: Overall Orientation.** **c: Variable Segment.**

Figure 1.5: Three Independent Components of Seat Configuration.

Orientation of the Ergometer and the Subject

When considered as an average over a complete crank cycle, the orientation of the ergometer with respect to gravity has minimal effect on the motion [122]. The net change in the potential energy of the linkage over one crank cycle is zero. Thus the net change in velocity due to gravity is also zero. Changes in the orientation of the ergometer with respect to gravity affect the instantaneous crank velocity however, and therefore can affect the muscle forces being generated. Nevertheless simulations showed that orientation does not significantly affect either the strength required to maintain constant cadance, or the metabolic energy utilized [122].

Seat-Back Angle

The ability of the muscles to power the crank was considered at seat angles between -15° and 90°. The probability that any given SCI patient can pedal is low in the configurations where the hip is most extended (i.e. the seat-back is most reclined (90°)). The probability is also low in configurations where the hip is most flexed (-15°). At seat-back angles around 30°, the probability is substantially higher (i.e. almost twice as likely as when the seat-back angle is 90°) [122].
Both the strength requirements and the energy demands to maintain pedalling appear to be minimized at seat back angles between 30° and 45°, and are higher in more

reclined and more upright configurations. However the metabolic energy utilized is relatively unchanged between 0 and 45 °, though the total strength required for the same range of seat configurations shows a 20 % variation.
It was found that the strength requirements appear to be more sensitive than the rate of metabolic energy utilization to changes in seat-back angle. At all seat-back angles, the rate of metabolic energy utilization varies by at most 18 %, even when the probability that a given SCI subject will be strong enough to pedal varies by about 100 % [122].

Horizontal Distance from Seat to Crank

Changing the horizontal distance from the seat to the crank from the standard configuration decreases the number of individuals expected to have sufficient strength to pedal. The hamstrings are less effective when the seat is moved farther from the crank. The quadriceps are less effective when the seat is moved closer to the crank. The strength required of the gluteals is relatively insensitive to the horizontal distance from the crank to the seat. It was found that even though the number of individuals capable of pedalling is maximized in the standard configuration, the standard configuration is the most effective horizontal distance from the seat to the crank for the quadriceps only.
The rate of metabolic energy utilization is also minimized in the standard configuration. In the most forward configuration however, the rate of metabolic energy utilization is 49 % higher. The rate of metabolic energy utilization is more sensitive to changes in the horizontal distance from the seat to the crank than to changes in the seat-back angle [122].

1.4.3 Stimulation Pattern

A major factor in the low efficiency of paralysed cycling is the timing and coordination of muscle actions required to produce external forces [101]. The stimulated muscle recruitment patterns during FES-cycling are crude compared to those inherent in voluntary exercise, involving only a few muscle groups and simplistic control of these muscles. If muscle recruitment patterns are not ideal, then it is probable that relatively larger muscle forces would be required to produce a given amount of external work at the pedal. Larger muscle forces would generate higher metabolic costs from both aerobic and anaerobic energy sources, and this may explain the lower mechanical efficiency and higher blood lactate levels observed during FES-exercise [91].

Generally the control of stimulated muscle can be achieved by adjusting the stimulation patterns and its intensities. The adjustment of stimulation patterns is to provide a sequence of stimuli for the coordinated activation of both legs. The change of stimulation intensity would overcome muscle fatigue and effectively achieve the training goal. For a closed loop FES-cycling system, the adjustment of both simulation pattern and intensity for each cycling angle could be technically difficult [18][19][108].

Since muscle stimulation has a time delay of about 1/10th to 4/10th of a second, the stimulation pattern is also a function of the desired pedal frequency, except the pedal frequency is fixed to a constant value [100].

The thresholds of the muscles are further variables. This is because various muscles have different sensitivities to electrical stimulation due to differences in their physiology, as well as varying thicknesses of the adipose tissue layer separating the electrodes from the muscle [100].

One possibility to find a stimulation pattern is electromyographyc (EMG), where surface electrodes are used to measure muscle activity. In [108] only 'a poor correlation' was found between the experimental stimulation sequence (EMG) and the stimulation sequence finally chosen. It was also mentioned that the transposition of EMG patterns to FNS may not give the best motion.

Although [56] showed that the pattern of muscle action potentials of three subjects during exercise on a stationary bicycle was consistent, research should be done in the area of individualisation and simplification of the identification of the stimulation pattern, because no two people are alike [122].

1.5 Effects after FES-Cycling

Physiologic adaptations to exercise training may be categorised as peripheral and central in nature [28]. Peripheral adaptations include local (i.e. within the muscle) histochemical changes such as hypertrophy of muscle fibres, increased concentration of oxidative enzymes and mitochondria, increased storage of fuel substrated and high energy compounds, and greater capillary density [29][87][88]. These result in enhanced muscle strength and endurance capabilities.

Central adaptations result in improved functional capacity of the Cardio Respiratory (CR) system. Such adaptations support higher levels of muscle performance by enhancing the capability to deliver blood, O_2 and fuel to the exercising muscles [53][106][107]. Therefore a desirable outcome of aerobic exercise training is to induce both central and peripheral adaptations to enhance the ability to pickup, deliver and consume O_2. Typically, improved muscle performance capability and CR fitness would be manifested by lower levels of CR responses at rest and during submaximal exercise tasks.

This section will present all peripheral and central effects of SCI-cycling published so far. The focus will be also on skeletal and physiologic body responses.

1.5.1 Cardiopulmonary

Because FES- cycling is peripherally induced by electrodes directly over the paralysed muscles, it essentially bypasses control by the central nervous system. In addition, most SCI results in the interruption of some autonomic sympathetic outflow, which is required for appropriate CR responses to exercise. Thus, automatic sympathetic stimulation of the CR system may not occur to the same extent during FES- cycling by SCI patients as for able-bodied individuals during voluntary exercise [22][50][51]. Common causes of morbidity and mortality in persons with SCI include cardiopulmonary disorders [67][135]. A mostly upright sitting position in a wheelchair results in changes of the cardiopulmonary system. Inactivity of the paralysed lower limbs appears to increase the risk factors involved, since there is less muscle mass available for exercise training. Furthermore, the inactivity of the skeletal muscle pump can lead to venous return, imperfect cardiac output, peripheral edema, thrombosis, pulmonary embolism, blood pressure regulation problems, and breathing complications [40].

In [62] it was found that SCI cycling exercise elicits relatively high magnitudes of aerobic metabolic and cardiopulmonary responses, as well as positive central and peripheral responses. [102] found that all three pulmonary parameters (Forced Vital Capacity (FVC), Forced Inspiratory Capacity (FIC), and the Forced Expiratory Volume at 1 second (FEV1)) were increased post training at a statistically significant level. It was also found, that the resting heart rate was increased, where this trend is in the opposite direction than the training effect observed in normal individuals. The explanation for this is not certain, but has been discussed in some detail by [24]. Exercise heart rate, although increased from resting levels, remained low, and muscle fatigue was always the reason for discontinuing the sessions described in [128]. This suggests a peripheral (muscular) rather than central (cardiorespiratory) training effect. The lack of a central effect was reported by [13][111]. It may indicate either a poor cardiac response due to decreased sympathetic effects or a low intensity of work performed by weak muscles [111]. It has been reported that when there is complete transection on the spinal cord above T1, the sympathetic influence on the heart is disrupted and the heart will not exceed 100/110 bpm [34]. [104] found no increase in heart rate during leg exercise in individuals with complete lesion while the largest response was in the subject with the most incomplete injury. In a similar manner an increase in blood pressure was not found in complete paraplegics but was obvious in incomplete paraplegics and tetraplegics. This effect was also true for arterial blood gases. Other investigators, reporting similar findings [50][98], have concluded that the level and completeness of the injury are the important factors determing how normally a subject responds to exercise. [90] reported that FES induced exercise caused a huge load on the heart of quadriplegics (blood pressure increased 60 %), whereas the heart rate was quite variable and depended on the level of injury.

Studies on relatively untrained individuals with SCI indicate that FES cycling can attract several physiologic adaptations that probably reflect both skeletal muscle and cardiopulmonary benefits [62]. Generally, after 6 weeks to 6 months of FES-cycle training, there were significant performance gains in which endurance increased from a few minutes to 30 minutes per session and PO capability increased by 6 to 30 W. Correspondingly, there were significant increases in peak $\dot{V}_{O_2}$ (Oxygen Consumption), heart rate, stroke volume, cardiac output, and pulmonary ventilation [62].

Thus, the progressive increase in aerobic exercise capability with the initial training experience can enhance the capability for subsequent cardiopulmonary training efforts.

1.5.2 Metabolic

Thrombosis and subsequent Pulmonary Embolism, which often occur during the acute phase after SCI, may be due to several factors like venous stasis for instance [62]. Although several mechanical (e.g. elastic stockings) and pharmacolog (e.g. heparin) prophylactic techniques are usually applied, thrombosis risk remains, and the existing techniques all have drawbacks.
A study by [63] showed that FES-induced contractions may reduce coagulation risk by enhancing venous blood flow in the legs. [75] demonstrated that the incidence of thrombosis could be reduced after SCI when FES - induced contractions were applied along with low-dose heparin, compared with low-dose heparin alone or a placebo. Hence, use of rythmic FES-induced contractions may reduce the risk of thrombosis and of circulatory disorders, especially during the acute rehabilitation phase. A report by [132] indicated that several weeks of FES-induced cycling exercise effectively reduced amoung other things, swelling and discomfort in one individual with quadriplegia. FES-induced pulses appeared strengthened, which suggested that lower limb circulation had improved.
[71] described that persons with SCI, especially those with quadriplegia, are of higher risk for infections. Respiratory system infections may be largely due to the reduced ability to cough, and urinary tract infections may be largely due to neurogenic dysfunction. [71][80] mentioned that it is conceivable that an attenuated function of the immune system adds to this susceptibility. [80] expressed the possibility that FES-induced cycling could improve immune responses and reduce the risk of infections. In eight individuals with tetraplegia, he found a significant increase in the number and natural killer cells, and this increase lasted for at least 30 minutes following sessions of cycle exercise. Although there is some evidence that FES-induced exercise training can improve immune system function, there is currently no evidence that this effect will translate into reduced incidence of infection in this population [62]. Promising data were shown by [89], who reported a 50 % reduction in the incidence of kidney and bladder infections in those participating in a 2-year FES exercise program. Furthermore, [45] found that the incidence of some infection problems in 19 individuals with SCI became markedly reduced (11 versus 2) while these individuals participated in a program for an average of 4.8 years.

1.5.3 Skeletal

Osteoporosis and with it an increased risk for fractures are a common problem in SCI [35][113]. The greatest bone loss occurs in the 2-year-post-SCI period, followed by a markedly reduced rate of bone loss [17][36]. Since increased muscular activity and bone loading appear to be important in retarding or possibly reversing the progression of osteoporosis, FES-induced exercise may help to damp this problem.

[9] found that there was no significant difference in specified bones after a 42 week training program. Nevertheless, there was a trend toward increased bone density in one case. The study did not indicate a statistically significant increase in the upper leg bone density for chronic SCI patients after an exercise training program of up to approximately 1 year.

Previous results of FES on osteoporosis in chronic SCI individuals support these findings. In the study by [85], the results implied that FES had no impact on osteoporosis. With immobilisation the, usually loaded with the body mass, bone seems to be more susceptible to osteoporosis than others [76]. This was confirmed by [15], where it was found that although all of the involved areas become osteoporotic, the amount of increased porosity appears to be site-specific. [9] had 12 men who were 5-15 years post SCI participating in a training program consisting of FES- cycling exercise sessions in a total of 68 sessions on average. Bone density before and after the training period did not significantly change in the investigated bones. The lack of increase in bone density in these studies may be related to the short duration of the training programs, insufficient exercise intensity, or the possibility that with increased time after SCI, osteoporosis may not be markedly reversible. The data however, may also suggest that the FES exercise retarded the osteoporosis progression [62].

Studies by [119] showed that bone density loss after FES-cyle training of subjects whose time since SCI varied was lower than the expected loss, suggesting a potential osteoporosis-retarding effect. Moreover, results from [79] and [127] suggest that, in patients with more recent SCI, bone loss may be reduced and osteoporosis progression retarded using FES-exercise. This was confirmed by [59] who showed that the rate of bone density loss in patients with acute SCI who had undergone FES-cycle training was lower than that in a control group.

Thus, the available data suggest that FES-induced cycling may be helpful in retarding osteoposis progression, especially in the acute phase of SCI, when bone loss is rapid [62].

1.5.4 Psychological Effects

Psychological benefits resulting from FES-cycle training have been reported. [126] surveyed 47 individuals with SCI who participated in an FES-cycle home training program and reported that approximately 60 % of their subjects indicated improved self-image and assessed their appearance to be better following training. Likewise [2] found improved self-reliance, self confidence, and social fortification following training. [133] found markedly improved scores (i.e. less depression) on both a subjective depression scale and an observer scale.

19 participants of a training study involving FES-cycling by [111] indicated not only that they felt stronger, more energetic, and less fatigued, but also that they had an increased feeling of well-being.

These studies suggest that mood disorders, which are common in SCI may be improved with regular FES exercise training. However, those with unrealistic expectations for the FES exercise program may demonstrate adverse changes in mood [12].

1.5.5 Muscle Size

Many investigators have examined changes in specified muscle areas after a programme of stimulation induced cycling, either using common measure methods (measure leg diameters, circumferences e.g.), or quantitative computerized tomography (CT).

Using CT, [84] indicated that the muscle area of the upper leg was increased by 27 % after 10 weeks of FES-cycle training. Also, [137] showed that the rate in muscle loss in patients with acute SCI was reduced by 20 % after daily contractions of the quadriceps of one leg, when that leg was compared with the nonstimulated control leg. Similarly, FES-cycle training has been shown to support hypertrophy of the muscles employed, as indicated by increased thigh circumference [5][29][111]. In [128] both the quadriceps and the total muscle area of the upper leg were significantly increased after a 3 month training, regardless of the initial strength of the patient or the completeness of the injury. The hamstrings remained unchanged, which may be due to the lower stimulation levels used in order to prevent spasm, or to the nature of cycling, which requires more work from the quadriceps than the hamstrings [27].

[8] used dual-energy X-ray absortiometry (DEXA) to find that FES-induced cycle training during the first 6 months post injury could prevent gluteal muscle atrophy

seen in a nonexercising group. Thus, FES-cycle exercise appears to reverse the disuse atrophy of paralysed muscles or retard the rate of its progression [62]. Subjective comments by many of the participants indicate that the mass and appearance of their lower limbs greatly improved, which in part motivates them to be involved with this therapy [62].

1.5.6 Spasticity

Spasticity often leads to significant discomfort, muscle and joint contractures, severe functional impairments, and disruption of daily life activities, all of which can limit rehabilitation outcome [62]. Pharmacologic methods are often employed in an attempt to control spasticity. However, they may not be completely effective and may produce side effects [130].

One technique to alleviate spasticity use cyclic stimulation of the opposite muscle group to block motor neuron activity to the spastic muscle groups [117]. Based on these data it seems that FES can be useful in some individuals for short-term reduction of spasticity, and it has been suggested that such techniques may be especially useful just before exercises or sleeping [123].

Studies investigating effects of long term FES-induced exercise have shown more equivocal results. A study by [46], in which six individuals with incomplete SCI underwent 9 to 12 months of FES-induced quadriceps muscle training, showed that in four of the six subjects, quadriceps muscle spasticity was reduced; one subject showed opposite results. In contrast [118] detected a trend toward increased spasticity in persons with incomplete quadriplegia after 4 to 8 weeks of FES induced pulsed contractions. [125] surveyed 19 individuals with SCI who performed FES-cycle training at home. Although 6 subjects reported a decrease in spasticity, nine could not detect a change, and four noted an increase in spasticity. Subjects in a training study by [5] indicated that although the periods of spasticity had become less frequent, they were often more intense, probably because of the increased muscle strength [62].

Chapter 2

The Tricycle and the Modifications

Paraplegic cycling via Functional Electrical Stimulation requires not only an appropriate cycle device, but also some modifications in terms of sensor feedback to the computer. This Chapter will give a technical description of the device used, the mechanical and electrical modifications made, and the place and the type of sensor chosen for this project. The stimulator and the data acquisition card are also described.

2.1 General Description

The main goal of the project is the development of a cycle device for the use of paralysed subjects, which combines the demands for low cost, safety, high effectiveness of the stimulated muscles, high individuality through the adjustability of important details, and optimal in terms of transfer from the wheelchair to the device.
A commercially available tricycle was chosen. Figure 2.1 shows the tricycle ordered.

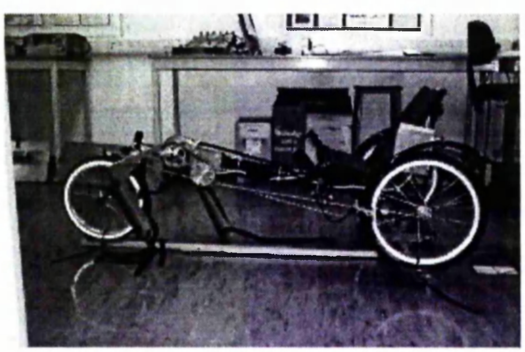

a: Tricycle.

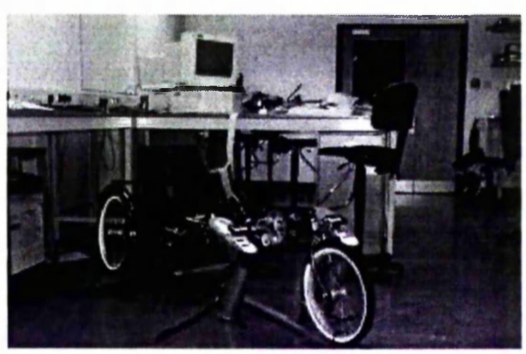

b: Experimental Setup.

Figure 2.1: Experiment.

The wheel in the front is steered, whereas one of the rear wheels is driven. Only one rear wheel is driven via a chain to avoid a differential, which would result in a higher weight of the whole setup. The device is equipped with a 9 gear chain shift on the rear transaxle. The brake affects the rear wheels. The tricycle was chosen not only for its low costs and its light weight, but also for its design, which allows paralysed individuals a safe and easy transfer from the wheelchair, since the steering can be turned down (see Figure 2.2 a).
The adaptation of the tricycle to different body sizes is achieved by a tube in tube bracket system of the main frame. The tricycle guarantees high stability due to its three wheels. This specific tricycle also offers foot protection in the case of a frontal crash with an obstacle, since the crank and therewith the feet are placed behind the front wheel. All technical data of the parts ordered for the mechanical modifications made are listed in Appendix A.

2.2 Mechanical Modifications

The first and most important modification to be made in paraplegic cycling is the certain fixation of the foot to the pedal, and also the conduct of the legs in the sagittal plane. Many possibilities developed in former projects were presented in Chapter 1. High foot orthoses which cover the calves and keep the ankle fixed at 90 degrees were chosen for this project. The orthoses are made from steel and therefore easy to attach to the pedals. Because of their stiffness they also keep the legs in the cycle plane. Picture 2.2b shows the orthoses ordered. The supplier can be found in Appendix A.

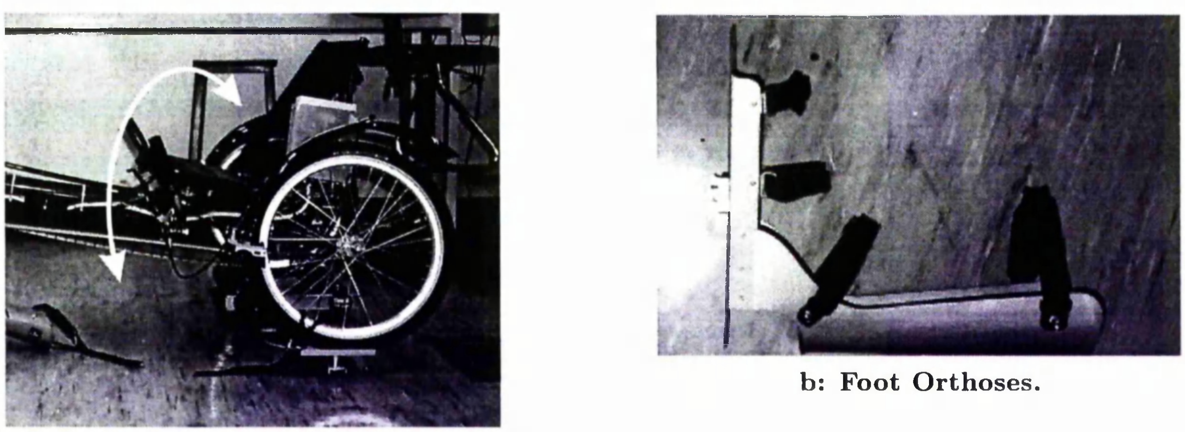

a: Steering Adjustability.

b: Foot Orthoses.

Figure 2.2: Details.

For the fixation of the orthoses to the pedals, a freely adjustable adapter was invented. The adapter guarentees a certain fortification, and also allows a very simple assimilation of the orthoses to each individual cycling. As can be seen in Figure 2.3 the orthoses are rotatable in the x-y plane, movable in x- direction, and also pivoted in the z-y plane. This might be very essential for future optimisation work.

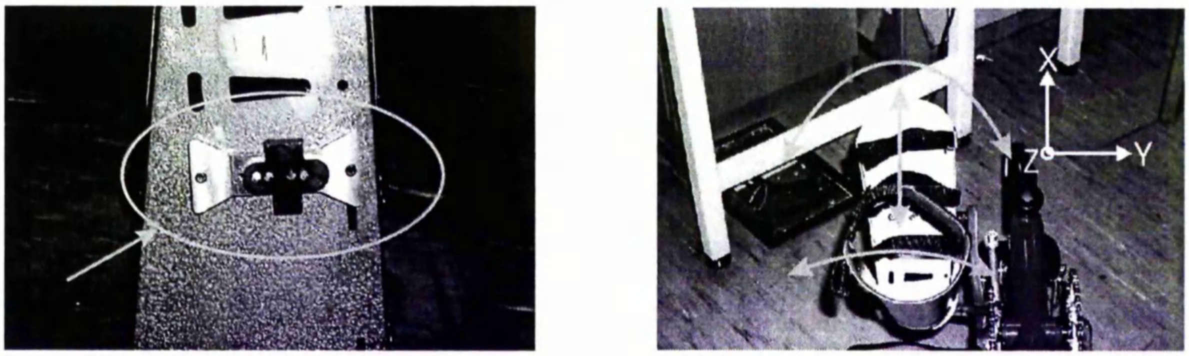

a: Adapter.   b: Adjustability.

Figure 2.3: Adapter and Adjustability of the Orthoses.

The adapter designed is also very easy to manufacture and of very low cost. Clamp compound pedals are used to attach and secure the orthoses via the adapter. On the other hand the orthoses are easy to detach with a single screw. In this case the pedals can be turned, and the setup can be used by healthy individuals in the usual manner. Technical drawings of the adapter can be found in Appendix B. Supplier information about the pedals used are listed in Appendix A.
To protect the stimulator against vibration, a box, made of aluminium and lined with rubber gum, was designed, and placed on the frame reachable for each cyclist. Its technical drawing can be found in Appendix B. The box can be seen in Figure 2.4.
Sensor feedback is needed for the closed loop control system. The crank velocity, as

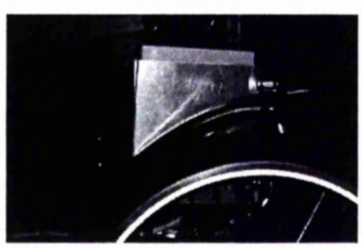

Figure 2.4: Stimulator Box.

described in [124], was chosen as the control parameter. A 10 bit optical shaft encoder is used, because of its low friction, high durability, and high accuracy.
As can be seen in Figure 2.5 a plate with brackets was designed to place the sensor close to the crank. The sensor is driven via a chain from the left crank. A left hand tandem crank with a 27 teeth chainwheel is used. Another chainwheel is mounted on the shaft encoder, using an adapter. Technical drawings of the plate and the adapter can be found in Appendix B. Supplier information for the tandem crank and the chainwheel are listed in Appendix A.

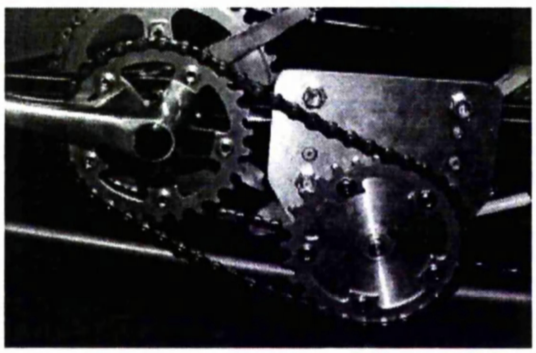

a: Chain to Drive the Sensor.

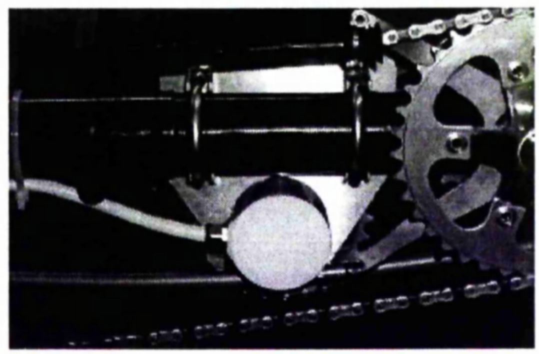

b: Sensor.

Figure 2.5: Crank Feedback.

Finally, a hometrainer had to be optimized for the static use of the tricycle for experimental work in the lab.

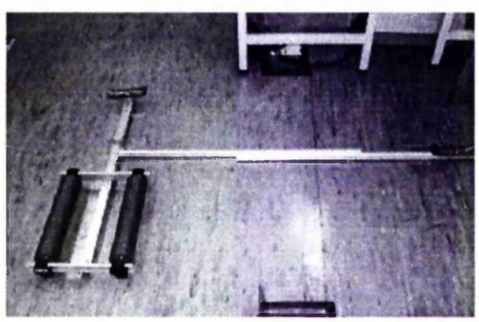

Figure 2.6: Modified Hometrainer.

The substructure is a commercially available trainer with two parallel rolls for the driven rear wheel on one side and a bracket on the other. The trainer is directly placed under the tansaxle of the tricycle, where one wheel is spinning on the rolls

and the other one is strapped to the frame. After initial tests the trainer showed instability, since it moved under the tricycle.
Figure 2.6 shows the modification made in order to achieve safe stability during exercise.

2.3 Electrical Modifications

As already mentioned in Section 2.2 feedback is needed for the design of a closed loop control system. In addition to the shaft encoder data other information have to be transmitted to a PC or controller as well.

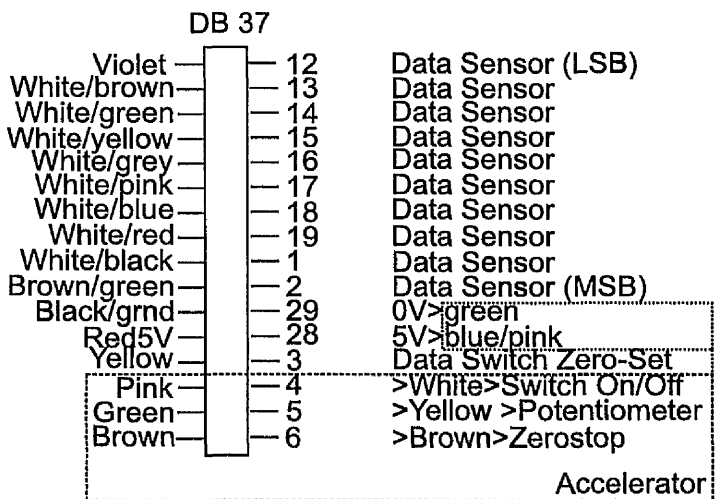

Figure 2.7: Wiring Plan of the Main Connector.

In open loop mode a throttle, based on a potentiometer, can be used to feed back desired reference conditions, such as torque or velocity, to the PC. The tricycle and its control is thus comparable to a motorbike, where the motor is being replaced by the stimulated muscles.
To indicate zero stimulation (throttle in zero position), a microswitch is part of the throttle. Next to the zero switch in the throttle an additional emergency stop switch is part of the tricycle as well.
The shaft encoder feeds back information on the crank position to the PC. The zero position on the encoder is fixed, so that the zero position of the cranks could only be roughly defined by the chain. For this reason an additional 'zero set' button is

installed on the tricycle, which is a further input channel in the evaluation software (see Chapter 3). The whole electric wiring diagram of the tricycle is presented in Figure 2.7. It shows the pins and the colours of the wires used in the main connector, which is placed directly behind the shaft encoder beneath the main tube.
The connection of the tricycle and the PC is solved via two conductors. One conductor is used to transfer the generated measure data (shaft encoder, throttle position, emergency stop, and zero set) of the tricycle to a PC. A DB 37 connector with an appropriate 37 pin wire is connected to the cable harness of the tricycle and to the parallel port of the PC.
The second conductor transmitts the calculated signal from the PC to the stimulator, which is fitted on the tricycle. In this case the connection is solved via the typical serial port connectors and a 5 pin wire.

2.4 The Stimulator

A portable stimulator was used for the experiments in this project. 5 integrated, rechargeable cells of 1.2 V and 1200 mAh each, provide the power supply of the stimulator.

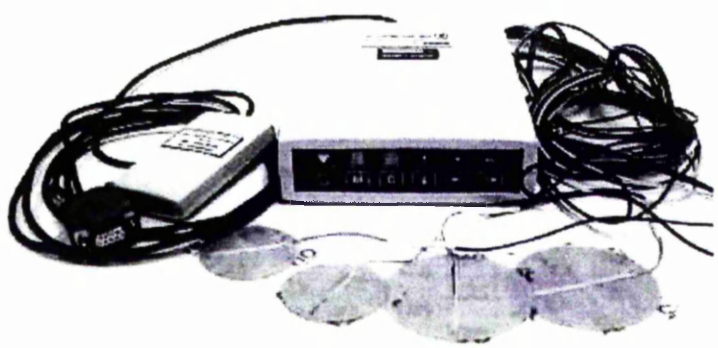

Figure 2.8: Stimulator, Wiring, and Electrodes.

Up to 8 output-channels of the stimulator can independently be controlled, the generated impulses are monophasic in their progression. A stimulation pattern can either

be programmed directly, or be transferred online from a PC using the serial acquisition port. An optical coupler galvanically isolates the stimulator from the PC.
Pulsewidth and current of the generated signals are possible control parameters for the stimulation intensity. The amplified voltage of the impulses is kept constant to 140 V. The pulsewidth can be chosen between 0 and 800 μs, the current is limited to a maximum value of 120 mA.
In this project the pulsewidth is the control parameter for the stimulation intensity. Its maximum output is limited to 500 μs. The current was set to 60 mA for each experiment. Figure 2.8 presents the stimulator used, including the wiring and electrodes.

2.5 AD 512 Data Acquisition Card

The AD 512 acquisition card consist of eight 12-bit analog channels, two 12-bit analog output channels, and 8 digital input-output channels respectively.
The maximum sampling rate is limited to 100 kHz. The A/D ranges as well as the voltage output are programmable. Analog input and output ranges can be chosen between ±10 V, ±5 V, 0-10 V, and 0-5 V. All digital in- and output lines are TTL compatible.
The maximum output current is limited to 10 mA, which was always enough to run the shaft encoder on the tricycle.

Chapter 3

Data Import and Pattern Generator

The development of an open loop controller for the cycle system is the content of this Chapter.

In Chapter 1 it was found that the quadriceps, hamstring and gluteal muscle groups are of highest interest in cycling. Exactly these muscle groups will be recruited in this project. Each of the mentioned muscles has a specific working range during one whole cycle. The variables to be defined are the stimulation start-stop angles for each muscle with respect to the angle velocity of the crank. The stimulation pattern results directly from these 12 parameters, and is probably of highest importance for the effectiveness of SCI FES cycling.

The control of all of the six (left and right) muscle groups with respect to their interaction seems to be a hard multiple input - single output (miso) control problem, where the stimulation amplitude for each muscle is the input, and the pedal frequency the system output.

For this project the complex interaction of the stimulated muscles is abstracted and only described by the stimulation pattern. A single input - single output (siso) system, with stimulation intensity as the input and pedal frequency as the output, is the result.

As described in Chapter 1 the system used for the ankle orthoses is of one degree of freedom. The crank position and angular velocity are the measured and calculated system parameters.

This Chapter treats the software to be written to calculate and to apply a stimulation pattern via the stimulator to the muscles. The first results achieved after initial experiments were done, will be described at the end of this Chapter.

3.1 Abstraction of the Cycle System

Figure 3.1 gives an impression of the cycle system to be developed. The shaft encoder delivers data of the crank angle to the pattern generator, where the stimulation pattern and the stimulation intensity are calculated. The calculated pattern is compiled in the export block and sent, via the serial port, to the stimulator, where the signal is converted to electrical impulses for each stimulated muscle.
In this stage the system runs in the open loop mode. Stimulation intensity is directly related to the input signal, which can be defined either via the throttle, or directly in the PC with an artificially designed input sequence.

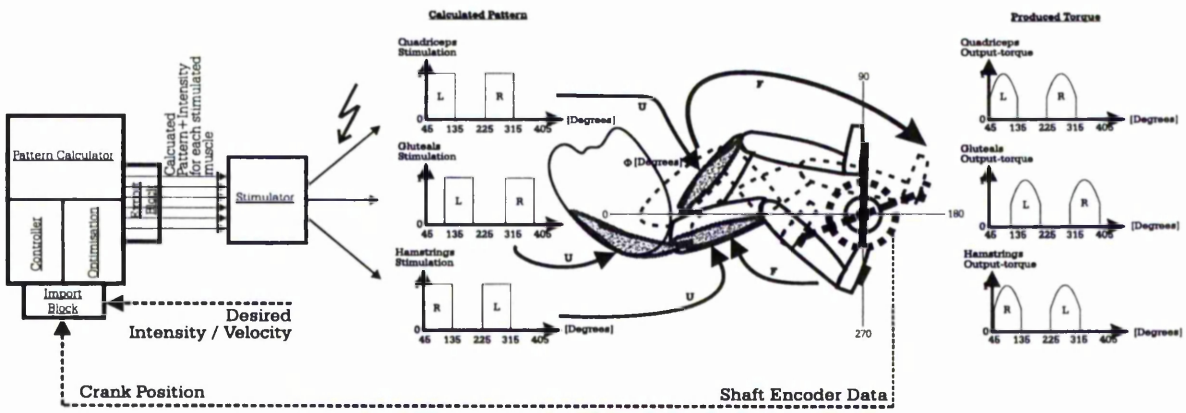

Figure 3.1: Cycle System (Muscle Stimulation and Contraction).

When the system operates controlled in closed loop mode the input signal changes from desired stimulation intensity to a desired pedal frequency. At this point a mathematical model of the system is required. A closed loop control will be described in Chapter 4.
The stimulation pattern is based on the fixed start-stop angles for the stimulation. These parameters are not only highly individual but also time varying. Chapter 5 describes one possibility of an online variation and optimisation routine for the stimulation pattern.
As can be seen in Figure 3.1 the position of the crank, next to the desired input information, is necessary input parameter for the pattern calculator. The pattern for each muscle is the pattern calculator output to the stimulator.
Summarizing the things said the pattern generator in its final version must include

the following parts: data import block, closed loop controller, optimisation routine, pattern calculator, and a connector, the export block to the stimulator.
Figure 3.2 presents the simulink function developed for FES cycling. Each of the parts mentioned above can be found in the model as well.

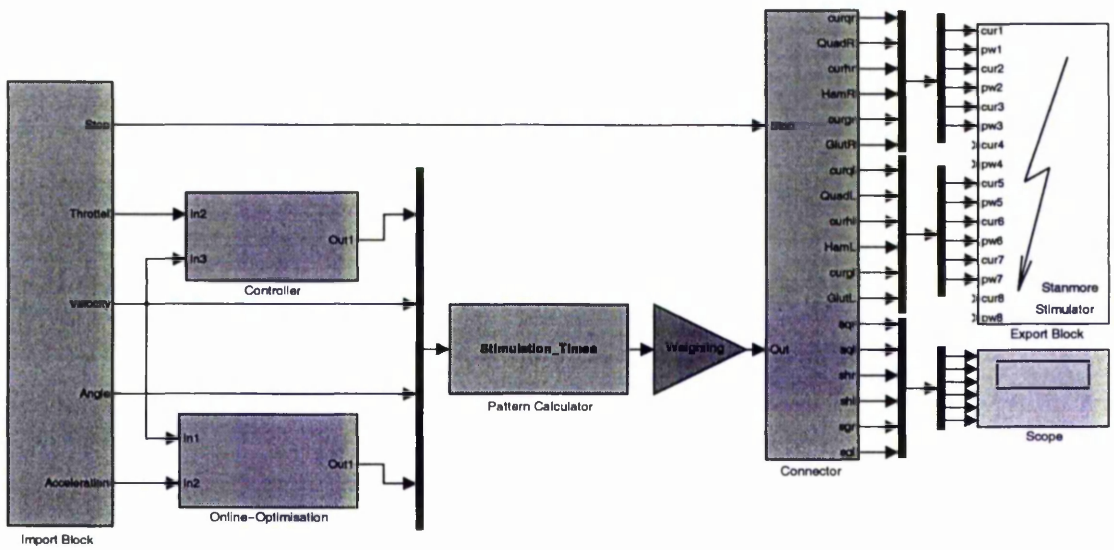

Figure 3.2: Pattern Generator.

3.2 The Pattern Generator

The Simulink Blockdiagram in Figure 3.2 presents the evaluation and calculation software of the FES-cycle system. The data Import Block on the left side, Controller and Optimization Blocks as the input to the Pattern Calculator. The Connector Block, which separates the pattern signals for each muscle is connected with the Export block, the communication block with the Stimulator.

3.2.1 The Import Block

The Import Block reads shaft encoder data from the data acquisition card and calculates a decimal value (Angle [deg]) from the binary signals. It also reads the information from the additional switches mounted on the tricycle, such as the 'Emergency Stop', 'Zero-Set', and 'Throttle'. In Figure 3.3 the main parts of the data evaluation can be seen, such as the Derivatives, the Angle Calculation, Zeroset Input and Memory, and the Reference Signal block.

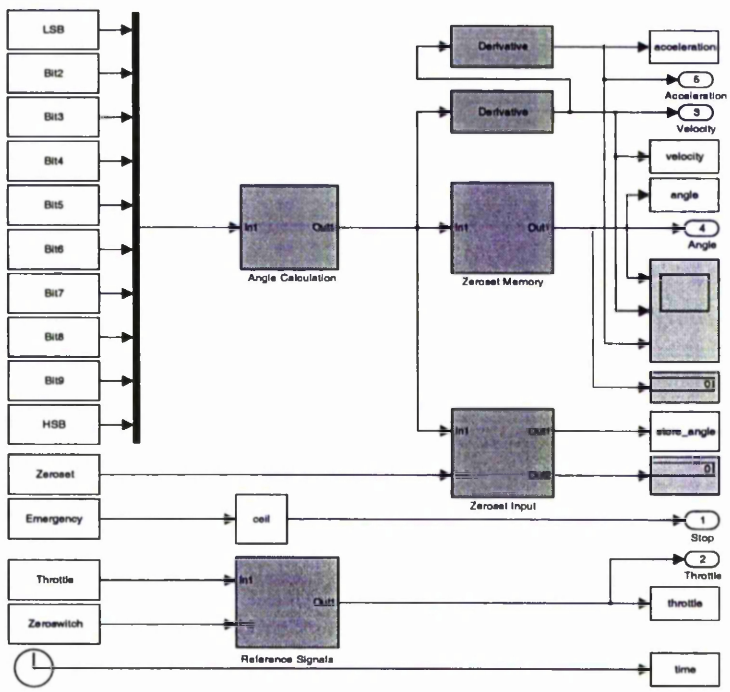

Figure 3.3: Import-Block

The import blocks for each channel can be found on the left side. Channels 1 to 10 (bit) are the binary information produced by the shaft encoder. The throttle input requires 2 channels, since the throttle is not only based on a potentiometer, but also on a zero-position switch. Furthermore an emergency-stop-channel and a zero-set-channel for the positioning of the pedal-zero are input information of 1 bit each.
All blocks on the right side in Figure 3.3 contain the export signals of the Import Block. Each signal is transferred to the workspace of matlab and can thus be stored for later evaluation. The input and output parameters of the Import Block are listed below.

Input parameters: shaft encoder, 10 channels; stop and zero set, 1 channel each; throttle, 2 channels.

Output parameters: crank angle, -velocity, -acceleration, emergency stop, reference signal, time.

Angle Calculation

Figure 3.4 shows the calculations to be done to transfer the 10 bit shaft encoder signals into a decimal value. Input (In 1) is the 10 bit vector of the shaft encoder

([LSB Bit1 Bit2 Bit3 Bit4 Bit5 Bit6 Bit7 Bit8 Bit9 HSB]).

All its values have to be rounded to 0 and 1 (because of measurement noise) in the ceil block. The resulting binary vector is multiplied with the Binarycode- vector *[1 2 4 8 16 32 64 128 256 512]* to calculate a decimal value.

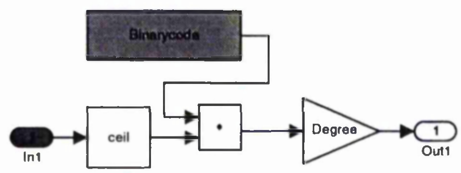

Figure 3.4: Angle Calculation.

The block Degree is a factor to transform the 1024 resolution into a 360 resolution of one turn in degrees.

Zeroset Input and Zeroset Memory

The zero position of the shaft encoder is mechanically fixed, but desired to be a free parameter to overcome the range of different body sizes for the adaptation of each cyclist to the tricycle (see Chapter 2). Figure 3.5 presents the uncovered blocks Zeroset Memory and Zeroset Input to solve this task.

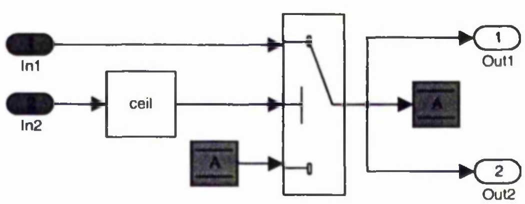

a: Zeroset Input.

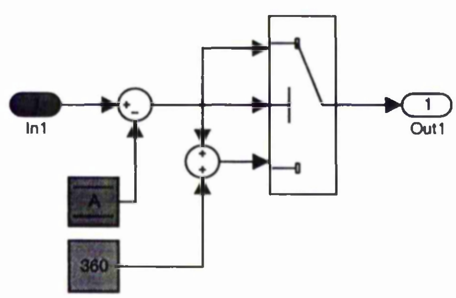

b: Zeroset Memory.

Figure 3.5: Zero Set Blocks Input and Memory.

The zeroset input (Figure 3.5a) consist of two block inputs and two outputs. Input 1

(In 1) is the crank position [deg] measured by the shaft encoder, and input 2 the zeroset switch input, rounded to the binary values [0 1]. The block Output is the current, non-corrected crank position, which can be seen either directly on the scope, or on the workspace, using the variable 'store-angle'.
The main parts of this block are the switch and the memory block A. The switch passes through input 1, when input 2 is greater than or equal to threshold, otherwise passes through input 3. The threshold was defined to 1, and zero is the standard input value of input 2, as long as the switch zeroset is not pressed. After running the programme, the memory A is initialized with zero. After pressing the zeroset button on the tricycle, memory A is overwritten with the current crank angle. Thus, memory A always contains the value for the correction calculation.
Figure 3.5b presents the correction calculations to be done. The value of memory A is subtracted from input 1 (not corrected crank position). The threshold in the switch is defined to zero, the corrected angle is, unless positive in its value, directly passed through input 1 to the output.
As long as the corrected angle is negative in its value (current angle < memory value), 360 is added, and the new value passed through input 3 to the output. Thus, the output value of the Zeroset Memory block is the corrected current crank position.

Reference Signals

Finally the desired reference signal (stimulation intensity for open loop control, pedal frequency for closed loop control) had to be transformed from a 0 to 5 V input signal from the throttle into a corresponding normalized signal in [0-100 %] (stimulation intensity or pedal frequency). Figure 3.6 presents the subsubsystem 'Throttle Calibration' of the 'Reference Signal' block.

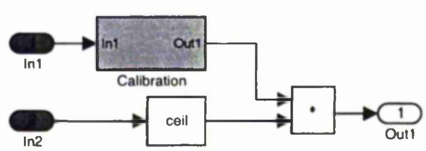

Figure 3.6: Throttle Calibration.

The two block inputs (throttle position and zero switch) are multiplied only after the throttle position input (0-5 V) was normalized in the range of 0 and 100 %, and

the zero switch input rounded, to guarantee zero output if the throttle rests in that position. Block output is a normalized signal in the range of 0 and 100 in [%].
To run the system with a designed input signal, not via throttle as the reference, another subsystem was created, which can be seen in Figure 3.7.

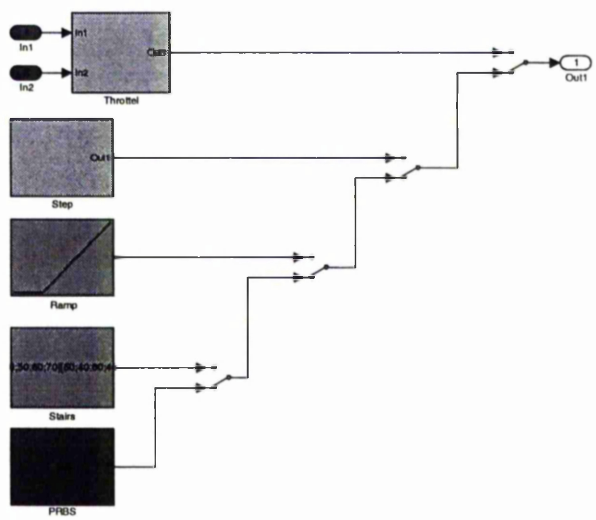

Figure 3.7: Reference Signals.

The manual switches in this block can be used to define the input (reference) signal. The tricycle can thus be controlled either directly, using the throttle, or by computer, with the outputs of a step, a ramp, or a staircase function. A PRBS input signal for the identification of the system for closed loop control (see Chapter 4) can also be chosen.

Derivatives

In addition to the information on the current angle, the speed and the acceleration of the crank are important data as well.
Since the speed is the first derivative of the angle, and the acceleration the second, a discrete derivative was written in Matlab. The S-function block 'Derivative' contains the code. The signal from the angle had to be low pass filtered, since the angle signal jumps from 360 to 0 deg after completing one cycle, which would result in peaks of the velocity and acceleration at these times. Both the derivative as well as the low pass filter of the S-function Derivatives can be found in Appendix C.

3.2.2 Controller and Optimization Blocks

Chapters 4 and 5 describe the Controller and the Optimization Block. Presently the FES-cycle system is open loop controlled and there is no online optimization. For this reason data are transferred directly through the controller and the optimization blocks and these systems have no influence on the data whatsoever. That means the input and output values of these blocks are equal.
The position of the blocks can be seen from Figure 3.2.

3.2.3 Pattern Calculator Block

Cycling is an intermittent process, where each muscle is stimulated only during a limited range of one cycle. The S-function block 'Stimulation Times' (see Figure 3.2) calculates, dependent on the crank position and the crank velocity, the output signal for each muscle. The amplitude of the output signal is the normalized reference output from the Import Block, like the throttle position, for instance.
The whole algorithm basically depends on the start and stop angles for each muscle defined in the Matlab script 'fescyclingstart' (see Appendix C).
The algorithm compares the actual angle with the defined angles and either feeds the reference signal directly through to the dependent muscle, or sets the output signal to zero. But due to the time delay, which occurs between muscle stimulation and muscle contraction, the crank velocity is a further input parameter in this algorithm.

3.2.4 Compensation of the Velocity

For the derivation of the velocity-compensation routine the force produced by each stimulated muscle is, due to the short period of activation in one cycle, assumed to be constant by neglecting nonlinearities and the influence of muscle fatigue. In this case the maximum torque produced in cycling is initially approximated by Figure 3.8, where the stimulation-force-delay of muscle activation is shorter than the time delay of relaxation [66]. However, when muscles are electrically stimulated fibres are recruited differently and all fibres are excited synchronously. As a result, the overall rates of activation and force development are slower. For example, the 10-90 % rise time in force in paralysed quadriceps muscles electrically stimulated at 50 Hz, ranges from 120-360 ms; relaxation times for the same muscles are between 90 and 180 ms [66]. When muscle is stimulated at 30 Hz, the rise time is expected to be longer [16].

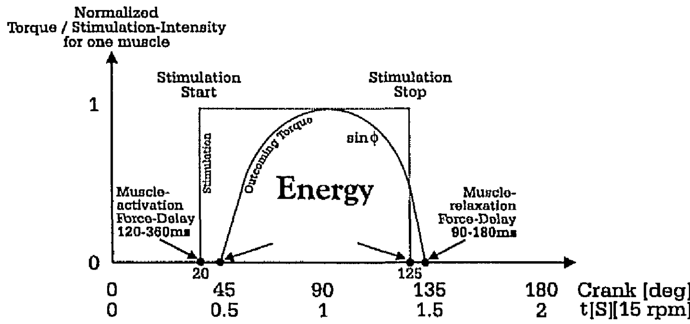

Figure 3.8: Muscle Stimulation and Contraction.

In [3] it was found that the optimal control for minimum time cycling is bang bang input. The dotted line in Figure 3.8 shows the progression of the stimulation and the equivalent stimulation times for a crank velocity of 15 rpm.
Basically two methods were used in former projects to find a general stimulation pattern. Either static force measurements were done to find the times where each muscle generates force which can be used effectively for cycling, or dynamic experiments were done with a constant velocity, using the technique of EMG (see Chapter 1). Both methods result in a stimulation pattern valid only in a small velocity range, since the time delay for the muscle stimulation is constant, and the angle, through which the pedal passes per sample time, changes with the velocity.

Example: A muscle stimulation delay of only 0.1 s is assumed although in [66] a delay up to 0.36 s was found. It is also assumed that the start-stop angles for stimulation were found in static experiments, meaning 0 rpm.
Using the angles found, the system is assumed to be operated by 90 rpm, where the pedal passes through an angle of about 54 deg per tenth of a second. The point of muscle contraction without compensation would be shifted forward to 54 deg of the crank, where probably the muscle effectiveness is reduced significantly.

The algorithm invented calculates the angle to be compensated, depending on the crank velocity. The algorithm was combined with the algorithm found for the intermittent stimulation pattern, and compensates the time delay between stimulation and contraction. The algorithm can be found in Appendix C. The evaluation of the individual contraction-delay will be discussed in Chapter 3.4.

3.2.5 Connector Block

As can be seen in Figure 3.9, the Connector Block works basically as a connection-box, where the outputs of the function 'Pattern Calculator' are connected with the 'Export Block', the compiler block for the stimulator.

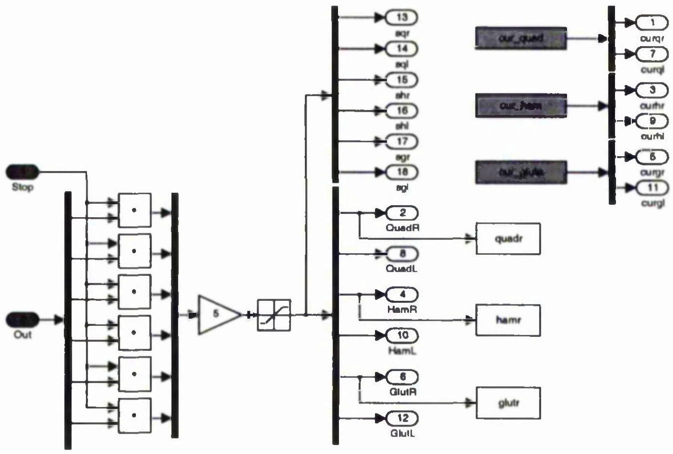

Figure 3.9: Connector Block.

The tricycle's emergency stop intervenes at this point, to exclude calculation errors in the function caused by emergencies.
The signals for each muscle are factored by five, to calculate the necessary pulsewidth [0-500 μs] from the signal intensity in [%]. The saturation block protects the stimulated subject from calculation errors, since it limits the maximum pulsewidth to 500 μs. As can be also seen in Figure 3.9, only the pulsewidth is used as a control parameter, although the current, which is fixed to a constant value of 60 mA for this application, could be controlled as well.
Output parameters of this function are the calculated pulsewidths for each muscle, as well as the constant currents for each muscle.

3.2.6 Export Block

The Export Block is a C-function, which compiles the calculated pulsewidths and currents for each muscle into a special format, to successively transfer the data via the serial port to the stimulator.

3.3 The Stimulation Pattern

As can be found in Chapter 1, basically 2 methods exist to find an individual stimulation pattern. Both of them are not only time consuming, but also highly expensive, since either force plates or an EMG-unit is needed.
Another approach, not only very fast and cheap, but also highly individual, was invented for this project.
The approach works as follows. One muscle of the lower limbs is stimulated with constant pulsewidth and current values. Then the leg is moved back and forward on the tricycle to find out the range where the muscle contraction produces a torque on the crank. The 'Start' and 'Stop' angles found for each muscle are written down in the 'fescyclingstart' Matlab-script, which can be found in Appendix C.
Another important influence in effective cycling is the position of the whole body, and especially the lower limbs on the cycle device. As described in Chapter 2 the developed tricycle offers a wide range of adjustability. The shaft encoder zero is a free parameter after its modification in the Pattern-Generator.

3.3.1 The Standardized Cyclist Position

All the experiments in this project were done with one healthy subject. To produce results, which are not only optimal for one special subject, but also comparable for test sessions on different days and different individuals, the important cycle parameters had to be normalized. Figure 3.10 shows the parameters of the highest influence.

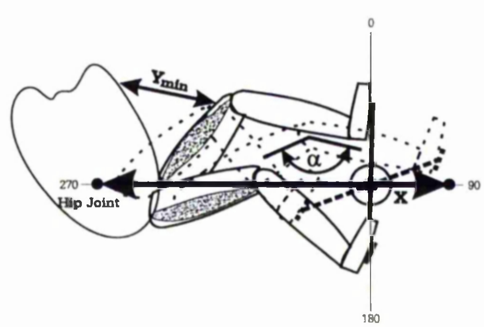

Figure 3.10: Parameters x, y_{min} and α.

The distance x was defined to be optimal if the knee never extended to 180 deg over a whole cycle. This must be guaranteed also for high pedal frequencies, when the upper body of the cyclist probably moves in a small range. The knee angle in its maximum extension was chosen to be about 160 deg. Another important parameter is the shaft encoder zero, because the whole stimulation pattern found is based on this position. The zero was set in a position of the right leg, where the distance between the knee and the upper body of the cyclist is a minimum y_{min}.

3.4 Initial Experiments

In Chapter 1 it was found that the quadriceps, hamstrings and gluteals are of highest effectiveness in cycling. For the investigations in this project precisely these muscle groups were stimulated. A 27 year old intact male subject, name it MR, was recruited for the experiments.
The initial experiments done to find a basic setup for one cyclist are divisible in two parts: a static part to find the start-stop angles for the stimulation of each muscle, and a dynamic part, where the pedal frequency changes in such a way that the parameter of the stimulation delay can be verified.

Static Experiments

The first part, described in Section 3.3 was done after the zeroset calibrations for the normalized distance x, y_{min} and angle α (Section 3.3.1) were found. The static-stimulation ranges for each muscle, presented in Figure 3.11 were established.

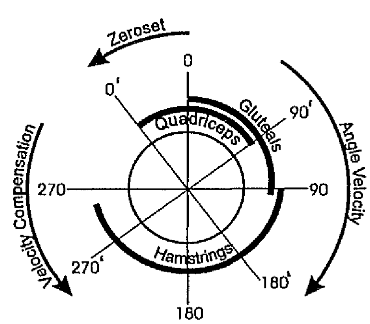

Figure 3.11: Static Stimulation Times, Zeroset Correction, and Velocity Compensation, Right Side

With the next step, a typical muscle-stimulation delay of 0.2 s was chosen. A step of low pedal frequencies was applied to the whole system. Figure 3.12 presents the results of this initial cycle test.

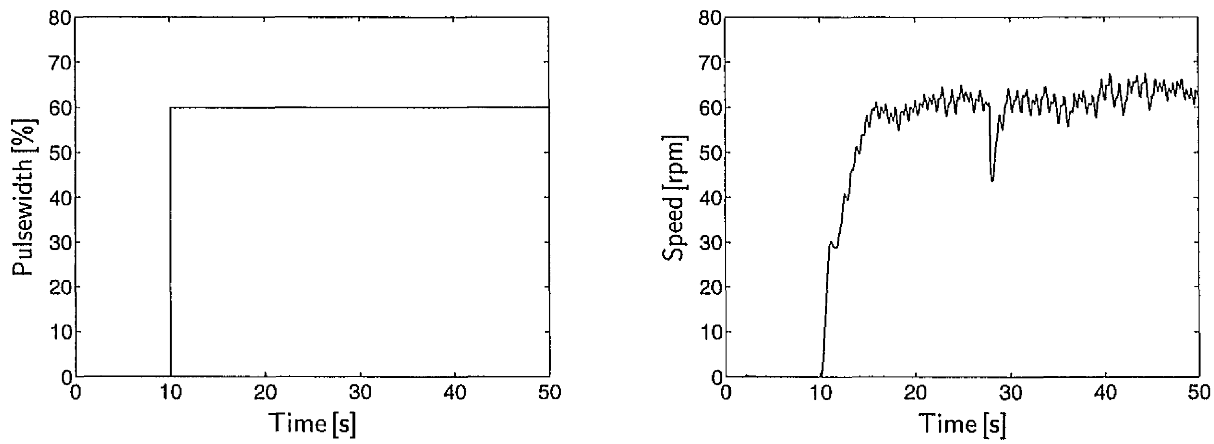

a: Step Input. **b: System Response.**

Figure 3.12: Step Response of the Tricycle (Velocity of the Crank).

As can be seen the velocity of the crank achieved is nearly constant, it oscillates with a small amplitude only, which is probably due to the acceleration and deceleration of the lower limbs during one whole cycle.

Dynamic Evaluation of the Time Delay

For the second part, in order to create a standard setup for one individual, the dynamic investigations for the determination of the muscle-stimulation delay have to be done.

For this reason a ramp input is applied. The function increases the stimulation (via the pulswidth) from 0 to the maximum, so that the whole stimulation range is covered. The parameter 'time delay' has to be changed in such a way that the crank velocity (system output) is also increased over the whole velocity range.

Figure 3.13 presents the system input and output, comparing a good approximation of the delay parameter with a setup without compensation. The Figure shows the major influence of this parameter in dynamic cycling.

At velocities over 100 rpm the system starts to oscillate. This effect is caused by the limited computation power and is not due to the stimulated subject. About 100 rpm is too fast for the evaluation software, whereas the subject still increased the pedal frequency.

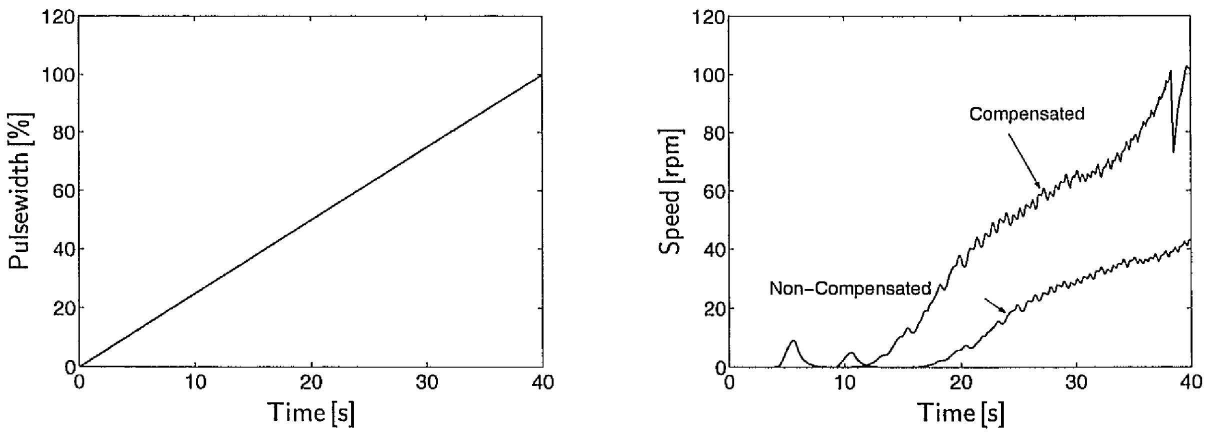

a: Ramp Input. **b: System Response.**

Figure 3.13: Responses with and without Velocity Compensation.

3.4.1 Results

After this initial test to adapt the hardware and software to the cyclist, some more complex tests were done.

For this reason a staircase function was applied to the system. Using this test the efficiency of the system in dynamic and static activity is reflected.

Figure 3.14 presents the input (pulsewidth [%]) and the system response (pedal frequency [rpm]).

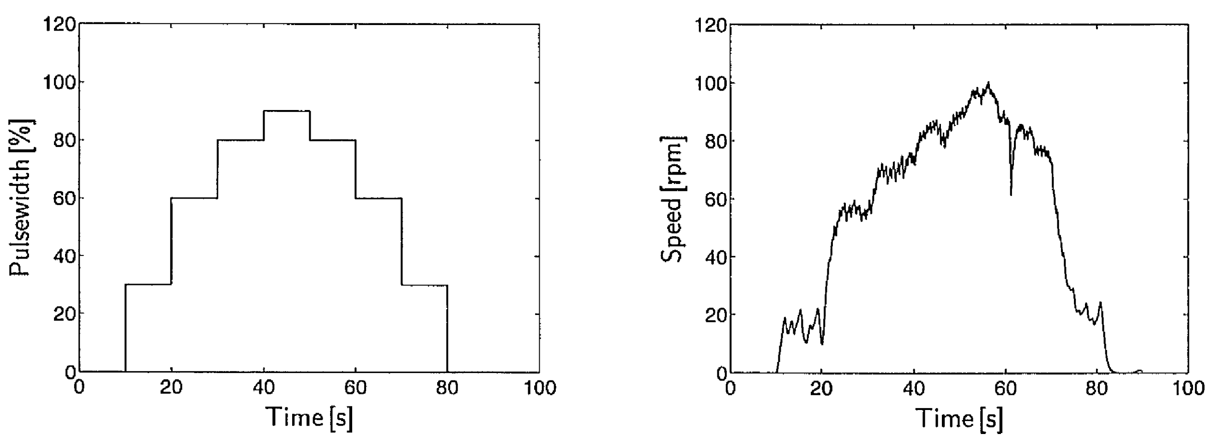

a: Stair Input. **b: System Response.**

Figure 3.14: Stair Response of the Tricycle.

As can be seen the crank velocity is increased with every step and static between steps, which confirms a good static and dynamic approximation of the corresponding parameters. This is true for the minimum speed as well as for the maximum. Muscle fatigue is not evident, which is probably due to the healthy and very sportive subject MR.

As also can be seen from Figure 3.14 the signal oscillates in every working point. This is probably due to the normal cycling dynamic which affects some areas of acceleration and some of deceleration during one cycle. FES cycling supports this effect further, since its stimulation pattern is hybrid between the on and off points of each muscle. On the other hand the system runs in open loop mode at this point. If a very fast controller with a good adaptation was used, a smoother signal with a decreased oscillation might be achieved.

Finally the different system dynamics in the modes of increasing (first half) and decreasing (second half) can be seen in Figure 3.14. One possible explanation for this effect could be that the muscle power increased after it warmed up in the first 40 s, and the required stimulation value for a specific velocity decreased.

Chapter 4

System Identification and Controller Design

The identification of the tricycle and the design of an RST-controller for the speed of the crankshaft is the content of this Chapter. For the system identification a physical model, based on differential equations, could be derived. But due to the many uncertainties and nonlinearities of the system, like individual muscle parameters and their time variance, an estimated model can be very helpful.
The coefficients of the transfer function can be estimated by the criterion of Least Squares, using the measurement of the system response. The Identification Toolbox of MatLab was chosen to estimate transfer functions of the system.

4.1 Step Responses

The first step to identify a system is to examine step responses. The sample time is deducible from the rise time of the step response. Starting from this point, the amplitude and the bandwidth of the PRB-Signal may be established for the later estimation of the transfer function. In case of the tricycle, the step response is not chosen as the range between zero and the maximum velocity output, but as the range of normal cycle speed, meaning the range 0 to 80 [rpm]. Figure 4.1 shows a PRBS response of the system within these limits.
As a first attempt, the sample time is chosen as T_S=100 ms. The rise time, defined as the time between 10 % and 90 % of steady state value, can be seen in Figure 4.1. As already mentioned, the response is not constant with time and is also nonlinear. The rise time varies in a range of 0.5 s and 1.5 s. The rise time probably depends on the

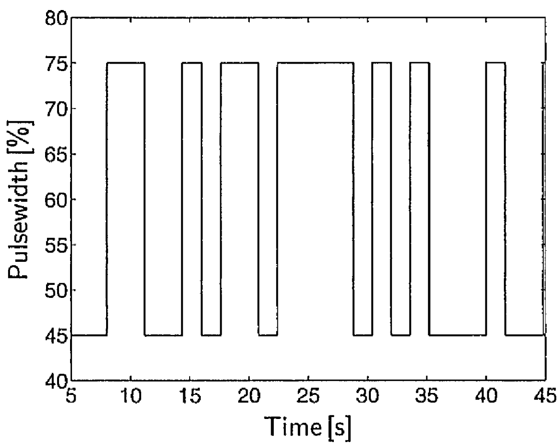

a: PRBS-Input.

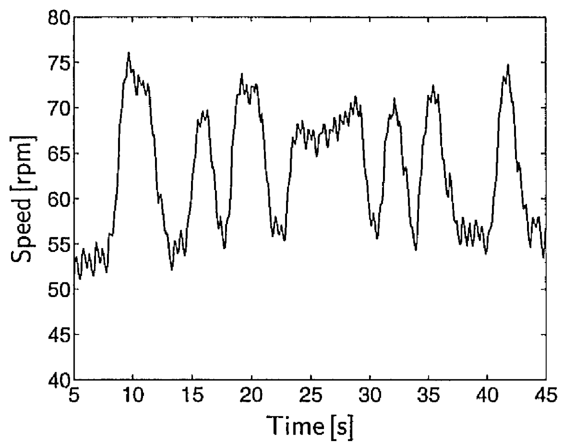

b: System Response.

Figure 4.1: PRBS-Response of the Tricycle (Velocity of the Crank).

crank -and leg- position. If the step occurs, for instance, in maximum power output crank positions, the rise time might be positively influenced. On the other hand, if the step occurs in one of the dead-angles where no muscle is stimulated and the system itself is driven forward only by its inertia, the rise time might be increased.

The Nyquist-Frequency limits the frequency range within control action is possible if the controller is to be realized in discrete time fashion, as in this case. For a sampling rate of 10 Hz which corresponds to a sample time of 100 ms, the Nyquist Frequency is $w_N = 31.4\, rad\, s^{-1}$. On the other hand the bandwidth of the system w_b is calculable by the approximation $w_b t_r \approx 2.2\ (\pm 0.15)$ [131]. The maximum bandwidth of the system can thus be estimated by choosing the fastest rise time of the system, which is about 0.7 s. With this estimation the bandwidth is $w_b \approx 3.14\, rad\, s^{-1}$. In this case the system is controllable over its whole frequency range.

Time delays of the system are also important to identify. Like the rise time, the time delay of the system is not constant, but varies in a range from 100 to 500 ms (see Figure 4.2). This effect is probably based on the same system attributes as the variability of the rise time.

This initial test displays the nonlinearity and time variance of the system very well. The controller design for systems like this is not trivial. Using an ordinary linear controller in this case could result in an unsatisfactuary performance, if the rise time is faster on the tricycle than predicted. On the other hand a controller, which is faster than the tricycle, could result in crude control signals and finally in instability.

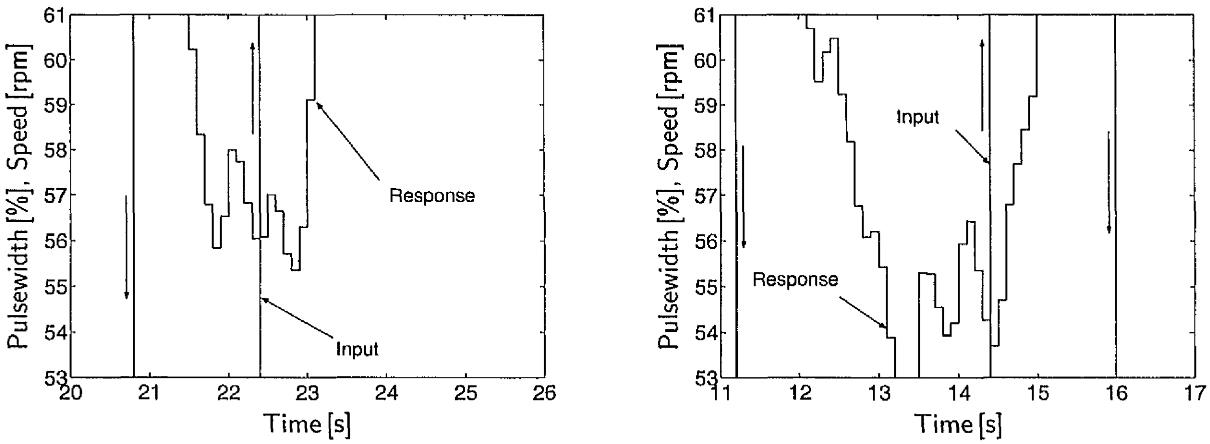

Figure 4.2: Step Time Delays.

As a first attempt a linear controller will be designed. Since the time delay can not be accurately specified, different controllers based on different models have to be designed and to be tested for each individual.

4.2 The PRB-Signal

A Pseudo Random Binary Signal (PRB-Signal) was calculated to identify the system. PRB-Signals are well suited for identification tasks because of their stochastic attributes which are comparable to white noise. PRB-Signals are deterministic and therefore repeatable.

The input range of the one used is normalized in the bounds of [0 100], which corresponds to the min-max range in percent of the stimulation intensity (pulsewidth). Since the plant was assumed to be highly nonlinear, the system should be identified at different input operating points [45 60 75]. The amplitude of the signal was chosen to be ± 15 to ensure that the difference between the lower and the upper bound is obvious in the systems response. The amplitude should be selected, on the other hand, to be as small as possible to identify only the local models.

The bandwidth of the PRB-Signal has to be within the bandwidth of the system which is to be identified. Furthermore, the PRB-Signal has to be periodic in the test interval so one part can be used as estimation data and the other as validation data. The PRB-Signal used for the identification of the system in operating point 60 is depicted in Figure 4.3a. The system response we measured is shown in Figure 4.3b.

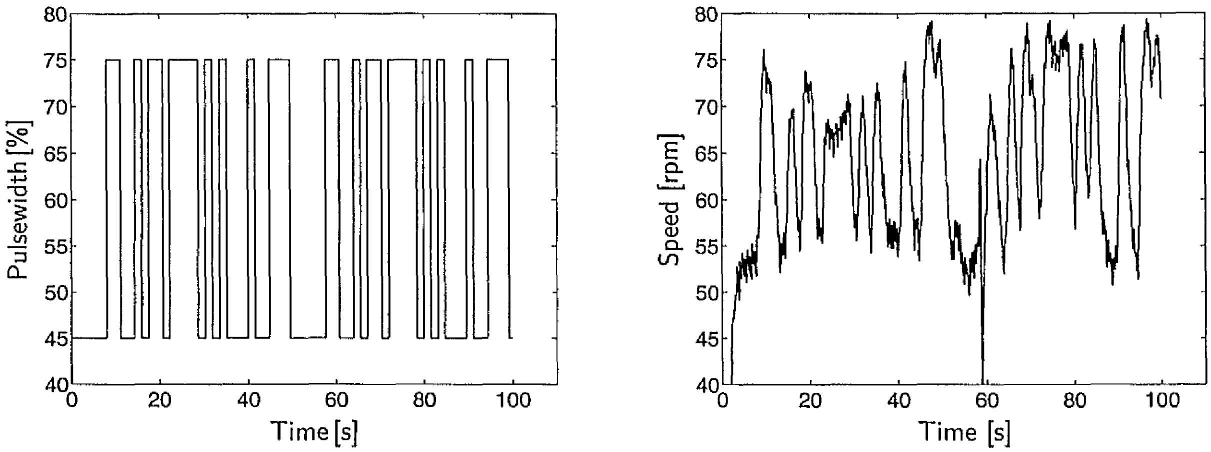

a: Input (Stimulation Intensity). **b: Output (Velocity).**

Figure 4.3: System Identification.

4.3 The ARX Model

A simple ARX-model can be estimated directly from the measured input-output plant data. The model is described by

$$y(k) = \frac{B(q^{-1})q^{-n_k}}{A(q^{-1})} u(k) \tag{4.1}$$

where the polynomials A an B are defined as [131]

$$A(q^{-1}) = 1 + a_1 q^{-1} + \ldots + a_{n_a} q^{-n_a} \tag{4.2}$$

$$B(q^{-1}) = b_0 + b_1 q^{-1} + \ldots + b_{n_b} q^{-n_b} \tag{4.3}$$

$y(k)$ is the output, $u(k)$ is the input and q^{-n_k} a time delay of n_k samples. A and B are polynomials in the unit delay operator q^{-1}. The coefficients of the polynomials are determined by the standard least squares method [70] using the input / output data in Figure 4.3.

4.4 Order Selection

In the literature survey it was found that stimulated human muscles feature a time delay between stimulation and muscle action. This delay depends for instance on the thickness of the skin and differs for each human - and each muscle - between 150 ms and 350 ms. This was confirmed with the initial cycle tests done in this project, where the optimum time delay, for the same cyclist and for the step response, was found at about 200 ms. It has to be admitted, that 6 muscle groups are stimulated during cycling, and that these 200 ms are probably the mean value of them all. This would explain the variation in the step responses even better, since rise time and time delay not only depend on the high or low power output crank positions (see Chapter 3), but also on the stimulated muscles.

Numerator and denominator order, as well as the number of sample times representing the delay of the system, are input parameters for the model estimation. The delay differs between 100 ms and 500 ms. A muscle delay of up to 360 ms is known from Chapter 3. This result in a model of 3 or 4 sample times delay. Considering the step responses, a very well damped model of first or second order is expected as well. The number of zeros can thus not be more than 1 in case of a causal system.

6 ARX models were estimated and compared by their mean square errors. The mean square error is defined by

$$\sqrt{\frac{1}{N}\sum_{k=1}^{N}[y(k)-y_s(k)]^2}, \tag{4.4}$$

where $y_s(k)$ is the model output. The ARX models are defined by $[na\, nb{+}1\, nk]$, where na is the order, nb the number of zeros, and nk the sample times delay (Equations (4.1)-(4.3)).

Table 4.1 presents the deviations of the investigated models with different prediction horizons. The models with the best approximation are the ARX [1 1 4], [2 1 3], and

	prediction horizon			
ARX-Model	1	5	20	∞
1 1 3	1.1285	3.178	4.8442	4.9467
1 1 4	1.1163	3.1008	4.7029	4.7582
1 1 5	1.177	3.34	4.9767	4.9909
2 1 4	0.88852	3.0241	4.7933	4.8685
2 1 3	0.88392	2.8691	4.4981	4.595
2 2 3	0.87502	2.8608	4.5046	4.5936

Table 4.1: Model-Deviations with Different Prediction Horizons.

[2 2 3]. The ARX [2 2 3] is the most accurate, but also the most complex one. Still its deviation is not much better than the one from the ARX [2 1 3]. In this case the model with the simpler transfer function is to be preferred. The ARX [1 1 4] is even less complex than the ARX [2 1 3], but its deviation to the real system is evidently worse than the one of 2nd order. Figure 4.4a shows the system response (dots) and

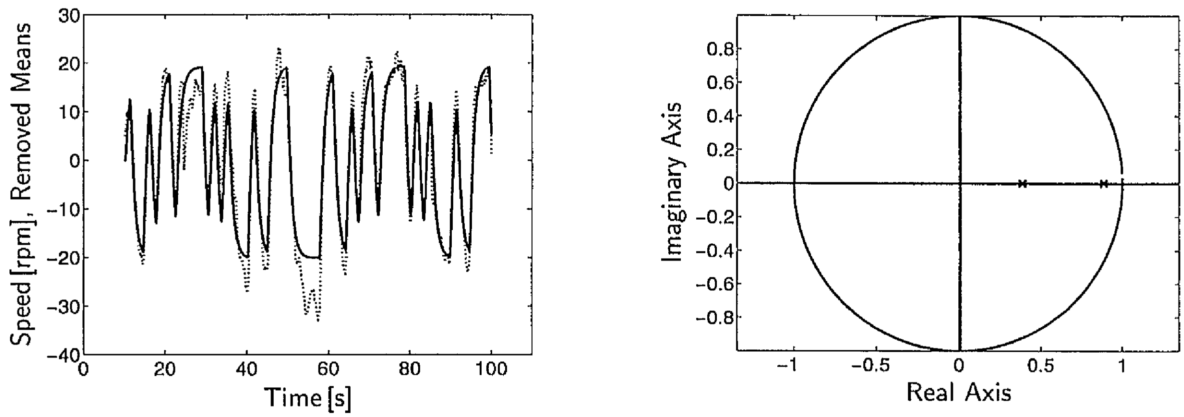

a: Measured and Estimated Output.

b: z^{-1}-Plane.

Figure 4.4: Simulated Output and Poles of the ARX [2 1 3] -Model.

the output of the ARX [2 1 3]-model (solid line). The poles of the estimated model are shown in Figure 4.4b. In the step response Figure 4.5 can be seen that the rise

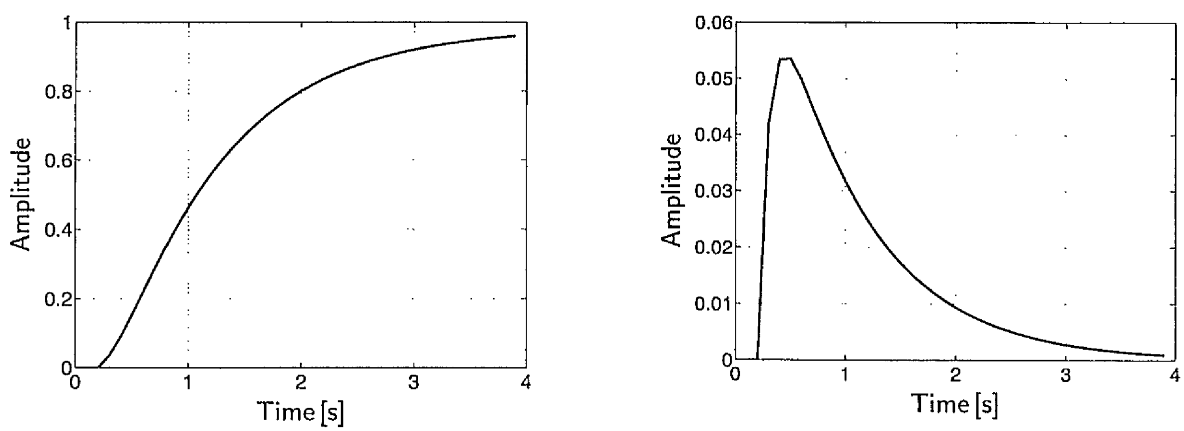

a: Step Response.

b: Impulse Response.

Figure 4.5: Step and Impulse Response of the ARX [2 1 3] -Model.

time of the system is about 3.5 s. With its 2 poles on the real axis it is, as predicted, very well damped. The impulse clarifies the huge inertia of the system.

4.5 Controller Design

The identified ARX model [2 1 3] is the basis for the design procedure of a linear discrete input-output pole-placement controller. The controller is to be designed with two degrees of freedom for one selected operating point [131].
The starting point is the general equation of a pole-placement controller (see Figure 4.6):

$$u(k) = \frac{1}{R}(Tr(k) - S(y(k) + n(k))) \tag{4.5}$$

where $r(k)$ is the reference, $u(k)$ the control signal, $y(k)$ the system output, $n(k)$ the measurement noise, and R,S and T are the controller polynomials in the delay operator. The polynomials are defined by:

$$R(q^{-1}) = 1 + r_1 q^{-1} + ... + r_{n_r} q^{-n_r} \tag{4.6}$$
$$S(q^{-1}) = s_0 + s_1 q^{-1} + ... + s_{n_s} q^{-n_s} \tag{4.7}$$
$$T(q^{-1}) = t_0 + t_1 q^{-1} + ... + t_{n_t} q^{-n_t} \tag{4.8}$$

The main goal of the controller design is to determine these polynomials in a way that the relationship between output $y(k)$ command signal $r(k)$ becomes:

$$y(k) = H_m(q^{-1})r(k) = \frac{B_m(q^{-1})}{A_m(q^{-1})}r(k) \tag{4.9}$$

Using a pole-placement controller it is possible to cancel stable poles and zeros in the plant. It is assumed that the polynomial coefficients A and B are factorized as $A = A^+A^-$ and $B = B^+B^-$ where A^+ and B^+ are the factors that will be cancelled. The factor $q^{-n_k}B^-$ cannot be cancelled. For this reason it must be part of the desired numerator polynomial. $B_m = q^{-n_k}B^-\bar{B}_m$. Important, especially in case of the tricycle, is the attenuation of input and output disturbances. For this reason the controller is required to have integral action, which means that the denominator-polynomial of the controller R has to contain the factor $(1 - q^{-1})$. Considering the things said, the controller polynomials can be written as [131]:

$$R = (1 - q^{-1})B^+\bar{R} \tag{4.10}$$
$$S = A^+\bar{S} \tag{4.11}$$
$$T = \bar{B}_m A_O A^+ \tag{4.12}$$

The polynomial A_O is called the observer polynomial. To obtain the controller, the Diophantine equation has to be solved. The Diophantine equation is the denominator polynomial of the whole closed loop system, which is represented in the following equation [131]:

$$A_{cl} = A^+B^+(A^-(1-q^{-1})\bar{R} + q^{-n_k}B^-\bar{S}) = A^+B^+A_oA_m \tag{4.13}$$

The specifications of the tracking performance are governed by the pulse transfer function $H_m = B_m/A_m$. The desired regulatory behaviour is given by the observer polynomial A_O. The control structure is shown in Figure 4.6.

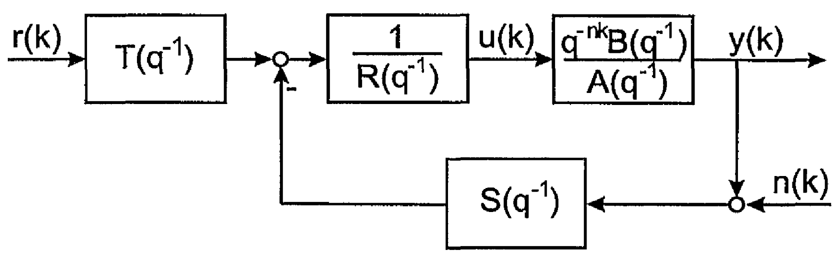

Figure 4.6: Controller Structure.

4.6 Experiments

After completing the controller design procedure, closed-loop speed control was tested. All initial experiments were done with the healthy subject MR for two reasons. Firstly, to test the system. If the system had been tested with a paralysed individual, the detection of disfunctions would become much harder, since SCI people usually do not feel their lower limbs, even if stimulated. In this case the cycle system was tested step by step with low stimulation intensity, and the feedback from the stimulated subject was used to detect disfunctions.
Secondly, to get an impression whether an effective muscle stimulation causes a more convenient skin-sensation than one of low efficiency. This might be the case, because a muscle stimulation in the right time forces a muscle contraction with lower resistance. This effect could simplify the process of data evaluation and interpretation in order to find an optimal setup.
As described in Chapter 3, a staircase function as the reference signal fulfills the evaluation demands of static and dynamic system behavior. For this reason a staircase function was designed and used in the closed loop control experiments. The velocity reference signal operates the tricycle in a normal cycle frequency between 30 and 80 rpm. The staircase function consists of 6 velocity levels, each level operates for 10 s. The function is defined by the following vector: [50 30 60 30 40 80 70 30]. The overall time for one experiment is about 80 s.
All the plots presented in this Chapter include 4 signals. The staircase function as the reference input in [desired rpm], the output of the estimated model [rpm], the controller output (pulsewidth [%]), and the crank velocity [rpm]. With the exception of the controller output (pulswidth) the signals describe the crank velocity. As described in Chapter 4 the current is kept constant at 60 mA.
The stimulated subject was not able to see the monitor with the reference signal. He also guaranteed not to do any voluntary work on the tricycle. All the mechanical adjustabilities of the tricycle were adapted to the cyclist as described in Chapter 3.

The main goal of the experiments was to see if and how the tricycle closed loop control works. Different models are to be tested, and the free parameters of the RST-controller are to be varied, to see their influence on cycling.
Since the controller design is based on the identified model, the model is probably of highest influence for closed loop cycling. It should be the first parameter to be

varied. As rise time and damping are the free control parameters they are going to be changed when an appropriate model was found.

For the first experiment the control parameters were set at conservative values. So the damping of the system was defined to be 1 and the rise time set to 5 s, to exclude hard control signals based on the performance.
A controller was designed based on the ARX [2 1 3] model, and the experiment was started.
Figure 4.7 presents the measured and calculated system inputs and outputs. It is

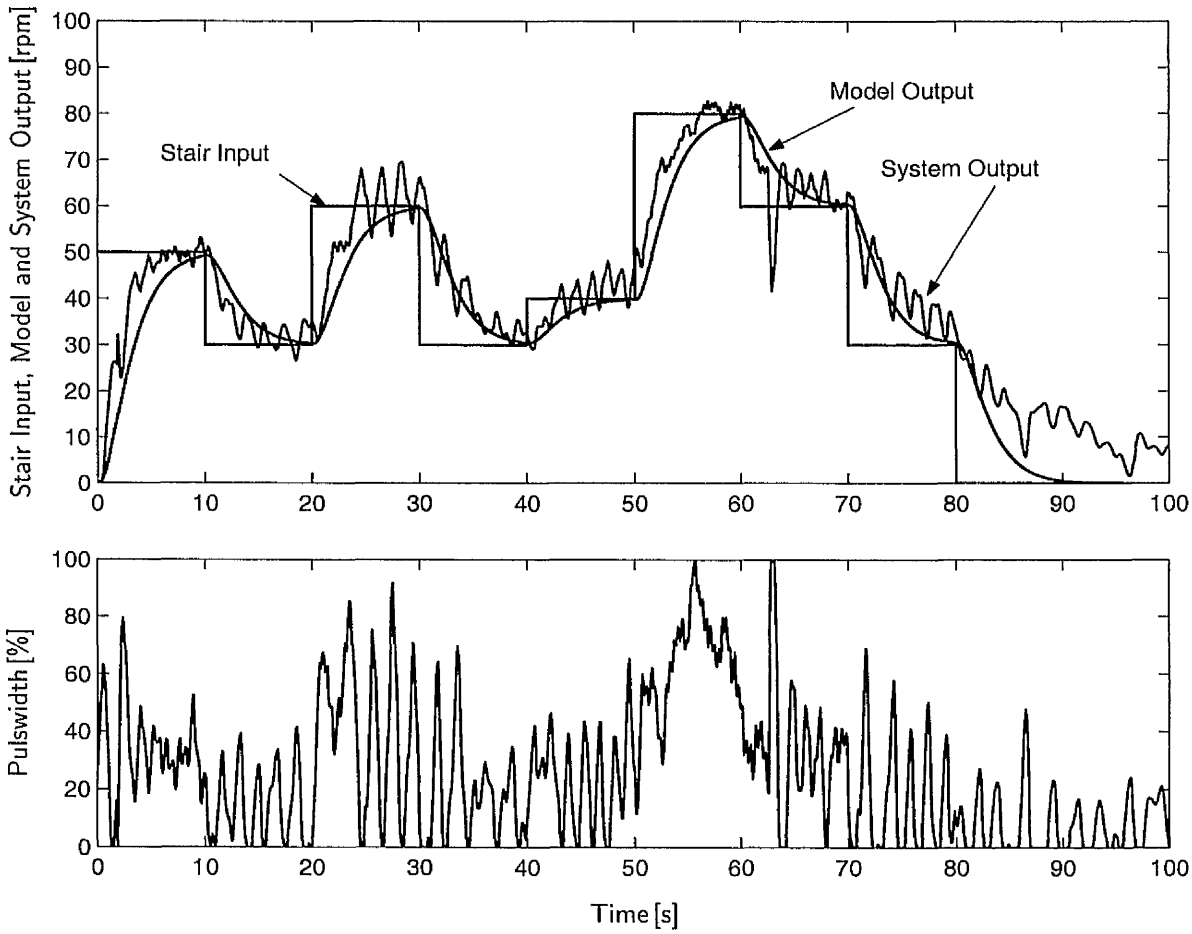

Figure 4.7: ARX [2 1 3], Damping Factor 1.0, Rise Time 5 s.

obvious that the control signal oscillates in a huge range for the whole time. The

stimulated subject felt quite uncomfortable during the experiment.
Compared to the initial cycle tests described in Chapter 3 the measured velocity oscillates with a large amplitude. This is not the case when the velocity surpasses 80 rpm. The dynamics of the estimated model do not reflect the systems real behavior. Especially in times of deceleration the model differs from the real system. In times of acceleration the mean value of the velocity approximately coincides with the estimated model.
As described in [66] and confirmed in Chapter 3 the time delay of muscle stimulation and muscle contraction varies in a wide range. For this reason different ARX models were tested for the design of different controllers. The controller design based

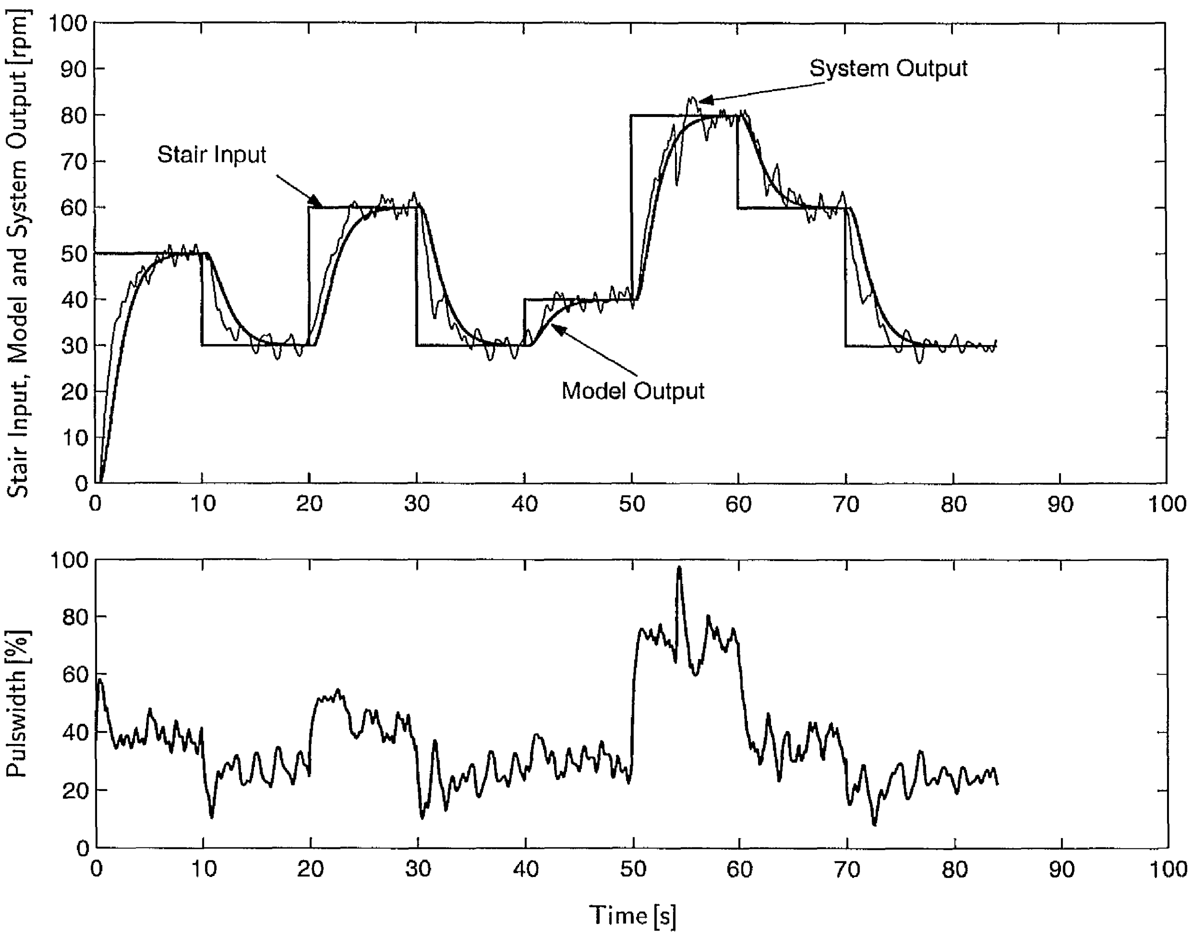

Figure 4.8: ARX [2 1 4], Damping Factor 1.0, Rise Time 5 s.

on the ARX [2 1 4] model produced the best results. Figure 4.8 presents the systems behavior with the modified controller, based on the model with 4 sample times delay. The control signal is smooth in comparison to the one obtained in the first test. The model's dynamics for acceleration and deceleration tasks fully reflects the real system behaviour. Only at static cycling the velocity signal of the tricycle starts to oscillate. This might be due to the accelerated and decelerated masses of the lower limbs and the tricycle during one cycle. The stimulated subject felt comfortable with the stimulation over the whole velocity range. Thus the velocity compensation routine is necessary to guarantee efficient cycling. Nevertheless the free parameters of the

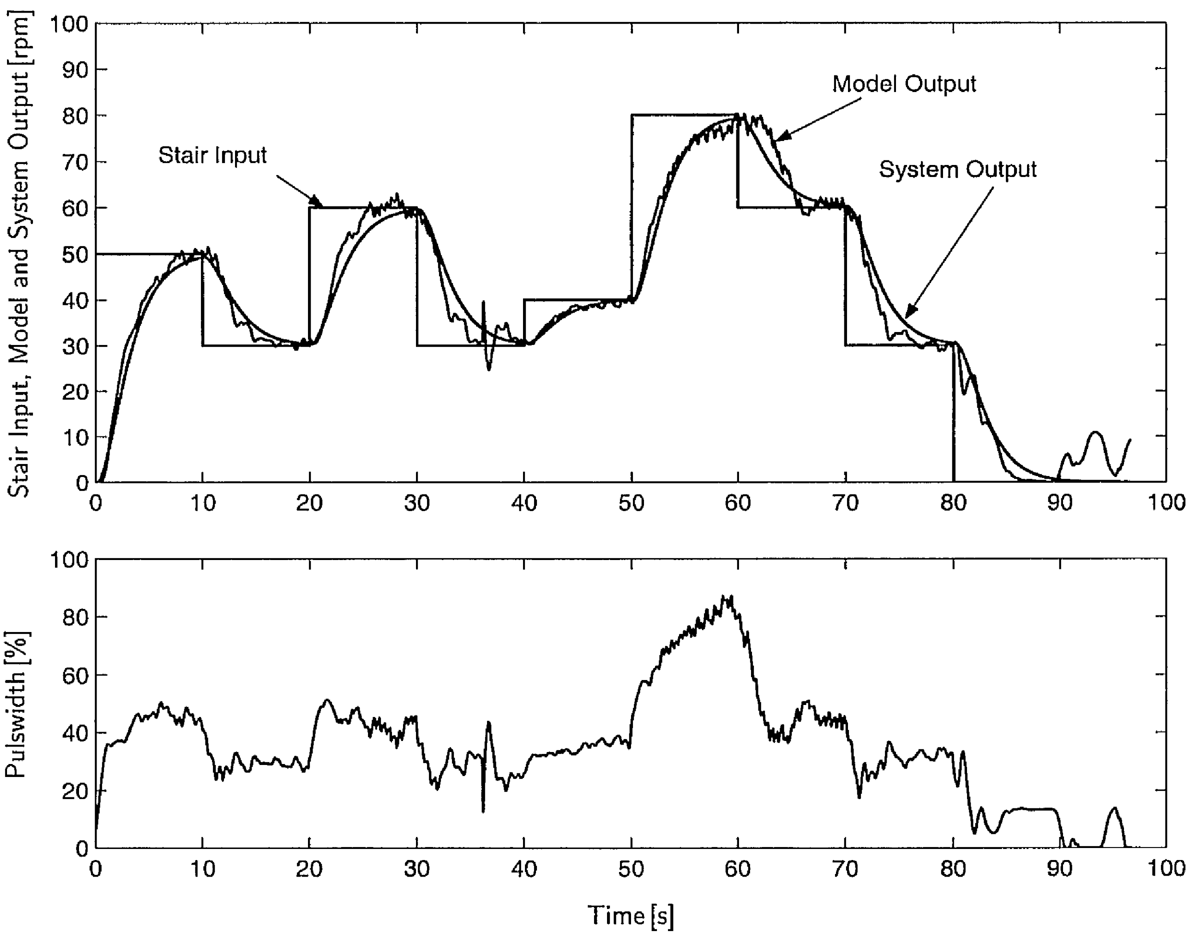

Figure 4.9: ARX [2 1 3], Damping Factor 1.3, Rise Time 7 s.

controller should be used to additionally modify the systems behavior. A decreased

rise time and a smoother control signal are desirable system attributes.
It was found that the desired rise time can not be decreased below 4 s. The controller signal started to oscillate in a manner comparable to the oscillation shown in the first experiment. Further experiments showed that the control signal can be smoothed, if rise time and damping are increased. Figure 4.9 presents the final solution, after increasing the damping factor to 1.3 and the rise time to 7 s. Although the control signal and the velocity are much smoother and the stimulated subject felt even better, the performance of the whole system decreased. The area below the control signal reflects the energy needed for the muscle stimulation during the whole experiment. The area between 0 and 80 s was calculated by the trapezoid rule

$$I \approx (x_2 - x_1)\frac{f(x_1) - f(x_2)}{2} + \ldots + (x_x - x_{x-1})\frac{f(x_{x-1}) - f(x_x)}{2}. \tag{4.14}$$

Comparing the size of this area in Figure 4.8 with Figure 4.9 shows, that the energy needed to stimulate the muscle is increased in the last setup (3.0694 e 3 against 3.3413 e 3). The efficiency of the stimulated muscle with the modified controller is not as good as with controller 2. Also the model does not reflect the systems dynamic behavior as accurate as in Figure 4.8.

Conclusions

The time delay between stimulation and muscle contraction is of major influence on the speed control in FES cycling. Its determination is difficult, since it can not be identified directly, using a PRB-signal for instance. A model based on a wrong stimulation delay results in rough control signals.
The controller designed was able to solve dynamic and static cycling tasks in a very precise manner, although the interaction of 6 muscles was controlled.
The velocity signal oscillates, especially in static cycling tasks. This effect was minimized using the control parameters 'rise time' and 'damping'. The modifications indeed decreased the performance of the system and also the muscle effectiveness. It seems that some oscillation is normal for some reasons (inertia of the accelerated and decelerated muscles and the 'hybrid' muscle stimulation).
A healthy subject is able to sense the quality of a model with the aid of the stimulation. As suspected, a muscle contraction at the right time, with lower resistance, feels more convenient than one with higher resistance.

Chapter 5

Summary and Future Work

The development of a tricycle for the use of people with spinal cord injury and the development and testing of a closed-loop speed controller for FES-cycling were the major contributions of this work. Therefore a detailed literature survey was done during the early stages of this project.

A commercially available tricycle was ordered. The tricycle was modified with a shaft encoder on the pedal crank for the control of the muscles in the lower limbs via Functional Electrical Stimulation. Other parts, such as an electric throttle, an emergency switch, and a calibration switch were mounted as well. Foot orthoses, for the fixation of the paralysed feet on the pedals, were ordered additionally.

Software for the control of the cycle system was developed, where data acquisition is done using Matlab / Simulink and the Real Time Toolbox.

Initial cycle experiments were realized with one healthy subject. A stimulation pattern was found, using a new identification technique based on an experiment with a static and dynamic part. The pedal frequency was taken in account as well. It was possible to use the tricycle in a velocity range never documented before.

A closed loop Pole Placement Controller was designed for the speed control of the tricycle. The speed control worked well, whereby the healthy subject MR was not able to see the monitor with the reference signal at any time.

The results show that a simple second order transfer function is able to accurately model the pulsewidth-speed dynamics. The closed loop controller based on this model is in turn able to provide accurate tracking of arbitrary speed reference patterns. The closed loop speed signal shows some intra cycle variation, which might be due to the underlying stimulation pattern.

The identification and controller design process is simple and can be applied rapidly to each cyclist at the start of an exercise session. The controller is tuned to each individual to ensure that the best feedback control performance is achieved. Thus, feasibility of this new methodology for the design of an automatic speed controller for FES cycling has been proven. Still the single subject data achieved with a healthy subject has to be evaluated by further tests to determine the wider applicability of the results. The work has been published lately [58] and is now being utilized within a pilot study with three volunteer paraplegic subjects at the General Hospital in Glasgow.

Nevertheless a few things have to be developed and to be investigated in the future. The distance between hip and crank should be adjustable with the seat, and not, like in this version, with the front tube of the tricycle. Another mechanical modification could be safety belts for free cycling experiments.

Next to the mechanical modifications to be made, stimulation parameters need to be further individualized to increase the effectiveness of the cycle system. Because of its major influence on the effectiveness of cycling, a further optimization and individualisation of the stimulation pattern might be highly reasonable.

One straightforward solution to meet these requirements could be the accurate mathematical modeling and the later simulation and optimization of the pattern. The model from Riener [116] could be used for this task. But although individual parameters, such like body masses and lengths, are utilized, the simulation will never represent the real system behaviour with respect to its time variance, evoked by the individual influence of muscle fatigue, or the changes of the skin dampness for example. If these stimulation parameters are kept constant over the time, the muscle effectiveness decreases and fatigue occurs even faster. This might be one major reason for the low longterm performance of FES cycling.

Another feasible method to overcome changing plant attitudes might be the design of a robust controller. But since the robustness of this type of controller is only based on a conservative design procedure, which does not change control parameters during control action, robust controller are not able to overcome fatigue either. Additionally, because of their conservative design, they are of lower performance than other controller structures, which is, especially in case of the stimulated muscle with low performance, an undesirable property.

Time depending and highly individual system parameters could be taken into account, if only they could be detected directly from the operating system (online). In this case the parameters could be varied and thus be optimized as well.

Start and stop angles of the stimulation pattern as well as the time delay between muscle stimulation and contraction are the parameters to be optimized. The variation of each of these parameters is the task of running an optimization. The optimization would evaluate after every variation, if the systems efficiency is increased or decreased. The variations further direction is based on the evaluation result.
The pedal frequency could be used to measure the systems efficiency. Therefore the stimulation intensity as well as the working rate (friction) has to be kept constant, an increased efficiency thus results in increased velocity.
Considering this, the variation and optimization are straightforward. Assuming constant stimulation intensity and friction of the system, the start-stop angles as well as the time delay have to be varied, and the pedal frequency has to be measured. If the frequency increases after a parameter is varied, the variation is continued in the same direction. If not, the variation is continued in the opposite direction.
A first attempt was done to vary and to optimize system parameters online. The location of the Optimization block in the cycle system can be seen from Figure 3.2 in Chapter 3. The routine used to vary and optimize one of the parameters can be found in Appendix C. (Online Optimization)
The routine developed was tested in initial tests. One stimulation parameter (start angle quadriceps, right side) was varied in one direction (-2 deg), the pedal frequency increased slightly.
In conclusion the routine does basically work, but work will be necessary to fully extend the possibilities this 'Online Optimization' provides.

Appendix

Appendix A

Parts Ordered

Trice	Ben Cooper [1] Kinetics - www.kinetics.org.uk 15 Rannoch Drive, Bearsden Glasgow G61 2JW, UK Tel.: 0141 - 942 2552	Kett-Wiesel
Hometrainer	[1]	Tacx 'Eco Track'
Orthoses	Eric Askew Orthotic Centre North Hampshire Hospitals NHS Trust Aldermaston Road Basingstoke Hampshire RG 24 9NA Tel.: 01256 - 314 764 FAX: 01256 - 811 326	-
Pedals	-	Shimano SPD PD-M323
Shaft Encoder	Fenwick Electronics Unit 10A Vulcan Works Floors Street Johnstone PA5 8QS Tel.: 01505 - 351091 FAX: 01505 - 336 423	RA58-S/0010 EK.42KBPB-F
Left Crank	[1]	Tandem version
Chainwheels	[1]	26 th
Throttel	[1]	Domino
Connector Stimulator Output	FC Lane Electronics Ltd Slinfold Lodge Horsham West Sussex RH13 7RN Tel.: 01403 - 790 661	9 pin plug M9PH19C

Appendix B

Technical Drawings

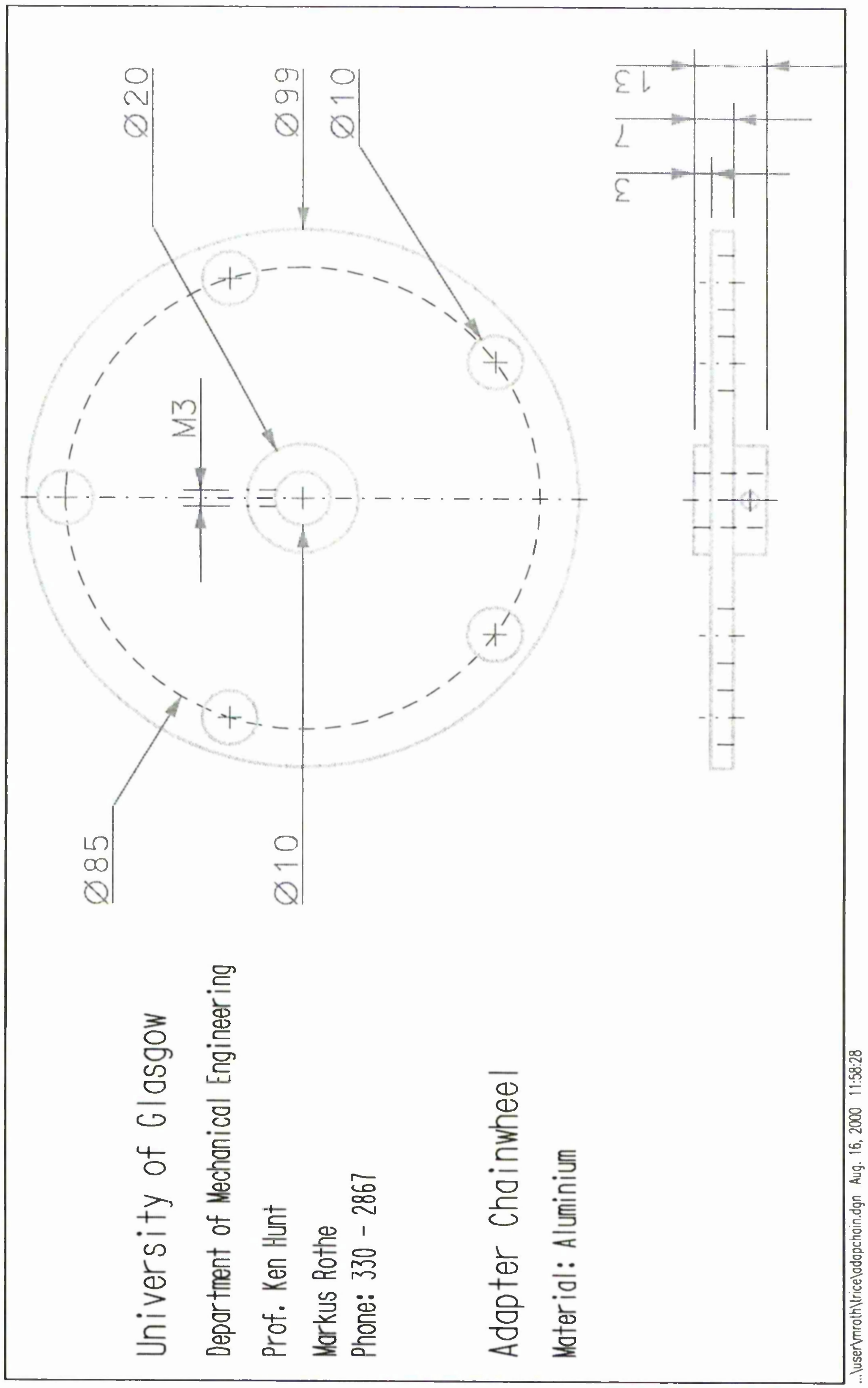

University of Glasgow
Department of Mechanical Engineering
Prof. Ken Hunt
Markus Rothe
Phone: 330 - 2867
Adapter Chainwheel
Material: Aluminium
Ø85
Ø10
Ø20
M3
Ø99
Ø10
3
7
13
...\user\mroth\trice\adapchain.dgn Aug. 16, 2000 11:58:28

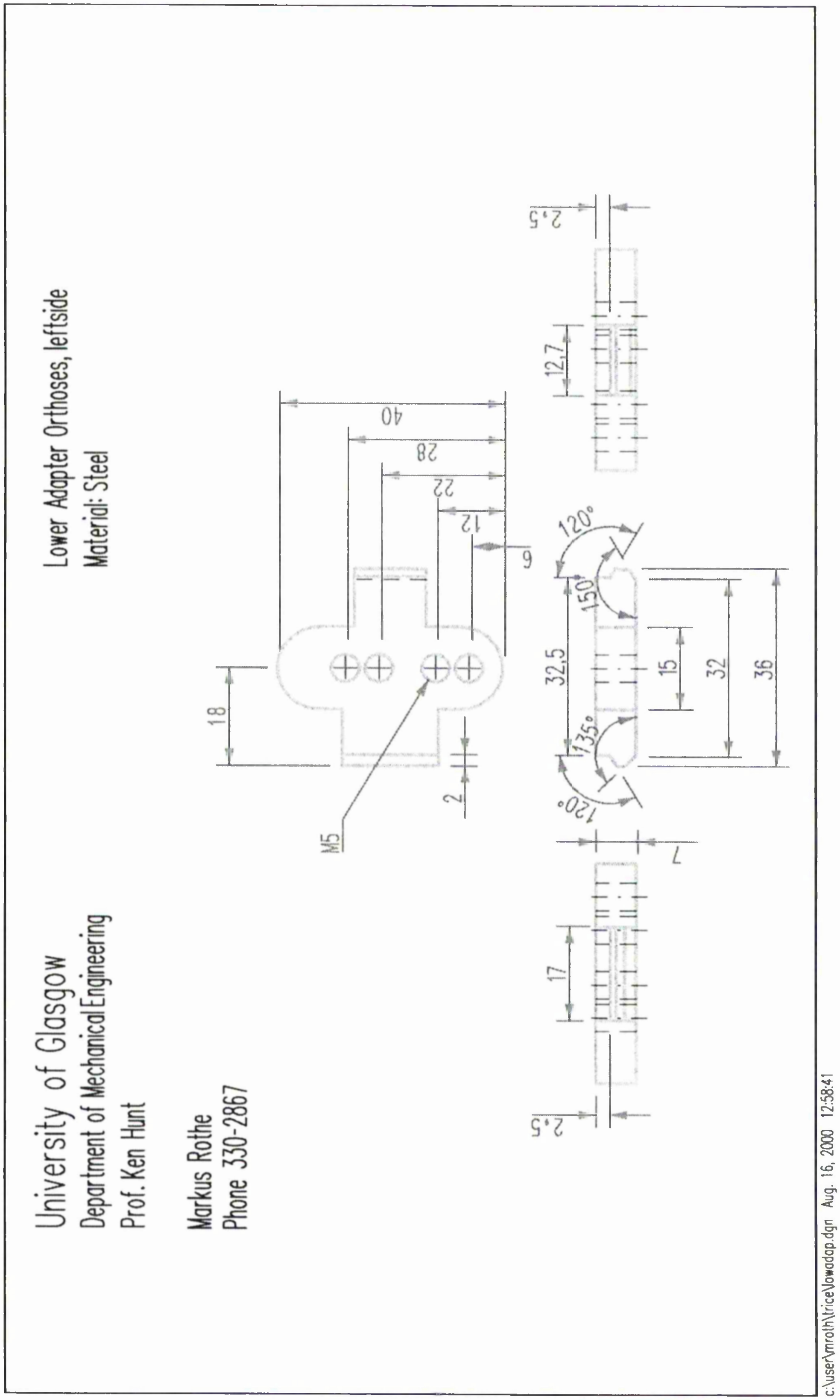
University of Glasgow
Department of Mechanical Engineering
Prof. Ken Hunt
Markus Rothe
Phone 330-2867
Lower Adapter Orthoses, leftside
Material: Steel
M5
40
28
22
12
6
18
2
120°
150°
135°
120°
32,5
15
32
36
17
12,7
2,5
2,5
7
c:\user\mroth\trice\lowadap.dgn Aug. 16, 2000 12:58:41

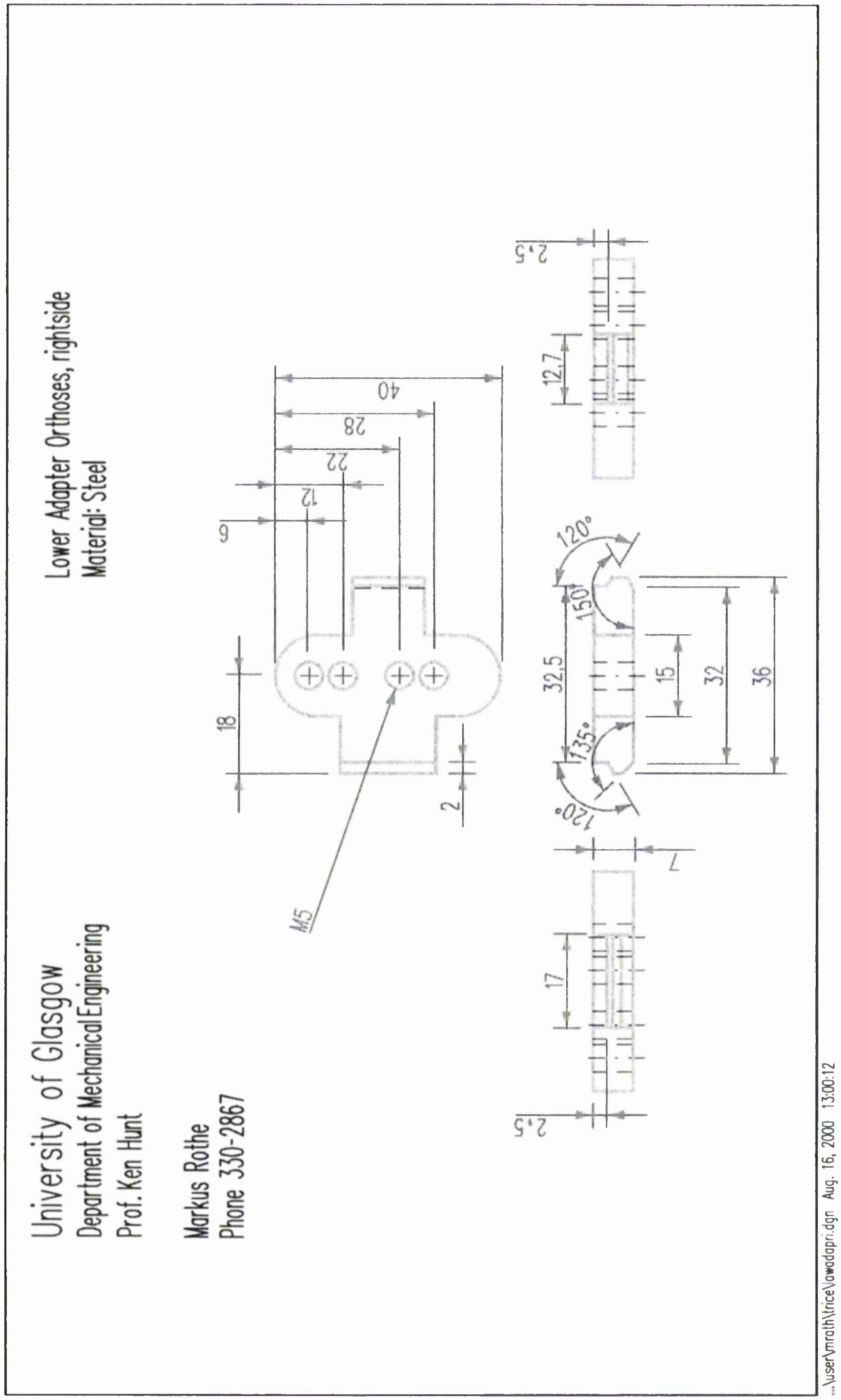
University of Glasgow
Department of Mechanical Engineering
Prof. Ken Hunt
Markus Rothe
Phone 330-2867
Lower Adapter Orthoses, rightside
Material: Steel
M5
6
12
22
28
40
18
2
2,5
17
7
120°
135°
32,5
150°
120°
15
32
36
12,7
2,5
...\user\mroth\trice\awadapri.dgn Aug. 16, 2000 13:00:12

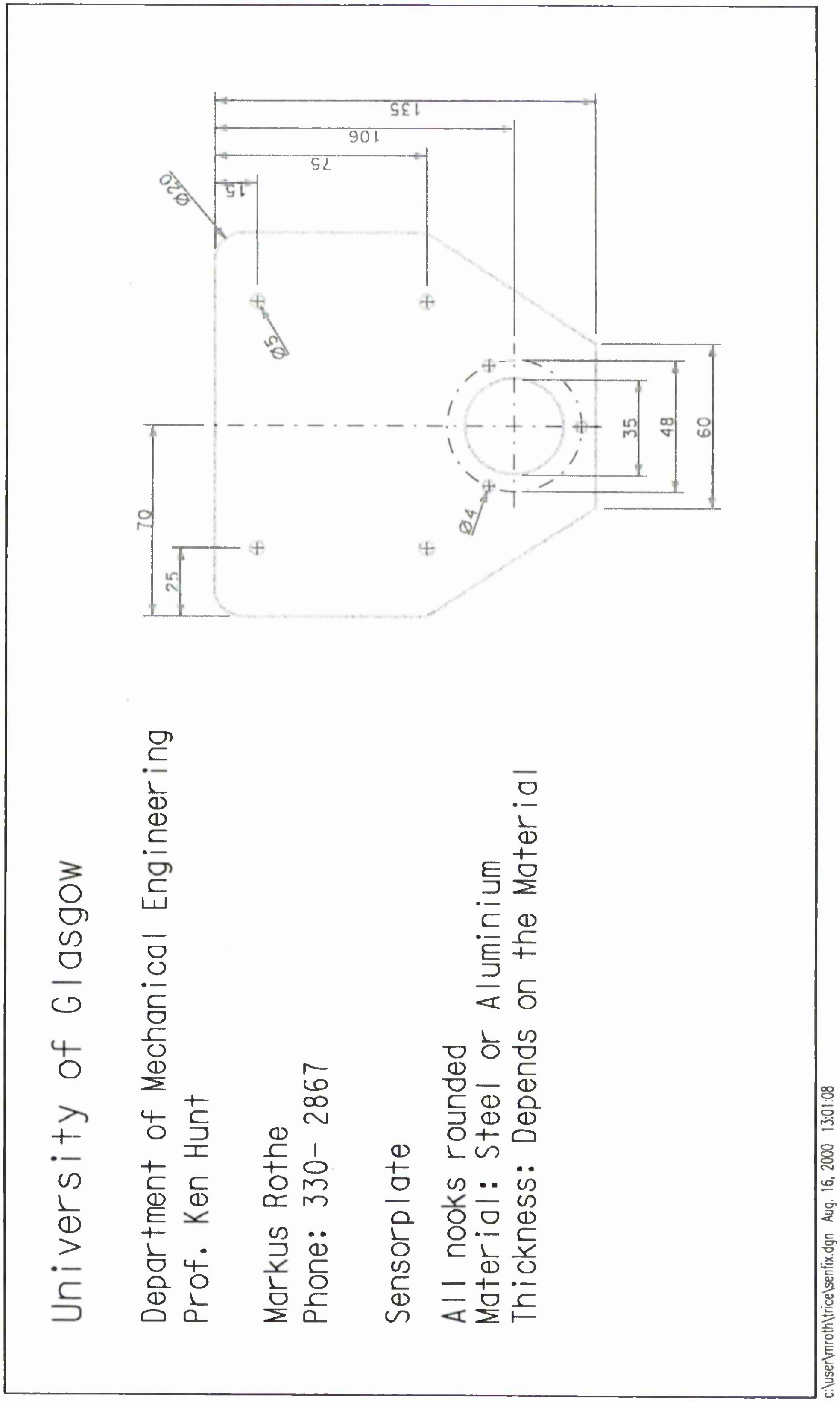
University of Glasgow
Department of Mechanical Engineering
Prof. Ken Hunt
Markus Rothe
Phone: 330- 2867
Sensorplate
All nooks rounded
Material: Steel or Aluminium
Thickness: Depends on the Material
135
106
75
15
Ø20
Ø5
Ø4
70
25
35
48
60
c:\user\mroth\trice\senfix.dgn Aug. 16, 2000 13:01:08

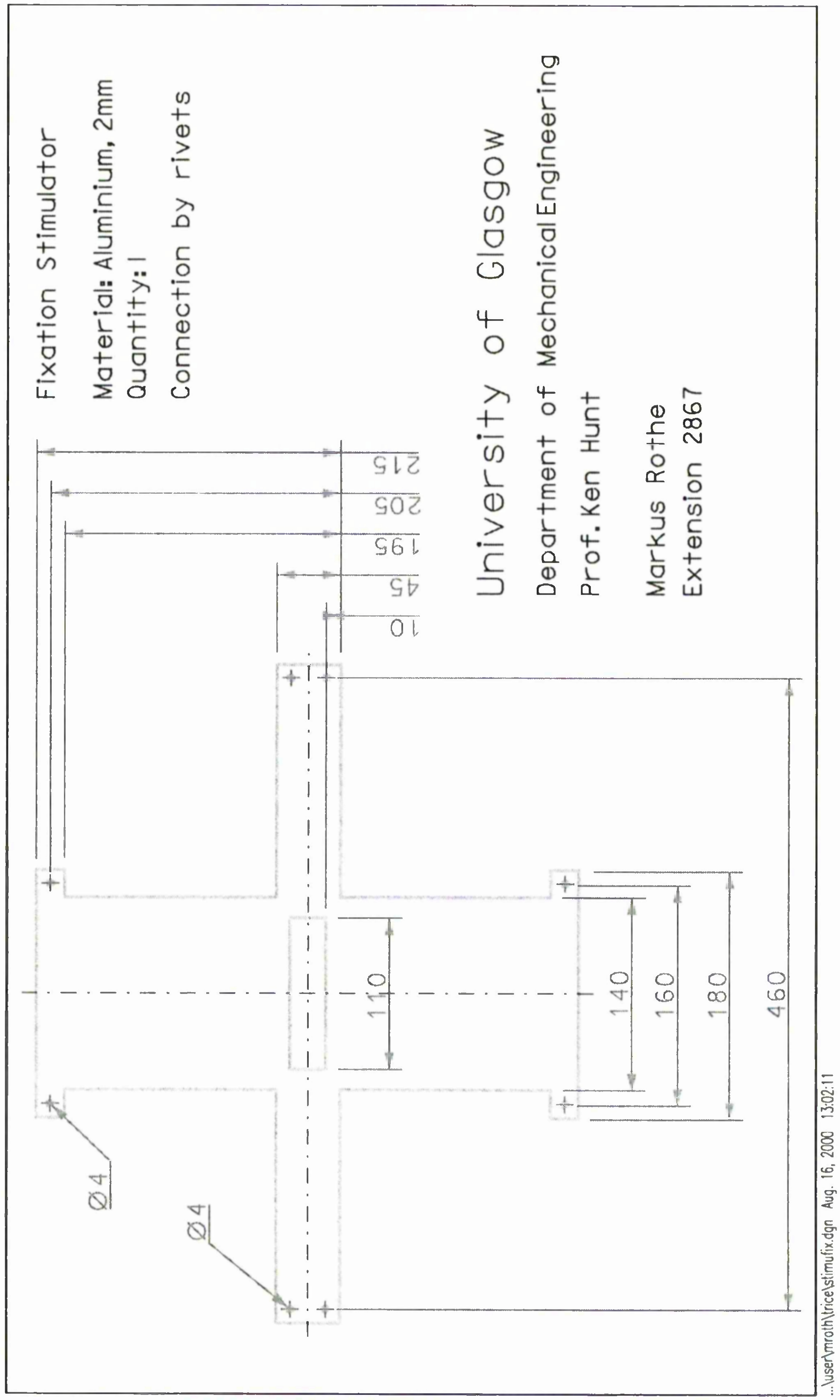
Fixation Stimulator
Material: Aluminium, 2mm
Quantity: 1
Connection by rivets
University of Glasgow
Department of Mechanical Engineering
Prof. Ken Hunt
Markus Rothe
Extension 2867
215
205
195
45
10
110
140
160
180
460
Ø4
Ø4
...\user\mroth\trice\stimufix.dgn Aug. 16, 2000 13:02:11

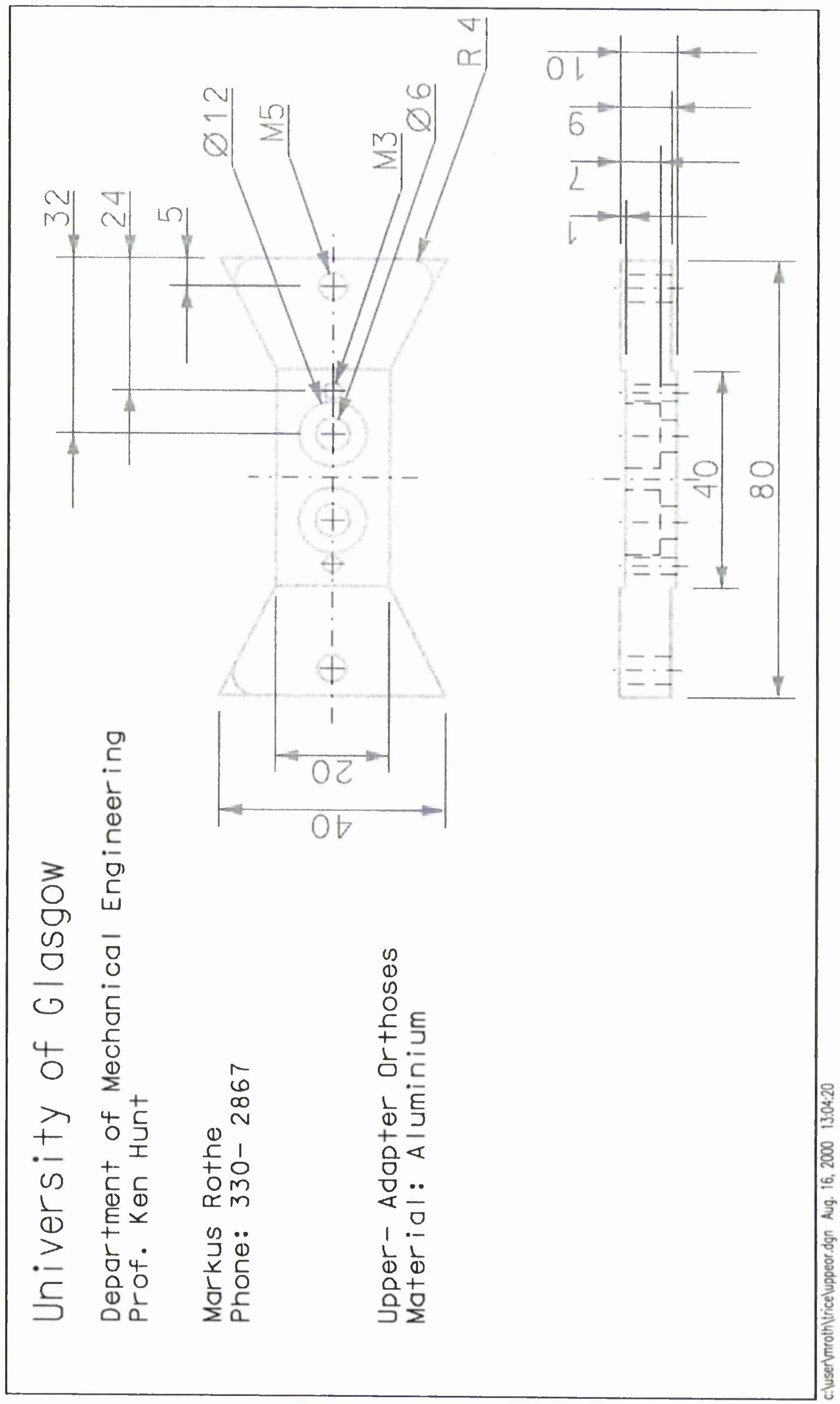
University of Glasgow
Department of Mechanical Engineering
Prof. Ken Hunt
Markus Rothe
Phone: 330- 2867
Upper- Adapter Orthoses
Material: Aluminium
32
24
5
Ø12
M5
M3
Ø6
R 4
10
9
7
1
40
80
20
40
c:\user\mroth\trice\uppeor.dgn Aug. 16, 2000 13:04:20

Appendix C

S-Functions

S-Function Stimulation Pattern

```
function [sys,x0,str,ts]= hamstring(t,x,u,flag,Ts);
switch flag,
case 0,
[sys,x0,str,ts]= mdlInitializeSizes(Ts);
case 2,
sys=mdlUpdate(t,x,u,Ts);
case 3,
sys=mdlOutputs(t,x,u,Ts);
case 1,4,9,
sys=[];
otherwise
error(['Unhandled flag = ',num2str(flag)]);
end;
function [sys,x0,str,ts]=mdlInitializeSizes(Ts);
sizes = simsizes;
sizes.NumContStates = 0; sizes.NumDiscStates = 3;
sizes.NumOutputs = 1; sizes.NumInputs = 1;
sizes.DirFeedthrough = 0;
sizes.NumSampleTimes = 1;
at least one sample time is needed
sys = simsizes(sizes);
initialize the initial conditions
x0 = [0 0 0];
str is always an empty matrix
str = [];
initialize the array of sample times
ts = [Ts 0];
end mdlInitializeSize
=========================================
Update
=========================================
function sys=mdlUpdate(t,x,u,Ts);
deru=1/Ts*(u-x(1));
sys(1)=u; sys(2)=deru;
if abs(deru)>700
velunpeaked=x(2)/6;
else
velunpeaked=deru/6;
end
filtered unpeaked velocity alpha=-0.85;
sys(3)=-alpha*x(3)+(1+alpha)*velunpeaked;
```

```
========================================
mdlOutputs
Return the block outputs.
========================================
function sys=mdlOutputs(t,x,u,Ts);
deru=1/Ts*(u-x(1));
if abs(deru)>700 velunpeaked=x(2)/6;
else
velunpeaked=deru/6;
end;
alpha=-0.85; sys=-alpha*x(3)+(1+alpha)*velunpeaked
```

S-Function Online Optimization

```
function [sys,x0,str,ts]= optimisation(t,x,u,flag,Ts,LowerAngles,UpperAngles);
switch flag,
case 0,
[sys,x0,str,ts]=mdlInitializeSizes(Ts,LowerAngles,UpperAngles);
case 2,
sys=mdlUpdate(t,x,u,Ts,LowerAngles,UpperAngles);
case 3,
sys=mdlOutputs(t,x,u,Ts,LowerAngles,UpperAngles);
case 1,4,9,
sys=[];
otherwise
error(['Unhandled flag = ',num2str(flag)]);
end;
function [sys,x0,str,ts]=mdlInitializeSizes(Ts,LowerAngles,UpperAngles);
sizes = simsizes;
sizes.NumContStates = 0;
sizes.NumDiscStates = 40;
sizes.NumOutputs = 14;
sizes.NumInputs = 2;
sizes.DirFeedthrough = 2;
sizes.NumSampleTimes = 1;
sys = simsizes(sizes);

initialize the initial conditions
x0 = zeros(40,1);

str is always an empty matrix
str = [];

initialize the array of sample times
ts = [Ts];

end mdlInitializeSizes

=============================================
Update
=============================================

function sys=mdlUpdate(t,x,u,Ts,LowerAngles,UpperAngles);
acceleration=u(2);
velocity=u(1);
```

```
a(2:(length(x)-20))=x(1:(end-21));
a(1)=acceleration;
b(2:(length(x)-20))=x(21:(end-1));
b(1)=velocity;
c=[a b];
sys=c;
============================================
mdlOutputs
Return the block outputs.
============================================
function sys=mdlOutputs(t,x,u,Ts,LowerAngles,UpperAngles);
global
global oldangle newangle oldstdacc
variables
dd = LowerAngles;
ee = UpperAngles;
input
velocity=u(1);
acceleration=u(2);
calculate average velocity and average acceleration last 2sec
newstdacc = std(x(1:20));
averagevel = mean(x(21:40));
averagevelnew = mean([velocity x(21:39)']);
reset
oldangle = newangle;
start optimisation conditions
if (t == 0)
oldstdacc = 10;
oldangle = dd(1);
newangle = dd(1);
outlowangles = [newangle (dd(2)-(dd(1)-newangle)) dd(3) dd(4) dd(5) dd(6)];
outupangles = [ee(1) ee(2) ee(3) ee(4) ee(5) ee(6)];
sys = [outlowangles outupangles newangle newstdacc];
elseif ((averagevel > averagevelnew)AND (averagevel>40))
[newangle, oldstdacc, outlowangles, outupangles]=
=optimisationyes(oldangle, newstdacc, dd, ee);
sys = [outlowangles outupangles newangle averagevel];
elseif ((averagevel < averagevelnew)AND(averagevel>40))
[newangle, oldstdacc, outlowangles, outupangles]=
=optimisationno(oldangle, newstdacc, dd, ee);
sys = [outlowangles outupangles newangle averagevel];
else
[newangle, oldstdacc, outlowangles, outupangles]=
=optimisation(oldangle, newstdacc, dd, ee);
```

```
sys = [outlowangles outupangles newangle averagevel];
end;

function optimisationyes

function [newangle, oldstdacc, outlowangles, outupangles]=
=optimisationyes(oldangle, newstdacc, dd, ee);
newangle = oldangle-0.05;
oldstdacc = newstdacc;
[outlowangles, outupangles]=muscle(newangle, dd, ee);

function optimisationno

function [newangle, oldstdacc, outlowangles, outupangles]=
=optimisationno(oldangle, newstdacc, dd, ee);
newangle = oldangle+0.2;
oldstdacc = newstdacc;
[outlowangles, outupangles]=muscle(newangle, dd, ee);

function optimisation

function [newangle, oldstdacc, outlowangles, outupangles]=
=optimisation(oldangle, newstdacc, dd, ee);
newangle = oldangle;
oldstdacc = newstdacc;
[outlowangles, outupangles]=muscle(newangle, dd, ee);

function muscle
function [outlowangles, outupangles]=muscle(newangle, dd, ee);

Lower
outupangles = [ee(1) ee(2) ee(3) ee(4) ee(5) ee(6)];
Quadricep
outlowangles =
=[newangle (dd(2)-(dd(1)-newangle)) dd(3) dd(4) dd(5) dd(6)];
Hamstring
outlowangles =
=[dd(1) dd(2) newangle (dd(4)-(dd(3)-newangle)) dd(5) dd(6)];
Gluteals
outlowangles = [dd(1) dd(2) dd(3) dd(4) newangle (dd(6)-(dd(5)-newangle))];

Upper
outlowangles = [dd(1) dd(2) dd(3) dd(4) dd(5) dd(6)];
```

```
Quadricep
outupangles = [newangle (ee(2)-(ee(1)-newangle)) ee(3) ee(4) ee(5) ee(6)];
Hamstring
outupangles = [ee(1) ee(2) newangle (ee(4)-(ee(3)-newangle)) ee(5) ee(6)];
Gluteals
outupangles = [ee(1) ee(2) ee(3) ee(4) newangle (ee(6)-(ee(5)-newangle))];
```

FES-Cycle Scirpt

```
Static Parameters
offset = [0 180]; calculats the stimulation times of the left limbs (fixed)
Binarycode = [1 2 4 8 16 32 64 128 256 512]; Binary => Decimal (fixed)
Degree = [0.352]; Convertion 1024 inctrements => 360 degrees (fixed)
Ts = 0.1; Sample Time

global oldangle oldstdacc newangle

Zero Set Shaft Encoder
zz = exist('storeangle'); if zz == 0
storeangle = 0;
else
end;

Static Parameters / Basic Setup for Variation-Optimisation
max values of current right / left
curquad = [60 60]; curham = [60 60]; curglute = [60 60];
Weighting Quads, Hams, and Glutes 1 == 100
y1 = 1; Quads
y3 = 1; Hams
y5 = 1; Glutes

Pattern Lower Angles (Symmetric).  Right Side.  Write -50 instead of 310
a1 = 0; Quads
a3 = 150; Hams
a5 = 50; Glutes

Pattern Upper Angles (symmetric).  Right Side.
b1 = 145; Quads
b3 = 325; Hams
b5 = 165; Glutes

Delay Stimulation-Force.  If >1 =>Delay > 0.15s
Constant = 1.5;

Calculations

Weighting Factors (Quads == 100)>Leftside, Symmetric
y2 = y1; y4 = y3; y6 = y5;
```

```
LowerAngles >Leftside, Symmetric
a2 = a1+180; a4 = a3+180; a6 = a5+180;

Calculates Angles in Range 0 < a(z) < 360
a=[a1 a2 a3 a4 a5 a6]; for z=1:1:6;
if a(z) > 360
aa(z) = a(z) - 360;
else aa(z) = a(z);
end;
end;

UpperAngles >Leftside, Symmetric
b2 = b1+180; b4 = b3+180; b6 = b5+180;

Calculates Angles in Range 0 < b(b) < 360
b=[b1 b2 b3 b4 b5 b6]; for z=1:1:6;
if b(z) > 360
bb(z) = b(z) - 360;
else bb(z) = b(z);
end;
end;

Output Values

LowerAngles = [aa(1) aa(2) aa(3) aa(4) aa(5) aa(6)]; UpperAngles
= [bb(1) bb(2) bb(3) bb(4) bb(5) bb(6)];

Weighting = [y1 y2 y3 y4 y5 y6];Weighting factors for stimulation current
```

Bibliography

[1] Controlled prehension and release in the c5 quadriplegic elicited by functional electrical stimulation of the paralyzed forearm musculature. *Ann. Biomed. Eng.*, 8:369–388, 1980.

[2] A.L. Aaronson, M.M. Rodgers, R.M. Glaser, and S.F. Figoni. Psychological changes resulting from electrical stimulation training of spinal cord injured. *Proc. Am. Psychol. Assoc. Annu. Conv. Anaheim, Calif.*, 1994.

[3] S.B. Abott. Analysis of Control Strategies for Human Skeletal System Pedaling a Bicycle. 1995.

[4] R. Acimovic-Janezic, N. Gros, T. Bajd, and A. Trnkoczy. New aspects in the determination of functional electrical stimulation for lower extremities. *PWN-Polish Scientific Publishers and University Park Press*, VIIA:288–293, 1981.

[5] P.B. Arnold, P.P. Vey, W.J. Farrel, T.M. Deurloo, and A.R. Grasso. Functional electric stimulation: its efficacy and safety in impoving pulmonary function and musculoskeletal fitness. *Arch. Phys. Med. Rehabil.*, 73:665–668, July 1992.

[6] T. Bajd, A. Kralj, and R. Turk. Standing-up of a healthy subject and a paraplegic patient. *J. Biomechanics*, 15(1):1–10, 1982.

[7] T. Bajd and A. Trnkoczy. Attempts to optimise functional electrical stimulation of antagonist muscles by mathematical modelling. *J. Biomech.*, 12:921–928, 1979.

[8] J.C. Baldi, W.J. Mysiw, R. Moraille, D.C. Owen, and R.D. Jackson. The effects of functional electrical stimulation on muscle atrophy in patients with acute spinal cord injury. *Med. Sci. Sports Exerc.*, S27:208, 1995.

[9] K.K. Bedell, A.M.E. Scremin, K.L. Perell, and C.F. Kunkel. Effects of functional electrical stimulation-induced lower extremity cycling on bone density of spinal cord-injured patients. *American Journal of Physical Medicine & Rehabilitation*, 75(1):29–34, January/February 1996.

[10] M. Bergstrom and E. Hultman. Energy cost and fatigue during intermittent electrical stimulation of human skeletal muscle. *J. Appl. Physiol.*, 65:1500–1505, 1988.

[11] H.B.K. Boom, A.J. Mulder, and P.H. Veltink. Fatigue during functional neuromuscular stimulation. *Progr. Brain Res.*, 97:409–418, 1993.

[12] M.B. Bradley. The effect of participating in a functional electrical stimulation exercise program on affect in people with spinal cord injuries. *Arch. Phys. Med. Rehab.*, 75:676–679, 1994.

[13] L.A. Bremner, K.E. Sloan, R.E. Day, and E.R. Scull. A clinical exercise system for paraplegics using functional electrical stimulation. *Paraplegia*, 30:647–655, 1992.

[14] W.F. Brown. Fatigue and neuromuscular block in mammalian skeletal muscle. *Proc. Royal Soc. (B)*, (136):182–189, 1949.

[15] D. Burr, R. Martin, and P. Martin. Lower extremity loads stimulate bone formation in the vertebral column: implications for osteoporosis. *Spine*, 3:681–686, 1983.

[16] S.G. Carroll, R.J. Triolo, H.J. Chizeck, R. Kobetic, and E.B. Marsolais. Tetanic responses of electrically stimulated paralyzed muscle at varying interpulse intervals. *IEEE Trans. Biomed. Eng.*, 36:644–653, 1989.

[17] A. Chantraine, B. Nusgens, and C.M. Lapiere. Bone remodeling during the development of osteoporosis in paraplegia. *Calcif. Tissue Int.*, 38:323–327, 1986.

[18] Chen, Yu, Huang, Ann, and Chang. Applying fuzzy logic to control cycling movement induced by functional electrical stimulation. *IEEE Transactions on Rehabilitation Engineering*, 5(2):158–168, June 1997.

[19] J.J. Chen, C.T. Shih, D.G. Huang, N.Y. Yu, M.S. Ju, and T.C. Huseh. Development of fes-cycling system with closed-loop control. *Chinese J. Med. Biologic. Eng.*, 14(3):195–209, 1994.

[20] J.J.J. Chen and N.Y. Yu. The validity of stimulus-evoked emg for studying muscle fatigue characteristics of paraplegic subjects during dynamic cycling movement. *IEEE Transactions on Rehabilitation Engineering*, 5(2):170–178, June 1997.

[21] H.J. Chizeck, R. Kobetic, E.B. Marsolais, J.J. Abbas, I.H. Donner, and E. Simon. Control of functional neuromuscular stimulation systems for standing and locomotion in paraplegics. *Proc. IEEE*, 76:1155–1165, 1988.

[22] S.R. Collins and R.M. Glaser. Comparison of aerobic metabolism and cardiopulmanory responses for electrical;ly induced and voluntary exercise. *Proc 8th Annual Conf. Rehab. Eng. Soc.*, pages 391–393, 1985.

[23] P.T. Croisant and R.A. Boileau. Effect of pedal rate, brake load and power on metabolic responses bicycle ergometer work. *Ergonomics*, 27(6):691–700, 1984.

[24] D. Danupolos, P. Kezdi, E. Stanley, J. Petrofsky, R. Stacy, C. Phillips, and L. Meyer. Changes in cardiovascular circulatory dynamics after a twelve week active bicycle rehabilitation in young tetraplegics. *J. Neuro. Ortho. Med. Surg.*, 7:179–184, 1986.

[25] R.R. Davis and M.L. Hull. Measurement of foot-pedal loads during bicycling: dataanalysis and results. *J. Biomechanics*, 14:857–872, 1981.

[26] Ericson, Nisell, Arborelius, and Ekholm. Muscular activity during ergometer cycling. *Scand. J. Rehab. Med.*, (172):53–61, 1985.

[27] M. Ericson. On the biomechanics of cycling: a study of joint and muscle load during exercise on the bicycle ergometer. *Scand. J. Rehabil. Med.*, Suppl. 16:1–43, 1986.

[28] P.D. Faghri, R.M. Glaser, and S.F. Figoni. Functional electrical stimulation leg cycle ergometer exercise- training effects on cardiorespiratory responses of spinal cord injured subjects at rest and during submaximal exercise. *Arch. Phy. Med. Rehab.*, 73(11):1085–1093, 1992.

[29] P.D. Faghri, R.M. Glaser, S.F. Figoni, D.S. Miles, and S.C. Gupta. Feasibility of using two fns exercise modes for spinal cord injured patients. *Clin. Kinesiol.*, 43:62–68, 1988.

[30] Z.P. Fang and J.T. Mortimer. Alternating motor unit activation in electrically stimulated muscles. *Physics in Med. Biol. Proc. World Congr.*, 33:385, 1988.

[31] S.F. Figoni, R.M. Glaser, M.M. Rodgers, S.P. Hooker, B.N. Ezenwa, S.R. Collins, T. Mathews, A.G. Suryaprasad, and S.C. Gupta. Acute hemodynamics responses of spinal cord injured individuals to functional neuromuscular stimulation-induced knee extension. *J. Rehab. R&D*, 28(4):9–18, 1991.

[32] S.F. Figoni, M.M. Rodgers, R.M. Glaser, S.P. Hooker, P.D. Faghri, B.N. Ezenwa, T. Mathews, A.G. Suryaprasad, and S.C. Gupta. Physiologic responses of paraplegics and quadriplegics to passive and active leg cycle ergometry. *J. Amer. Paraplegia Soc.*, 13:33–39, 1990.

[33] B.J. Fregly and F.E. Zajac. Interpretation of muscle activity during cycling based on a dynamical, two-legged biomechanical model. *XII Int. Congr. Biomechan.*, pages 29–33, 1989.

[34] U. Freyschuss and E. Knutsson. Cardiovascular control in man with traverse cervical cord lesions. *Life Sci.*, 8:421–424, 1969.

[35] D.E. Garland, Z. Maric, R.H. Adkins, and C.A. Stewart. Bone mineral density about the knee in spinal cord injured patients with pathologic fractures. *Contemp. Orthop.*, 26:375–379, 1993.

[36] D.E. Garland, C.A. Stewart, and R.H. Adkins. Osteoporosis after spinal cord injury. *J. Orthop. Res.*, 10:371–378, 1992.

[37] M. Gföhler, T. Angeli, T. Eberharter, P. Lugner, and L. Rinder. Measurements on pedaling by fes. Technical report, Department of Mechanics, Technical University of Vienna.

[38] M. Gföhler, M. Loicht, and P. Lugner. Exercise tricycle for paraplegics. *Med. Biol. Eng. Comput.*, (36):118–121, 1998.

[39] M. Gföhler and P. Lugner. Cycling by means of functional electrical stimulation. *IEEE Transactions on Rehabilitation Engineering*, 8(2):233–243, June 2000.

[40] R.M. Glaser. Arm exercise training for wheelchair users. *Med. Sci. Sports Exerc.*, 21:149–157, 1989.

[41] R.M. Glaser, J.A. Bruner, S.D. Feinberg, and S.R. Collins. Locomotion via paralyzed leg muscles, feasibility study for a leg propelled vehicle. *J. Rehab. Res. & Dev.*, 20:53–61, 1983.

[42] R.M. Glaser, W.P. Couch, T.W.J. Janssen, J.W. Almeyda, D.D. Pringle, S.R. Collins, and T. Mathews. A development system to enhance fes leg cycle ergometer technology. *RESNA*, (7-12):279–281, June 1996.

[43] R.M. Glaser, S.F. Figoni, W.P. Couch, S.R. Collins, and R.A. Shively. Effects of increased maximum current during electrical stimulation leg cycle ergometry. *Med. Sci. Sports Exerc.*, (26):111, 1994.

[44] R.M. Glaser, S.F. Figoni, and S.P. Hooker. Efficiency of fns leg cycle ergometry. *IEEE Engineering in medicine and Biology Society 11th Annual Internationational Conference*, pages 961–3, 1989.

[45] R.M. Glaser, T. Mathews, and S.F. Figoni. Evaluation and optimization of fes techniques for exercise. *Rehab. Res. Dev. Progr. Rep. 1994*, 32:77–78, 1995.

[46] M.H. Granat, A.C.B. Ferguson, B. Andrews, and M. Delargy. The role of functional electrical stimulation in the rehabilitation of patients with incomplete spinal cord injury-observed benefits during gait studies. *Paraplegia*, 31:207–215, 1993.

[47] H. Granek and M. Granek. Transcutaneous transducer garments: current mammalian usage and future applications. *J. Neuro. Ortho. Surg.*, 6:271–278, 1985.

[48] D. Graupe. Emg pattern analysis for patient-response control of fes in paraplegics for walker-supported walking. *IEEE Trans. Biomed. Eng.*, 36:711–719, 1989.

[49] R.J. Gregor. A biomechanical analysis of lower limb action during cycling at four different loads. *Doctoral Dissertation, The Pensylvania State University*, 1976.

[50] J.A. Gruner, R.M. Glaser, S.D. Feinberg, S.R. Collins, and N.S. Nussbaum. A system for evaluation and exercise conditioning of paralysed leg muscles. *J. Rehab. Res. Dev.*, 20:21–23, 1983.

[51] N. Hjeltnes. Oxygen uptake and cardiac output in graded arm exercise in paraplegics with low level spinal lesion. *Scand. J. Rehab. Med.*, 9:107–113, 1977.

[52] J.J.A.J.M. Hoes, R.A. Blinkhorst, A.E.M.C. Smeekes-Kuyl, and A.C.A. Vissers. Measurement of forces exerted on pedal and crank during work on a bicycle ergometer at different loads. *Int. Z. Angew. Physiol.*, 26:33–42, 1968.

[53] M.D. Hoffman. Cardiorespiratory fitness and training in quadriplegics and paraplegics. *Sports Med.*, 3:312–330, 1986.

[54] S.P. Hooker, S.F. Figoni, R.M. Glaser, M.M. Rodgers, and P.D. Faghri. Physiologic responses to prologned electrically stimulated leg-cycle exercise in the spinal cord injured. *Arch. Phys. Med. Rehab.*, 71:863–869, 1990.

[55] S.P. Hooker, S.F. Figoni, and M.M. Rodgers. Physiologic effects of electrical stimulation leg cycle exercise training in spinal cord injured persons. *Arch. Phys. Med. Rehabil.*, (73):470–476, 1992.

[56] S.J. Houtz and F. Fischer. An analysis of muscle action and joint excursion during exercise on a stationary bicycle. *J. Bone & Joint Surg*, (41a):123–131, 1959.

[57] M.L. Hull and M. Jorge. A method for biomechanical analysis of bicycle pedalling. *J. Biomech.*, (18):631–634, 1985.

[58] K.J. Hunt, M. Rothe, T. Schauer, A. Ronchi, and N.O. Negård. Automatic speed control in fes cycling. *Proceedings IFESS*, 2001.

[59] R.D. Jackson and W.J. Mysiw. Intermittent compressive forces, not muscle contraction, can reduce neurogenic osteoporosis. *Proc. 76th Annu. Meeting Endocrine Soc.*, 73(3):15–18, June 1994.

[60] R.P. Jaime. Entwurf und Erprobung eines linearen robusten Reglers für das Muskelmoment der Plantarflexoren zum nichtunterstützten Stehen von Patienten mit Querschnittslähmung. Master's thesis, Technische Universität Berlin, 1998.

[61] G.C. Jang, J.J. Chen, C.T. Shih, and T.C. Huseh. Design of fes-cycling system and its stimulation patterns. *Chinese J. Med. Biologic. Eng.*, 13(4):305–316, December 1993.

[62] T.W.J. Jansen, R.M. Glaser, and D.B. Shuster. Clinical efficacy of electrical stimulation exercise training: Effects on health, fitness, and function. *Topics in Spinal Cord Injury Rehabilitation*, 3(3):33–49, 1998.

[63] R.T. Katz, D. Green, T. Sullivan, and C. Yarkonv. Functional electrical stimulation to enhance systemic fibrinolytic activity in spinal cord injury patients. *Arch. Phys. Med. Rehab.*, 68:423–426, 1987.

[64] A. Kralj and T. Bajd. Functional electrical stimulation: Standing and walking after spinal cord injury. *Boca Baton, FL: CRC Press*, 1989.

[65] A. Kralj, T. Bajd, J. Krajnik, and H. Benko. Gait restoration in paraplegic patients: A feasibility demonstration using multichannel surface electrodes fes. *J. Rehab. R&D*, 20(1):3–20, 1983.

[66] A. Kralj and S. Grobelnik. Functional Electrical Stimulation- a new hope for Paraplegic Patients? *Bull. Pros. Res.*, 20:75–102, 1973.

[67] C.T. Le and M. Price. Survival from spinal cord injury. *J. Chronic. Dis.*, 35:487–492, 192.

[68] M. Levy. Fatigue of paralyzed skeletal muscle activated in- vivo by electrical stimulation. *D.Sc. Thesis, Technion, Israel*, 1990.

[69] M. Levy, T. Kushnir, J. Mizrahi, and Y. Itzchak. In vivo p nmr studies of paraplegic's muscles activated by functional electrical stimulation. *Magnetic Resonance in Medicine*, 29:53–58, 1993.

[70] L. Ljung. System Identification: Theory for the user. *Information and System Sciences, Prentince Hall*, 1987.

[71] M. Lyons. Immune infection in spinal cord injured males. *J. Neurosci. Nurs.*, 19:18–23, 1987.

[72] E.B. Marsolais and R. Kobetic. Functional walking in paralyzed patients by means of electrical stimulation. *Clin. Ortho. Rel. Res.*, 175:30–36, 1983.

[73] J.C. Martin, D.L. Millikin, J.E. Cobb, K.L.McFadden, and A.R. Coggan. Validation of a mathematical model for road cycling power. *J. of Applied Biomechan.*, 14:276–291, 1998.

[74] D.J. Maxwell, M.H. Granat, G. Baardman, and H.J. Hermens. Demand for and use of functional electrical stimulation systems and conventional orthoses in spinal cord lesioned community of the uk. *Artificial Organs*, 23(5):410–412, 1999.

[75] G.J. Merli, G.J. Herbison, and J.F. Dittuno. Deep vein thrombosis: prophylaxis in acute spinal cord injury patients. *Arch. Phys. Med. Rehab.*, 69:661–664, 1988.

[76] P. Minaire. Immobilization osteoporosis: a review. *Clin. Rheumatol.*, 8:95–103, 1989.

[77] J. Mizrahi, M. Levy, H. Ring, E. Isakov, and A. Liberson. Emg as an indicator of fatigue in isometrically fes-activated paralysed muscles. *IEEE Trans. Rehab. Eng.*, 2(2):57–65, June 1994.

[78] A. Dal Monte, A. Manoni, and S. Fucci. Biomechanical study of competitive cycling. *Medicine and Sport: Biomechanics III*, 8:434–439, 1973.

[79] W.J. Mysiw and R.D. Jackson. Hypercalciuria prevented by functional electrical stimulation. *Arch. Phys. Med. Rehab.*, 71(795), 1990.

[80] M. Nash. Immune responses to nervouse system decentralization and exercise in quadriplegia. *Med. Sci. Sports Exerc.*, 26(2):164–171, 1994.

[81] M.S. Nash, S. Bilsker, A.E. Marcillo, S.M. Isaac, L.A. Botelho, K.J. Klose, B.A. Green, M.T. Rountree, and J.D. Shea. Reversal of adaptive left ventricular atrophy following electrically-stimulated exercise training in human tetraplegics. *Paraplegia*, 29:590–599, 1991.

[82] J. Newmiller, M.L. Hull, and F.E. Zajac. A mechanical decoupled two force component pedal dynamometer. *J. Biomech.*, (21):375–386, 1988.

[83] American College of Sports Medicine. Guidelines for exercise testing and prescription. *Philadelphia, PA: Lea & Febiger*, 4, 1991.

[84] P.I. Pacy, R.H. Evans, and D.A. Halliday. Effect of anaerobic and aerobic exercise prompted by computer regulated functional electrical stimulation (fes) on muscle size, strength and histology in paraplegic males. *Prosthet. Orthot. Int.*, 11(75-90), 1987.

[85] P.J. Pacy, R. Hesp, D.A. Halliday, D. Katz, G. Cameron, and J. Reeve. Muscle and bone in paraplegic patients, and the effect of functional electrical stimulation. *Clinic. Sci. (Colch)*, 75:481–487, 1988.

[86] P.H. Peckham, M.W. Keith, and A.A. Freehafer. Restoration of functional control by electrical stimulation in the upper extremity of the quadriplegic patient. *J. Bone a Joint Surg.*, 70A:144–148, 1988.

[87] P.H. Peckham, J.T. Mortimer, and E.B. Marsolais. Alteration in the force and fatigability of skeletal muscle in quadriplegic humans following exercise induced by chronic electrical stimulation. *Cli. Ortho. Rel. Res.*, 114:326–344, 1976.

[88] P.H. Peckham, J.T. Mortimer, and J.P. Vander Meulex. Physiologic and metabolic changes in white muscle of cat following induced exercise. *Brain Res.*, 50:424–429, 1973.

[89] J.S. Petrofsky. Functional electrical stimulation: a two-year study. *J. Rehabilitat.*, 58:29–34, 1992.

[90] J.S. Petrofsky, R.M. Glaser, C.A. Phillips, and J.A. Gruner. The effect of electrically induced bicycle ergometer exercise on blood pressure and heart rate. *The Physiologist*, (25):253, 1982.

[91] J.S. Petrofsky, H. Heaten, and C.A. Phillips. Outdoor bicycle for exercise in paraplegics and quadriplegics. *J. Biomed. Eng.*, 5:292–296, October 1983.

[92] J.S. Petrofsky, H.H. Heaton, and C.A. Phillips. Feedback control system for walking in man. *Computers in Biol. & Med.*, 14(135-149), 1984.

[93] J.S. Petrofsky and C.A. Phillips. Constant velocity contractions in skeletal muscle by sequential stimulation of muscle efferents. *Med. Biol. Eng. Comput.*, 17:583–592, 1979.

[94] J.S. Petrofsky and C.A. Phillips. Active physical therapy- a modern approach to rehabilitation therapy. *J. Neuro. & Ortho. Surgery*, 4:165–173, 1983.

[95] J.S. Petrofsky, C.A. Phillips, J. Almeida, R. Briggs, E. Couch, and W. Colby. Aerobic trainer with physiological monitoring for exercise in paraplegic patient. *J. Clin. Eng.*, 10:307–314, 1985.

[96] J.S. Petrofsky, C.A. Phillips, H.H. Heaton, and R.M. Glaser. Bicycle ergometer for paralyzed muscle. *J. Clin. Eng.*, 9:13–19, 1984.

[97] J.S. Petrofsky, C.A. Phillips, P. Larson, and R. Douglas. Computer synthesized walking, an application of orthosis and functional electrical stimulation (fes). *J. Neuro. & Ortho. Med. & Surg.*, 6(3):219–230, 1985.

[98] J.S. Petrofsky, C.A. Phillips, and S.H. Petrofsky. Electronic physicians' prescription system for fes patient therapy. *J. Neuro. & Ortho. Surg.*, 6:239–246, 1985.

[99] J.S. Petrofsky and J. Smith. Computer aided rehabilitation. *Aviation Space and Environ. Med.*, 59:670–679, 1988.

[100] J.S. Petrofsky and J. Smith. Three wheel cycle ergometer for use by men and woman with paralysis. *Med. & Biol. Eng. & Comput.*, (30):364–369, 1992.

[101] J.S. Petrofsky and R. Stacy. The effect of training on endurance and the cardiovascular responses of individuals with paraplegia during dynamic exercise induced by functional electrical stimulation. *Eur. J. Appl. Physiol.*, 64:487–492, 1992.

[102] C.A. Phillips, D. Danopulos, P. Kezdi, and D. Hendershot. Muscular, respiratory and cardiovascular responses of quadriplegic persons to an fes bicycle ergometer conditioning program. *Int. J. Rehabil. Res.*, (12):147–157, 1989.

[103] C.A. Phillips and J.S. Petrofsky. A review of fracture cases in spinal cord injured individuals participating in closed loop functional electrical stimulation (fes) experiments. *Ibid*, 6:247–251, 1985.

[104] C.bA. Phillips, J.S. Petrofsky, D.M. Hendershot, and D. Stafford. Functional electrical exercise: a comprehensive approach for physical conditioning of the spinal cord paralyzed individual. *Orthopaedics*, 7:1112–1128, 1984.

[105] S.F. Pollack, K. Axen, N. Spielholz, N. Levin, F. Haas, and K. Ragnarsson. Aerobic training effects of electrically induced lower extrimity exercises in spinal cord injured people. *Arch. Phys. Med. Rehab.*, 70:214–219, 1989.

[106] S.F. Pollack, K. Axen, N. Spielholz, N. Levine, F. Hass, and K.T. Ragnarson. Aerobic training effects of electrically induced lower extremity exercises in spinal cord injured people. *Arch. Phys. Med. Rehab.*, 70:214–219, 1989.

[107] M.L. Pollock, J.H. Wilmore, and S.M. Fox. Exercise in health disease: evaluation and prescription for prevention and rehabilitation. *Philadelphia: Sanders*, 1990.

[108] D.J. Pons, C.L. Vaughan, and G.G. Jaros. Cycling device powered by the electrically stimulated muscles of paraplegics. *Med. & Biol. Eng. & Comput.*, (27):1–7, 1989.

[109] H.M. Popp. *Design and construction of a laoratory system for neuromuscular stimulation of the lower extremeties during cycling.* M.sc. dissertation, University of Cape Town, 1986.

[110] P.M.H. Rack and D.R. Wesrbury. The effects of length and stimulus rate on tension in isometric cat soleus muscle. *J. Physiol.*, 204:443–460, 1969.

[111] K.T. Ragnarsson, S. Pollack, and W. O'Daniel. Clinical evaluation of computertised functional electrical stimulation after spinal cord injury: A multicentre pilot study. *Arch. Phys. Med. Rehabil.*, 69:672–677, 1988.

[112] K.T. Ragnarsson, S. Pollack, W.O'Daniel, R. Edgar, J. Petrofski, and M.S. Nash. Clinical evaluation of computerized functional electrical stimulation after spinal cord injury: A multicenter pilot study. *Arch. Phys. Med. Rehab.*, 69:672–677, 1988.

[113] K.T. Ragnarsson and G.H. Sell. Lowerextremety fractures after spinal cord injury: A retrospectrive study. *Arch. Phys. Med. Rehab.*, 62:418–423, 1981.

[114] R. Redfield and M.L. Hull. On the relation between joint moments and pedalling rates at constant power in bicycling. *J. Biomech.*, (19):317–329, 1986.

[115] R. Riener. Model-Based Development of Neuroprostheses for Paraplegic Patients. *Medical and Biological Engineering and Computing*, 1999.

[116] R. Riener. Model-based development of neuroprosthesies for paraplegic patients. *In press for the Philosophical Transactions of the Royal Society: Biological Sciences*, 1999.

[117] C.J. Robinson, N.A. Kett, and J.M. Bolam. Spasticity in spinal cord injured patients: 1. short term effects of surface electrical stimulation. *Arch. Phys. Med. Rehab.*, 69:594–604, 1988.

[118] C.J. Robinson, N.A. Kett, and J.M. Bolam. Spasticity in spinal cord injured patients: 2. initial measures and long-term effects of surface electrical stimulation. *Arch. Phys. Med. Rehab.*, 69:8620868, 1988.

[119] M.M. Rodgers, R.M. Glaser, S.F. Figoni, S.P. Collins, T. Mathews, A.G. Suryaprasad, and S.C. Gupta. Musculoskeletal responses of spinal cord injured individuals to functional neuromuscular stimulation-induced knee extension exercise training. *J. Rehab. R&D*, 28(4):19–26, 1991.

[120] M. Rothe. Design and realisation of a controller for an electric-motor-supported tricycle in therapeutic use for paraplegics. *Masterthesis*, 1999.

[121] L.M. Schutte, M.M. Rodgers, B.N. Glaser, and F.E. Zajac. Determining the direction of crank acceleration during electrical stimulation-induced leg cycle ergometry. *RESNA Int. Toronto, Ont., Canada*, pages 238–240, 1992.

[122] L.M. Schutte, M.M. Rodgers, F.E. Zajac, and R.M. Glaser. Improving the efficacy of electrical stimulation induced leg cycle ergometry: an analysis based on a dynamic musculoskeletal model. *IEEE Transactions on rehabilitation engineering*, 1(2):109–124, June 1993.

[123] T.P. Seib, R. Price, M.R. Reyes, and J.F. Lehmann. The quantitative measurement of spasticity: effects of cutaneous electrical stimulation. *Arch. Phys. Med. Rehab.*, 75:746–750, 1994.

[124] P.J. Sinclair, G.M. Davis, R.M. Smith, B.S. Cheam, and J.R. Sutton. Pedal forces produced during neuromuscular electrical stimulation cycling in paraplegics. *Clin. Biomech.*, 11(1):51–57, 1996.

[125] M.L. Sipski, C.J. Alexander, and M. Harris. Long-term use of computerized bicycle ergometry in spinal cord injured subjects. *Arch. Phys. Med. Rehab.*, 74:238–241, 1993.

[126] M.L. Sipski, J.A. Delisa, and S. Schweer. Functional electrical stimulation bicycle ergometry: patient perception. *Amer. J. Phys. Med. Rehab.*, 68(3):147–150, 1989.

[127] M.L. Sipski, T.W. Findley, R.M. Glaser, S. Schweer, and C. Ramach. Prevention of osteoporosis through early use of electrical stimulation afetr spinal cord injury. *Arch. Phys. Med. Rehab.*, 71:795, 1990.

[128] K.E. Sloan, L.A. Bremer, J. Byrne, R.E. Day, and E.R. Scull. Musculoskeletal effects of an electrical stimulation induced cycling programme in the spinal injured. *Paraplegia*, (32):407–415, 1994.

[129] P.D. Soden and B.A. Adeyefa. Forces applied to a bicycle during normal cycling. *J. Biomechanics*, 12:527–541, 1979.

[130] E.S. Stauffer. Long-term management of traumatic quadriplegia. *The Total Care of Spinal Cord Injury, Boston, Mass: Little, Brown*, 1978.

[131] K.J. Åstrom and B. Wittenmark. *Computer Controlled Systems.* Prentice Hall, 1997.

[132] D.J. Twist. Acrocyanosis in a spinal cord injured patient- effects of computer controlled neuromuscular electrical stimulation: a case report. *Phys. Ther.*, 70:45–49, 1990.

[133] D.J. Twist, J.A. Culpepper-Morgan, K.T. Ragnarsson, C.R. Petrillo, and M.J. Kreek. Neuroendocrine changes during functional electrical stimulation. *Amer. J. Phys. Med. Rehab.*, 71:156–163, 1992.

[134] P.H. Veltink. Control of fes-induced cyclical movements of the lower leg. *Med. & Biol. Eng. & Comput.*, 29:8–12, 1991.

[135] G.G. Whiteneck, S.W. Charlifue, and H.L. Frankel. Mortalidy, morbidity, and psychosocial outcomes of persons spinal cord injured more than 20 years ago. *Paraplegia*, 30:617–630, 1992.

[136] F.R. Whitt and D.G. Wilson. Bicycling science. *M.I.T. Press*, 74.

[137] Wilmot. Functional neuromuscular stimulation in acute spinal cord injury. *Am. Spinal Injury Assoc. Abstr. Dig.*, 9, 1989.

[138] G.T. Yamaguchi and F.E. Zajac. A planar model of the knee joint to characterized the knee extensor mechanism. *J. Biomechan.*, 22(1):1–10, 1989.

[139] L.A. Zadeh. Fuzzy sets. *Inform. Contr.*, 8:28–44, 1965.

Markus Rothe
Am grünen Hang 16
57078 Siegen
Germany